Consistency of Gravure Printers Output for Medicine Packaging

Thesis submitted by

by

Paulomi Kundu

Doctor of Philosophy (Engineering)

Printing Engineering Department,
Faculty Council of Engineering & Technology
Jadavpur University
Kolkata, India

2022

Index No. 295/16/E

Title of Thesis

Consistency of Gravure Printers Output for Medicine Packaging

Under the Guidance of

Dr. Swati Bandyopadhyay
Associate Professor,
Printing Engineering Department,
Jadavpur University, Kolkata – 700032, India

&

Prof. Alain Trémeau
Professor,Faculty of Sciences and Technologies
Hubert Curien Labarotory, UMR CNRS
Université de Lyon, Université Jean Monnet,
Saint Etienne, France

3. List of Publication:

Journal Publications (3) :

1. Paulomi Kundu , Swati Bandyopadhyay , Alain Tremeau "Authentication of a Gravure Printer from Color Values using an Artificial Neural Network", International Journal of Engineering Research & Technology (IJERT) , Vol. 11 ,Issue 02, February-2022.

2. Paulomi Kundu, Swati Bandyopadhyay, Alain Tremeau," Analysis of Spectral differences between Printers to detect the Counterfeit Medicine Packaging", Journal of Algebraic Statistics,Volume 13, No. 2, p. 798 – 806, 2022.

3. Paulomi Kundu, Swati Bandyopadhyay, Alain Tremeau," Study on Color Gamut to Authenticate the Gravure Printers Output", International Journal of Computer Applications (0975 – 8887), Volume 184– No.18, June 2022.

4. List of Presentations in National / International Conferences/ Workshops/Symposiums:

1. International Conference – Online Presentation,2nd International Conference on Engineering, Social- Sciences, And Humanities (IC-ESSU) 30th & 31st March, 2022 Philippines, Paper titled "Analysis of Spectral differences between Printers to detect the Counterfeit Medicine Packaging" , held on 30th & 31st March, 2022, Philippines.

"Statement of Originality"

I Paulomi Kundu registered on 01/04th July, 2016 do hereby declare that this thesis entitled" Consistency of Gravure Printers Output for Medicine Packaging" contains literature survey and original research work done by the undersigned candidate as part of Doctoral studies.

All information in this thesis have been obtained and presented in accordance with existing academic rules and ethical conduct. I declare that, as required by these rules and conduct, I have fully cited and referred all materials and results that are not original to this work.

I also declare that I have checked this thesis as per the "Policy on Anti Plagiarism, Jadavpur University, 2019", and the level of similarity as checked by iThenticate software is 6%.

Paulomi Kundu

Signature of Candidate:

Date : 21.10.22

Certified by Supervisor(s):

(Signature with date, seal)

1.

Sweta Bandyopadhyay
21.10.22
(Supervisor)

Associate Professor
Printing Engineering Department
Jadavpur University
Kolkata

2.

Prof. Alain Trémeau

LABORATOIRE HUBERT CURIEN
UMR CNRS 5516 Université Jean Monnet
18 rue Pr. Benoit Lauras - Bât. F
F-42000 SAINT-ETIENNE
(33) 04 77 91 57 80 / Fax (33) 04 77 91 57 81

Proforma-2

CERTIFICATE FROM THE SUPERVISOR

This is to certify that the thesis entitled **"Consistency of Gravure Printers Output for Medicine Packaging"** submitted by **Paulomi Kundu**, who got her name registered on 01/04th July, 2016, for the award of Ph.D. (Engineering) Degree of Jadavpur University is absolutely based upon her own work under the supervision of **Dr. Swati Bandyopadhyay** and **Prof. Alain Trémeau** and that neither her thesis nor any part of the thesis has been submitted for any degree or any other academic award anywhere before.

Signature of the Supervisor and Date
With Official Seal

Swati Bandyopadhyay
21.10.22
Associate Professor
Printing Engineering Department
Jadavpur University
Kolkata

Dr. Swati Bandyopadhyay
Associate Professor,
Printing Engineering Department,
Jadavpur University
Kolkata – 700 032, India

Signature of the Supervisor and Date
with Official Seal

A. TREMEAU
LABORATOIRE HUBERT CURIEN
UMR CNRS 5516 Université Jean Monnet
18 rue Pr. Benoît Lauras - Bât. F
F-42000 SAINT-ETIENNE
(33) 04 77 91 57 60 / Fax (33) 04 77 91 57 81

Prof. Alain Trémeau
Professor, Faculty of Sciences and Technologies
Hubert Curien Labarotory
UMR CNRS
Université de Lyon, Université Jean Monnet,Saint Etienne, France

ACKNOWLEDGEMENT

It gives us immense pleasure in presenting the Ph.D thesis entitled “Consistency of Gravure Printers Output for Medicine Packaging". It has given me a memorable worthwhile experience for completion of thesis which is floored by the guidance and support by several people, who are much esteemed for me. First and foremost, I heartily wish to express my deepest gratitude to my supervisors, Dr. Swati Bandyopadhyay and Prof. Alain Trémeau, for their invaluable advice, continuous support, and patience during my PhD study. Their immense knowledge and plentiful experience have encouraged me in all the time of my academic research.

I would like to convey my sincere gratitude to Indo French Centre for the Promotion of Advanced Research (IFCPAR/CEFIPRA) for their support.

I would like to thanks to Sergusa Solution Pvt. Ltd. and Etone India Pvt.Ltd. for their support.

My most sincere thanks go to members of Color and Tone Reproduction Laboratory, who have given me valuable suggestions and warm company in successfully completing this work.

I wish to express my warm and heartfelt thanks to my family, Parents, In-Laws for their tremendous unconditional, unequivocal, and loving support which keep me motivated and confident. My accomplishment and success are because they believed in me.

Foremost, my special thanks to my Husband for his joining to my life during my research work and stood by me and shared with me both the great and the hard moments of my life.
Thank you for your love and believing in me!

DEDICATION

I would like to dedicate my thesis to my Parents for their endless love, support, and encouragement throughout my pursuit for education. I hope this achievement will fulfill their dream they envisioned for me.

Table of Content

List of Figures

List of Tables

Abstract

Counterfeiting of pharmaceutical packaging has become amajor challenge to the society which causes severe health hazard. The easiest way of producing fake medicine is counterfeiting the packages of medicine. While counterfeiting the pharmaceutical product, printing and packaging takes very crucial role as the customer buy the product by the attraction and information provided by the package. So the counterfeiters emphasize more on packages and associated printing. Nowadays this issue has spreaded worlwide and it has become a major threat to the society and economy. The counterfeited pharmaceutical products are unauthorized, expired, reused and/or manipulated packages which are similar to the original. The main problem is that it is difficult to identify visual differences between original and fake packaging, and the lack of solutions to identify the authentic packaging. So packaging authentication is a very important need in pharmacetical industry.Through medicine packaging, valuable information such as manufacturing date, expiry date, and chemical composition etc. of product have been conveyed. Advanced technologies have made it easier to replicate the packaging of any products. The simpliest way to produce fake samples of printed packaging is to scan the image of the original package by different devices, such as digital camera, mobile camera, scanner etc.,then to print the scanned image by suitable printers.This work is focused on pharmaceutical package printing not only for its social implication but also for its technological variation. Since most of the medicines are packed in metal foil, the printing technology associated is gravure printing. Hence the work has been based on gravure printing on metal foil. Little work has been done on gravure printing on metal foils. Scanning or taking photographs of the package and re-printing is one of the methods to counterfeit the original package sample. However, the variation of color while reprinting it may be assessed to check whether the printing is done by the original manufacturer or their authenticated printer house. When the image of the original print is taken through different mobiles, camera or scanners, the color values are not the same as the original print even if it is printed on the same printer. However, when the scanned samples are reprinted with different printers, the differences are much higher in comparison to the original print. If it is a single color print, counterfeiters are trying to match the color by applying different color management solutions. Situations become difficult when multicolor printing is applied. Hence, color consistencies of multicolor printing have been studied for checking authenticity of a print. In this study, blister foil has been taken as substrate and a reference color chart (IT8.7/3) are printed with 4-color gravure printing machine. IT8.7/3 is the standard color chart designed by International Color Consortium for printer characterization. The spectral reflectance of the solid colors (Cyan, Magenta, Yellow, Black) and their different combination of color patches of printed color chart (original sample)and its scanned reprinted sample (mentioned as reprint) have been observed. The difference between the samples has been evaluated by color difference CIEΔE2000(ΔE_{00})**.**In this study, the reference image(color chart IT8.7/3) has been printed with three different gravure printers (P1, P2 ,P3 which are mentioned as prints). Then to simulate counterfeiting process, the images of print samples are taken by different input devices. The images are then printed in those three printers again. The scanned and reprinted samples are referred as reprints. Artificial Neural Network (ANN) model is used to predict the CIELAB color values of a print samples and reprint samples printed in different printers. In this study, 70% of color

patches (total 928) have been used to train the network, 15% of the data used as cross-validation and 15% of the data is used to verify the accuracy of the network. Then the predicted color values of one printer (reference Print) are compared with other print and scanned reprint samples to assess the differences. It has been observed that the differences of predicted color values with the print samples are much less when compared with the reference print. The difference becomes much higher for scanned reprint samples in comparison to the same reference prints. Hence it will be possible to identify the reprint sample (if someone tries to reprint it after scanning or taking images of original multicolor artwork and reprints it). Hence the predicted difference may be used to protect medicine packaging from counterfeiting. Yule-Nielsen spectral modified Neugebauer) (YNSN) model has been used to predict the reflectance spectrum for original and reprint sample for different dot areas for different color combinations of color patches. It has been taken to identify the authentic printed sample. It has been observed that the obtained predicted spectrum result is close to the print sample (original) and has wide difference with the scanned reprint samples. The volume of the color gamut has also been studied between print sample (original) and a scanned reprint sample to identify the difference between them. From the color gamut volume it has been analyzed that the gamut volume is lesser for scanned reprintsample than the print samples. The obtained result indicates that the difference could be used to identify whether a sample is original or counterfeited and it will be difficult for counterfeiters to copy the image with these combinations of colors on blister foils packaging and also may help to protect the medicine packaging from counterfeiting.

CHAPTER1

1. INTRODUCTION

Counterfeiting of medicine is a great challenge to the society. Duplicate medicines are creating serious health hazards. The pharmaceutical industries are also facing great challenge and huge loss for the counterfeiter. The simplest way to produce duplicate packages is to take images of the original packages or copy the text with suitable fonts and reprint the package. With the improvement of different new technologies and the increase of counterfeiters, packages have been counterfeited easily throughout the world and it has affected our society and also the economy.

In this study, gravure printing on blister foil for pharmaceutical products has been focused and basic color features such as spectral reflectance of color, colorimetric values of the printed multicolor chart have been used to get the difference between the original print sample (mentioned as print) and scanned reprint sample (mentioned as reprint) on blister foil using gravure printer. In this study, it has been observed that the color values have been changed to a significant extent after scanning or capturing any multicolored image which was printed on blister foil by gravure printing machines [64, 68]. It has been demonstrated that after the scan and print attack, the color distortion and spectral distortion on print and reprint blister foil samples could not be corrected by any color correction methods. This difference could be used as an indicator for differentiation between original and scanned reprinted samples. Thus the color consistency of the medicine packages may be used to detect counterfeiting in the pharmaceutical industry.

1.1 IDENTIFICATION OF PROBLEM

It has been observed that the important step is to investigate the authentication of packaging for suspected counterfeited pharmaceutical packaging. Initial request came from some package printers as the major pharmaceutical companies are facing challenges of huge financial loss and ill reputation for the Duplicate medicines available in the market. Printing and packaging have taken very crucial role as the customer has bought the product by the attraction and information provided by the package. Nowadays it has been difficult for the customers to detect the counterfeited

medicine sample by visual comparison. Due to increase of counterfeiters and improvement of new technologies, authentication and protection of packages has generated new series of challanging problem. The esaiest ways to generate the counterfeited or Duplicate package from scan and reprint the original product. Development of different devices like digital camera [101], mobile camera, scanner have been used to capture or scanned the image or text of original print sample and then produce the scanned reprint sample. Since most of the medicines have packed with metal foil (blister foil) then as a printing technology gravure printing machine has been associated with it. It has also challanging task to preserve the image quality of prints on reflective materials (blister foil) with a gravure printing technology and to check if a print is original or not.The main purpose of our study is to address the problem of authentication of printed artworks on blister foil using a gravure printer (CMYK printing process).Meanwhile most of papers of the state of the art have been studied the quality of prints based on ink jet printers, few studies have studied on the quality of gravure spot color reproduction. MMandal and Bandyopadhyay [64] studied the impact of printing parameters on quality of prints for gravure printing. Pandey et. al [68] analyzed the print quality relatively to different types of non-porous substrates for gravure printing. They have compared the density and dot gain values for Cyan, Magenta, Yellow and Black (CMYK) channels for three types of substrates (milky poly, polyester and BOPP). The stability of image quality with time on blister foil [64] printed by gravure printing machines have been studied and defined by colorimetric values and ANN [64] models. For gravure printing press the test pattern of authentication [80] has been proposed to identify the original cylinder using the process of chemical etching on blister foil. The shape of print dots [81] of processed colors (cyan,magenta,yellow,black) are different from the scanned reprinted dots on blister foil for gravure printer.

1.2 PROBLEM STATEMENT

Medicine package prining are mainly based on gravure since most of the packages are based on blister foils. Counterfeiting of print medicine packages are produced by scanning original using camera, scanner etc. and then printing it. Many of medicines have been packed with blister foil and the informations of medicines have printed on the package using gravure printing machines. Managing or manipulating a single color may be easy by different hardware as well as software solution. However, it will

be very difficult to manage colors in multicolor printing. Hence the present work is focuessed on color consistency of multicolor printing. Due to the reflective material (blister foil) it has been difficult to preserve printed image quality with gravure printing process.Meanwhile most of papers of the state of the art studied on the quality of prints are based on ink jet printers, few studies are based on the quality of gravure spot color reproduction. Various types of innovative technologies have been developed to identify the original samples and counterfeiters also increased their knowlegde to counterfeit any original samples and produced duplicate or counterfieted sample. Few papers have focused on the package printing with blister foil using gravure press. There exist different color management systems to edit colors to look good the image on display or as printed image. The color management system or color correction are not easy for gravure printing machines with reflective materials like aluminium blister foil. The majority of existing printing security features have not been adapted for such printing process and blister foil used as packaging in pharmaceutical industry. So the color features has explored as important feature to differentiate between original and scanned reprinted samples.

In this study, color features have been studied to analyze the differentiation between original and scanned reprinted sample. In this study, color parameters has been identified to find out the signified difference between the original and scanned reprinted samples. It has been demonstrated that scan and print processes create color distortions due to several parameters related to the printing press and gravure printing cylinders (print & reprint cylinders) used.When the original print is scanned and reprinted ,some color or spectral differences have been observed between the original print and reprint samples. In this study, it has been demonstrated that the color of a set of printed samples is changed depending on the input and output devices used for print and reprint processes. After scanning the printed image, when the printed image is reprinted again, the quality of the reprinted image is affected by different devices. The spectrum of color patches and the L*, a*, b* values of the original print and of its scanned reprints are significantly different. It has been assumed that these differences may be used to detect whether a print is original or not. It may be used to protect packages from the counterfeiting.

1.3 PURPOSE AND GOAL

This study has been considered the problem of protecting pharmaceutical products with blister foil packaging from counterfeiting. This research work aims to authenticate the printed blister foil sample used as medicine packagingwith the basic color features, such as color values of the printed substrate from counterfeited blister foil samples. The print and reprint samples have been represented as original and counterfeited samples respectively. So, in this study, the effect of change after the scan and print process has been analyzed by using the color feature of printed and scanned reprint images on blister foil which are used as packages for some medicines in the pharmaceutical industry. During the printing process with gravure machines cyan (C), magenta (M), yellow (Y) and black (K) inks have been used to print any multicolor image on the substrate. Here IT8.7/3 standard color chart has been used as artwork to print on blister foil. The print samples were taken in three different printers. Then the print samples are captured with different camera and scanner to simulate the process what counterfeiters do. Then the scanned image has been reprinted with the three printers again. It has been observed that the color values are changed to a significant extent as it is dependent on the color profile of input devices and printers. It has been known that the spectral signature is unique for specific ink-substrate combinations. If the original printed sample has been printed with different gravure printers then color values (cyan, magenta, yellow and black) and reflectance spectrum of inks also differ for other printers from the source printer. In this research, the inequality of reflectance spectrum and the color difference between printed and scanned reprinted samples have been observed when the printed sample is scanned and reprinted with the same output device even if printed with a different output device before the scanned process. For using different output gravure printing machines, the color distortion is lesser between printed samples than the print-reprint samples after scan & print process. Artificial Neural Network (ANN) and Yule-Nielsen modified Spectral Neugebauer (YNSN) models have been used to predict the CIELAB color values and reflectance spectrum for a different combination of color patches from the printed sample and compared with reprint samples collected from other gravure machines. The obtained predicted results closely similar to the printed sample but differ from the reprint sample. The color differences are less when

compared with print samples printed with different printers in comparison to reprint samples after scanning and reprinting the original ones. So, the obtained results have indicated that it may provide a solution which is cost effective to identify whether a print sample is original or not. It will be beneficial for the manufacturer in the pharmaceutical industry and it would be difficult to counterfeit any combinations of the color of images printed on foil substrate by gravure printing machines.

1.4 RESEARCH OBJECTIVES:

- To study the color consistency parameters which can differentiate original print with reprint samples.
- Characterization of the output prints from gravure printing machines on blister foil substrate to make print and scan attack difficult.
- Observe the CMYK color appearance on a printed and scanned reprinted sample collected from different gravure printing machines.
- Analyze any difference that appears in color for gravure printing and reprinting process on blister foil used for medicine packaging under standard conditions.

1.5 STATEMENT OF HYPOTHESIS

In medicine packaging, mostly gravure printing on blister foil is used to pack the products. So, the present work is focused on gravure printing on blister foil substrate. The foil samples are printed with cyan (C), magenta (M), yellow (Y), and black(K) colors by various gravure printing machines. The Reflectance spectrum, colorimetric values, color difference between solid colors (C,M, Y, K) and their combinations printed on blister foil have been used to differentiate original printed samples from counterfeited reprint samples. The color values of prints are statistically different from the color values of reprints, and spectral values of prints are statistically different from spectral values of reprints. It has been defined that print and reprint samples are statistically different by color values and spectral values.

1.6 LIMITATION

This study mainly focused on the colorimetric properties of printed and scanned reprinted samples as output from gravure printing machines. It will be beneficial for pharmaceutical companies to identify whether a print sample is original or counterfeited. In future, it may be studied how the end users can verify it in medicine shops or by sending images to the manufacturer.

1.7 THESIS OVERVIEW

The present work is based on the print output of the gravure printing machine for blister foil substrate used in the medicine packaging industry. The present work mainly focuses on the gravure printing on blister foil substrate used for medicine packaging. The present study has explored the study of color consistency of gravure prints on blister foil substrate using colorimetric values. The difference in the reflectance spectrums, colorimetric values of processed colors printed on foil was analyzed to differentiate between original and counterfeited sample. In the pharmaceutical industry, printed foil samples could be identified by the manufacturer using simple colorimetric values instead of using existing expensive methods (Hologram, Watermarking, RFID, etc.).

Chapter 1 includes introduction with problem statement.

Chapter 2 includes literature survey which summarizes the background work related to the present work. Different methods and prediction models have been discussed for printed sample authentication for different substrates and printing methods.

Chapter 3 has defined the material used for medicine packaging and their advantages.

Chapter 4 has defined the description of the gravure printing process used for pharmaceutical package printing. Various gravure cylinders making processes have been discussed to analyze the effect of printing output for different gravure printing machines.

Chapter 5 has discussed the color consistency of gravure prints and introduced the basic concept of basic color theories, color management, and printing colors parameters. Yule-Nielsen modified Spectral Neugebauer (YNSN) model used in this present work to identify the original samples and established the color difference for print sample authentication purposes has been discussed.

Chapter 6 presents the procedure of collection of data and devices used for the experimental measurement for the present work.

Chapter 7 has described an Artificial Neural Network prediction model. The general overview and its implementation in this present work have been discussed.

Chapter 8 has shown and analyzed the result with graphs collected from the experiments.

Chapter 9 summarizes and concludes the present research work. Future work has been discussed here.

CHAPTER 2

2. LITERATURE SURVEY

This chapter summarizes the background research for thispresent study. Different types of methods, algorithms with different equipment (directly or indirectly related to thepresent research work) are reported. Background papers based on different printer characterization methods, gravure printing processes, spectral differences analysis, gamut difference analysis, Artificial Neural Network model, Yule-Nielsen modified spectral Neugebauer model, are discussed herewith the aim to use these methods to identify an authentic gravure printer output from a counterfeited print.

2.1 Literature review on Printer Characterization

2.1.1 Reflectance spectral prediction and characterization of a printer

- *Methods based on the Yule-Nielsen modified Neugebauer model*

Silvia Zuffi and Raimondo Schettini [2] treated the four-ink inkjet printer as RGB printer for spectral base printer characterization. In this study they have measured the spectra of print sample and computed the spectral data using Yule-Nielsen modified Neugebauer (YNSN) model. To improve the performance of their model, they mostly concentrated on black ink. They have analyzed that the YNSN model has not suitable to predict the reflectance of colors which has been made of more than one ink. They have used RGB data as input to the printer model to compute the reflectance spectra as output. Then the color difference was used to compute the difference between the measured and computed spectra.

Roger David Hersch and FrédériqueCrété [3] improved the Yule-Nielsen modified Neugebauer model by combining the effective dot surface coverage computation model. The effective dot surface coverage values have been produced from the nominal dot surface coverage values by weighted mean of individual effective dot surface coverage depending on the different superposition conditions. They have computed the new method on 729 color patches as test sample for different printing technologies like offset at 150 lpi, thermal transfer prints at 75 lpi, inkjet prints at 100 lpi and defined the

prediction error using color difference (delta E_{94}). They have also showed the improved prediction factors for all printing technologies by using their prediction model. They have obtained better prediction accuracy of reflectance spectra for clustered dot halftones than the dispersed dot and error diffusion halftones.

Roger David Hersch and Adish Kumar Singla [4] improved the ink spreading model and developed an approach for dot-on-dot spectral prediction model with the Yule-Nielsen modified spectral Neugebauer model for halftone patches. They have applied their prediction model for dot-on-dot thermal transfer prints and for ink-jet prints at different screen frequencies (50, 75, 100 and 120 lpi). They predicted the spectrum of one single solid ink, printed on superimposed on one ink or two inks by their model, where nominal to effective surface coverage of an ink halftone has been mapped by ink spreading function and measured the error using delta $E_{94.}$ They have showed 50% higher prediction accuracy for thermal print technology and ink-jet prints.

R. D. Hersch et al. [5] provided accurate spectral prediction of calibrated color patch, they have enhanced the Yule–Nielsen modified spectral Neugebauer model (YNSN) enhanced for accounting for ink spreading in the different ink superposition conditions. In all superposition condition, they obtained better prediction result of the calibrated same image or similar color image than the performance of classical calibration on 50% halftone patches printed in all superposition conditions. Effective dot area coverage has been fitted by minimizing a difference metric between measured reflection spectrum and predicted reflection spectrum for all superposition condition. To characterize the physical dot gain of halftone ink on paper, they used multiple ink spreading curves for all solid inks superposition conditions.

L Iovineet al.[6] predicted the reflectance spectra on ceramic substrate for halftone prints the Neugebauer model has been applied. With the Yule-Nielsen correction factor (n = 20) they defined the best performance of prediction model for different ink and single ink mixtures. They assessed the incorporation of spectral prediction for overlap colors on ceramic substrate and the application of modified Kubelka-Munk theory.

N. P. Garg et al. [29] have described a calibration method using the Yule–Nielsen Modified Spectral Neugebauer Model. They have used digitized RGB images instead of measured reflection spectra to compute effective surface coverage for full ink spreading. They defined the comparison between predicted reflection spectra and measured refection

spectra and their color difference. Measured and predicted spectra first to CIE-XYZ and then to CIE-LAB to predict the accuracy of spectral halftone patch. They defined that the effective colorant coverage could be identified by cyan, magenta, yellow, red (superposition of magenta and yellow),green (superposition of yellow and cyan), blue (superposition of magenta and cyan), and black (superposition of cyan, magenta and yellow) with different percentage of colorant. They used two different printers (inkjet and thermal printer) for their experiment. For calibration they reduced the ink spreading curve by using intensity, mean and color difference of digitized images which has been digitized with scanner or microscope.

Thomas Bugnon et al.[88] introduced the ink spreading enhanced Yule-Nielsen modified Spectral Neugebauer model for recovering the ink surface coverage of cyan, magenta, yellow and black inks using reflectance spectra. Within the visible rangethe amount of pure black and chromatic black has unambiguously distinguished by their proposed method of ink spreading and near-infrared enhanced Yule-Nielsen modifiedSpectral Neugebauer model (IRYNSN). Due to the better absorbent of black pigment ink within the near-infrared domain than visible domain, their measurement has expanded to the near-infrared domain. They also showed that the IRYNSN model more consistent than extended YNSN (EYNSN) methodand used for recovery of gray component replacement strategies from halftone patches.

Pau Soler and Jordi Arnabat [31] proposed an Extended Neugebauer Spectral Model or Yule-Nielsen modified Spectral Neugebauer (YNSN) model to characterize the printer by using different substrates and two types of ink, such as pigment based and dye-based ink. Specific ink substrate combination creates printer profile to characterize the printer. They used IT8.7/3 color chart for prediction purpose, next reduced the data to 44 patches. They included Neugebauer primaries with two different inks using thermal inkjet printer for their experiment procedure. As a result, they showed that the performance of dye based ink is better than the pigment based ink by computed color difference.

From the survey of the previous papers it has been concluded that they were mostly applied the YNSN model for paper substrates and inkjet printer. The reflectance spectrum has predicted for different ink surface coverage of cyan, magenta, yellow and black inks to get the characterize halftone multicolor patches from inkjet printers. In this study, YNSN model is applied to predict the reflectance spectrum of multicolor halftone patches from solid color patches on blister foil substrate for gravure printing machines. This

method is also useful for authentication purpose of printed samples collected from gravure printing machines for medicine packaging.

- *Other methods*

*Roger D. Hersch et al. [1]*proposed a new spectral prediction model to improve the accuracy the prediction performance and showed considerable progress result compared with the classical Clapper-Yule model. At various screen frequencies, the proposed spectral prediction model has been applied with the method of effective surface coverage to offset and thermal transfer printing. They have defined that the proportionality of incident light and reflected light is more for same colorant than the other colorant. Their ink spreading model computed the weighted mean (ink coverage) of individual ink for different superposition condition of inks when ink densities remain same for offset and thermal transfer technologies.

Roger D. Hersch etal.[7] proposed spectral prediction model defined better result compared to the classical Clapper-Yule model on the basis of the reflection of light from colorant. For both offset (75 to 150 lpi) and thermal transfer printer (50 to 75 lpi) they combined the proposed spectral prediction model with the ink spreading model. The clustered dot color printed samples was used for spectral prediction purpose. They showed that more light has been reflected on to the same colorant surface than different colorant surface when light incident through the surface of the colorant. Effective dot coverage has defined and improved the spectral prediction by reducing the mean error between prediction and measured values. They have not computed their model for other printers and other half toning algorithms.

*Robert Chunget al.[8]*measured and predicted the color of overprint solid on the spectral based solution. The color of overprint solid been predicted by spectral based model for offset printer and as well as for digital printers. Due to the change of ink sequence in the wet on wet printing they have defined the color difference of overprint. In the Preucil equation with all variables they modified the Holub equation on the basis of spectral based overprint model. The Preucil equation is defined by the following Eq.(1).

$$t = \frac{D_{op} - D_1}{D_2 - D_0} \qquad \text{Eq.(1)}$$

Eq.(1) defines the density base ink trapping formula, where t is ink trapping as a function of overprint (D_{op}), paper (D_0), first ink (D_1), and second ink (D_2). And Holub equation is expressed by the Eq.(2)

$$R_{op(\lambda)} = R_{1(\lambda)} \times R_{2(\lambda)} \qquad \text{Eq.(2)}$$

Where, spectral reflectance of overprint color has been computed by the reflectance spectrum of 1st ink ($R_{1(\lambda)}$) and 2nd ink ($R_{2(\lambda)}$). Inks with the same tack and in different ink sequences, the performance of spectral based model has been tested to simulate wet-on-wet ink transfer for offset and dry-on-dry ink transfer for digital printing. They showed the importance of ink sequence for solid two-color overprint in offset and digital printing. They concluded that for wet-on-wet printing ink trap value is 0.7 and ink sequence has been required to compute the overprint color. The ink sequence is not required and trap value is 1.0 for dry-on-dry or wet-on-dry printing. They have not defined and predicted the color of different tint combinations of any spot color. This study has given better accuracy of color matching between predicted and measured color overprint as decreased the value of ink trapping.

HansjorgKunzlp et al.[9] proposed a method to reduce the measurement time of color patches in newspaper printing they have predicted the color values by neural network from two or three overprint and as well as single primary colors. They obtained more information from less number of color patches with minimum time and maintained the quality of newspaper printing. Reflectance spectrum is predicted from single and overprint primary patches. They derived the colorimetric and densitometry values from predicted spectrum of color patches for newspaper printing. They showed the lesser color difference between measured and predicted data and reduced the number of measurements of printed color patches of newspaper printing.

Mathieu Hébert and Roger Hersch [35] explained the spectral prediction model to develop the color patches with different screen frequencies. With the same support, same ink and same printers, classical or custom clustered-dot or dispersed-dot screens have printed. They defined the prediction accuracy for different models. They showed the variation of model parameters have changed according to the printing setup and so the predictive performance has also changed. Through the experiment they showed that the performance accuracy of the Cellular Yule-Nielsen model is better than other models like Yule-Nielsen model, the Clapper-Yule model and the Low Scattering Clapper-Yule

model under different printing support, different printing process, and the halftone screen frequency. Large set of halftone is required for calibration by using the Cellular Yule-Nielsen model, but fewer halftones are needed for other mentioned models. The Clapper Yule and low scattering Clapper-Yule models is preferred to predict the color of halftones with different illumination or viewing conditions. But when one knows the individual spectrum of solid inks, the inability of their model is to predict the reflectance spectrum of superimposed solid inks.

Mark Shaw et al.[11] evaluated to estimate printer characterization for different substrate. Three model-based methods and one empirical method (PCA) were approached to characterize the printer for a reference substrate and a small number of measurements on the new substrate. They compared these techniques to provide accurate color management for large set of substrates in different printing environment. CMYK Xerox graphic printer and three model-based approaches, like Beer's Law, Kubelka-Munk theory, Neugebauer model and an empirical method (principal component analysis)were used to evaluate the experimental methods. It has shown that the small improvement provided by the Beer's Law, Kubelka-Munk model-based methods based on the spectral data of new substrate. But based on PCA, an empirical method gave significant improvement than the Neugebauer model by direct use of the reference substrate characterization. Properties like fluorescence, optical brightness, gloss, roughness were not discussed in this study to improve the model in characterization accuracy of color management.

Théo Phan Van Song et al. [12] proposed a prediction model to predict reflectance and transmittance of different combinations of ink and substrates. Different inks (dye based, pigment based, etc.) and print support (paper, metallic panel, textile, plastic, etc.) both were characterized as distinct unit. Through the macroscopic measurement of four-flux metric model reflectance and transmittance were jointly computed for the superposition of the stack of inks on the support. The better prediction result was computed by their proposed model for weakly scattering print and diffusing supports.

Dmitry Tarasov et al.[14] proposed a color prediction model to predict colorants from observed spectrum using artificial neural network. They discussed different color prediction models which have been used to predict reflectance spectra from measured colorant and since in CMYK printer generated black channel algorithm reduced the certain amount of other colors in the mixture, so they defined that majority of those models worked with CMY colors instead of CMYK colors. The proposed model used

spectral density values as input to ignore the negative values of reflectance spectra. They showed that the predicted colors are indistinguishable from the original with color difference. They defined that their proposed model increased the color prediction accuracy and also discussed about the simplification of model and implication of the approach into real workflows of printing equipment characterization.

Oleg B. Milder et al.[15] defined a technique to predict spectral reflectance by artificial neural network for characterization and profile making. To reduce the complicacy of different color prediction models they worked with ANN training algorithm to define the applicability of the technique for spectral prediction and color accuracy. Spectral reflection coefficients are transformed into the spectral optical density to remove the negative values of individual spectral components. They predicted the spectral density values using artificial neural network and after prediction the spectral density, spectral reflectance is recalculated from predicted spectral density. The predicted quality is defined by the color difference (Delta E_{94}). They also discussed about the quality of ANN prediction on the base of ink zone (light or shades area).

Francisco Imai et al. [16] developed a multi-channel visible spectrum imaging (MVSI) color reproduction system to analyze the spectral reflectance of image. Using their proposed model, they compared the spectral reflectance of original image and hardcopy image for four color printing and they also defined the color accuracy between the original and printed image using reflectance factor and color difference. They showed the theoretical feasibility of their spectral based imaging system using eigen values and eigen vectors to reconstruct the reflectance spectra. They predicted the reflectance spectra using digital counts from the camera (input device) and printer inverse model and compared with measured spectral reflectance of the printed image (target image). They showed that the colorimetric accuracy has been achieved by their spectral reproduction system and the feasibility of the system.

Kateryna Savchenko et al.[18] defined the degree of emulsification and color stability for offset hybrid inks in the printed copies. They defined the spectral characteristics of real ink and observed that inks are influenced by such factors as coloring agent tone, binding agent, ink additives, whiteness of substrate and many others. They showed that on the amount of UV component, their hybrid model inks varied significantly and by their measurement they have observed that 2% to 10% of UV components are enough to optimal water-based ink and stable the printing process. They defined the reflective curve

of ink and observed that reflective coefficient value for magenta ink is maximum when it has been printed on PVC substrate other than other substrates. They compared the reflectance curve of experimental magenta ink for different substrates (absorbent and non-absorbent substrate) and showed that the reflectance curve of experimental magenta ink is closed to the ideal magenta ink and also higher reflective in red zone for printed on coated paper. But they showed that when 2% or 10% UV components are added to the inks, then the spectral characteristics of ink are been affected by these components and stabilize the color reproduction.

From the above literature of different spectral prediction model and Artificial Neural Network model it can conclude that these models have used to predict reflectance spectrum of two, three or multicolor superimposed color patches mostly for offset or other thermal printers on newspaper, coated paper etc. Few papers were worked on foil substrate and gravure printing machines together. These ANN or other models also applied on printed color patched to predict the reflectance spectrum and colorimetric values from multicolor CMYK color patches for blister foil substrate using different gravure printing machines and helped to identify the original printed sample over scanned reprinted printed samples. So, in this study these methods have been used to authenticate gravure printers output samples on blister foil used as packaging for pharmaceutical products.

2.1.2 Color prediction and characterization

Kiran Deshpande and Phil Green [10] defined a model to predict color from different combinations of spot colors by overprint model. Their prediction model has worked with different dot percentage of color patches in offset printing. They showed that with an increase of dot percentage color differences also increase. That means this model works well in light and mid-tone areas than shadow area. Solid and halftone overprint color can be predicted by their proposed model with good accuracy and lesser number of inputs than other model for offset printing.

Fred Hsu [13] described the effect of dot gain for printer calibration on color matching accuracy. For color matching accuracy he compared the result under two printer conditions, default and 0% dot gain by using two ICC profiles. He verified the spatial uniformity of substrate and printer and also color consistency and color gamut before the

performance test of color matching analysis using cumulative relative distribution curve. He analyzed the color matching by using default setting and 0% dot gain setting of printer. After the analysis of the performance of both settings he concluded that it does not have significant color matching improvement using 0% dot gain as the criterion for device calibration.

Haoxue Liu et al.[20] evaluated the color difference between digital images and printed images. Standard color image data were used as test images to compute the color differences. They defined the color difference between digital and printed using CIELAB, CIEDE2000, CIE94, and CMC methods. They found the threshold to detect the color difference for digital images and as well as for printed images depending on the different color difference methods. For digital cases, RGB image is converted into CIELAB color space and the image is modified with different coefficient of lightness of chroma and also hue angle. Then the modified digital image is transformed back into RGB image to compare it with original input digital image. For printed case, original and modified images are printed with calibrated inkjet printer and then compared between them. Perceptually and computationally color differences are computed between digital and printed images.

Bangyong Sun et al. [25] studied the performance of a polynomial regression method with different parameters over other conversion algorithm such as Neugebauer model, neural network, interpolation method for high color accuracy during color characterization. They showed that mean of color accuracy is reached as the polynomial terms increased. Different color errors were computed with different color connection spaces (CIEXYZ or CIELab). They compared the color errors between CIEXYZ and CIELab color spaces for RGB monitor and also for CMYK printer. They suggested that CIELab color space might be used as device connection space when polynomial less than 10 terms are used for rgb signal processing. CIEXYZ is used when the polynomial terms is between 10 to 20 terms. In CMYK signal processing, CIELab color space is preferred as device connection space for better high accuracy. Sometime before color conversion process, linearization is applied to calibrate the rgb device. So, they compared the effect of linearization on rgb device and showed that the impact of linearization has less for the polynomials of degree greater than or equal to three and linearization is not recommended by them for CMYK printer as decreased the color accuracy during color characterization.

Cheol-Hee Lee et al.[89] proposed a tone reproduction curve method for printer characterization. To compensate the printer non-linearity perceptually they defined the tone reproduction curve method and sigmoid function using neural network. The optimal tone-curve for printing is obtained by adjusting curve of the sigmoid function and this curve is used as input of the neural network to find the CMYKsignal. Samples are observed by observer to check the perceptual brightness. They showed the over compression in mid tone range area by lightness curve and color difference curves of linear CMYKsignals in CIELAB system and also enhanced the overall image contrast on the printing output.

*Abhay Sharma and Xiaoying Rong [19]*have defined the print quality by establishing of standard commercially available in the market for inkjet printers. They have collected different real data from different companies and provided then as input to the ISO committee to develop ISO 15311 standards for flatbed inkjet printing in large format. The obtained data were tested on some parameters such as color management accuracy , print uniformity, color gamut, CMYK cross-hair registration, print speed,repeatability from day to day, ink consumption etc. From these tests, they have identified the specific metrics to validate the international and local programs.

Paul D Fleming and Abhay Sharma[103] have reviewed on the necessity of ICC profiles and color management system to control the consistency and quality of color of images from input to output devices. Input devices like scanner, camera to output devices like display monitor, printers, maintaining of color is very essential part in imaging and printing industry. So, for different devices to obtain the color accuracy, devices are characterized with ICC color profiles using different standard color chart. They have mentioned the importance of ICC profile for gravure printing machines to manage the color quality.

From the previous papers of device characterization it can conclude that characterization is an important method to get accurate result from output devices as original sample. So, printer characterization is required for correct representation of colors with different printing devices to understand the originality. Most of the previous papers focused on offset press or other inkjet printers. But this research work is concentrated on gravure printer characterization using IT8.7/3 color chart (standard color chart) printed on blister foil using different four color gravure printing machines. This color chart has been used

to make a profile for particular printing device and characterize the gravure printer to get consistent output (printed sample) among different gravure machines.

2.1.3 Device Color Calibration

Patrick Jackman et al.[17] proposed a n-algorithm for robust color calibration of device. The proposed algorithm is combined with linear space conversion from device dependent to device independent and advanced multiple regression methodologies. This is possible to predict L*a*b* color data with less than 2.2 color units of error because this value of color difference is not recognized by human eyes. They compared different types of regression model which helped to reduce the error of color calibration. RGB valuesare transformed into a new color space that follows more closely the concept of L*a*b* by expressing brightness as a single variable and expressed color in firstly a variable that runs from green to red and secondly with a variable from blue to yellow, while remaining vectors are inside the RGB color cube. They showed that LASSO regression method is effective to reduce the color calibration error and achieved to an acceptable color difference.

Henry R. Kang et al.[22] defined the neural network application for scanner and printer calibration. Multiple polynomial regressions were defined by them to calibrate scanner and printer. They showed that six terms polynomials and fourteen terms of polynomial are accepted to calibrate the scanner and printer respectively. The distance between calculated and measured color specification in CIEXYZ or CIELAB space is measured by Euclidean distance and to minimize the distance they have showed that the performance of neural network is better than polynomial regression.

*Renée Charrière et al.[*21*]* described the performance of color calibration of an RGB camera. This method was achieved by RGB camera for microscope during strong color distortion. They showed that some color calibration methods are not very robust in the change of illumination. They used halogen lamp as external illuminant for microscopic imaging system because of uniform irradiance on the viewed surface. Their method was used to extract the color information from the distorted microscopic images and calibrate the captured image by white balance, gamma correction, and saturation enhancement. After the preprocessing correction color values are transformed from device dependent to device independent space. They defined the color difference between different spectral values obtained from color chart on different geometries positions. They described that

the choice of illumination and color chart patches are important in microscopic imaging system for better calibration accuracy.

Rui Gong et al.[23] described the calibration of color information between different digital cameras via a device-independent medium, by modified digital inputs. They worked with two digital cameras (test and target camera) by the method of forward and inversed colorimetric characterization respectively under respective lighting condition. Spectral power distribution of lighting condition and spectral reflectance of each color of color checker were used to calculate L*a*b* color coordinate. To keep the same color information for both test and target cameras the captured image is converted from device dependent color space (RGB) to device independent color space (CIELab) by using forward transform matrix and then it is transformed into manipulated digital input (R'G'B') by inverse transform matrix. They showed that the color difference delta E2000 is less by using their proposed method for digital camera calibration.

Zhihong Pan et al.[24] proposed color scanner characterization method for different media types. They characterized acolor scanner with color profile based on specific scan target type. Polynomial regression method was performed for conversion from device dependent color space to device independent color space. They defined acolor scanner characterization method based on three types of media like plain, coated and glossy paper and three different types of printing mechanism which are photographic developing process, inkjet printing and laser printing process. They worked with six different profiles for different media types and printing processes. One and three dimensional look up table was used for each color profile to store the color patches and the accuracy of color transformation is evaluated by color difference. They showed that the color difference is lesser when same color profile is used for inkjet and laser printed sample and for different media types. They also explained that two color profiles are needed, one profile is for halftoning printout targets, i.e. inkjet or laser printout, the other profile is for photographic developing process to minimize the noticeable color difference.

P. Emmel et al. [26] focused on the current approaches of color calibration and also proposed a new approach for calibrated color reproduction. They defined a calibration process for input device (scanner or digital camera), display device (monitor) and output device (printer). For input device tone reproduction curve is used to convert from device RGB to linear RGB and then it is converted to CIE XYZ connection space by using 3x3

linear transformation matrixes. The display calibration model is the inverse of input model. The transformation from the device independent (CIE XYZ) to output space (CMYK) is used to characterize the output device profile. The multi-dimensional look up table is used to contain the values of each channel and table entries are computed by interpolating them in the tetrahedron sample space. Reflection spectrum of halftone sample is used as color prediction model (Neugebauer model). They defined less number of samples. Physical parameters are needed to calibrate the input output devices.

V. Ostromoukhov et al.[27] presented two different table-based approaches for the calibration of desktop scanning and printing devices. The first approach is a process where device-independent CIE-XYZ colorimetric space is used as an intermediate standard space for device calibration from the conversion of RGB space to CMY space. Input-output device is calibrated separately by using tetrahedral interpolation method. In the second approach they described the closed loop approach for the calibration of scanner-printer pair. Their proposed method is used to calibrate the scanner-printer together using single 3D table without intermediate colorimetric space. They showed that when same paper, same spectral characteristics of the primary inks, same halftoning technique are used for test and target sample then the color difference is lesser by using their proposed method than other method.

*Juan Martínez-García [32]*explored a color calibration method for specular materials using microscope under constrained illumination condition. Since conventional color calibration methods do not performed well in general for specular samples, so they experimented on it. Color conversion is done from CIEXYZ color space to CIELAB color space for color calibration. They defined the result after applying their methods on 50 samples, polynomial 2^{nd} order was fitted to their data and computed lesser color difference using $CIEDE_{94}$.

Hui-Liang Shen et al. [28] proposed a characterization method for color scanner. To get high color accuracy they defined the colorimetric and spectral characterization for color scanner using local statistics. The performance of both characterization methods is closely related to the correlation between the device responses and the device-independent measurement data of color samples. Polynomial regression and minimum mean square error methods are used in colorimetric and spectral characterization process. They showed that the mean color difference decreases initially and then steadily

increases for characterization process. Characterization error might be small by using lower number of training samples with local statistics for both colorimetric and spectral characterization process. Acceptable color difference is provided by their defined characterization method but they defined that in terms of performance, the colorimetric characterization is better than the spectral characterization for training samples and the proposed method is limited to single media.

Bangyong Sun et al.[57] introduced a method for color printer calibration based on gamut division algorithm. To adjust the black color (K) for different images they proposed a CMYK separation algorithm method based on gamut division. This method divides the printer gamut into seven sub gamuts according to the K values of sample data. They showed that the color range of sub gamut decreases along the CIEL* coordinate asthe increase of K value. In CIELab color space the color might be contained by more than one sub gamut that means it has several CMYK colors. The method is used to convert the color sample from CIELab color space to CMYK color space and final CMYK is the combination of all CMYKs with black generation coefficient. When some color sample might not be enclosed with one sub gamut then gamut mapping process is used to enclose the color in one sub gamut after conversion. Polynomial regression method is used to convert the color sample from CIELab color space to CMY color space. They showed that, in comparison with other methods (Neugebauer equations and the neural network method), their proposed method produces less color differences.

2.1.4 Spectral and Color Differences Metrics

Francisco H. Imai et al.[43] analyzed and compared various types of metrics for spectral match. They evaluated different metrics such as CIELAB, CIE2000, Spectral error RMS factor, GFC (Goodness fit coefficient), Fairman metamerism index, Viggiano'sperception-reference method, and weighted RMS metrics between pairs of spectra to explore the advantages of each metric for spectrum matching process. They stated from their studies that no metric issuperior to another for spectrum matching purpose. Combinations of metrics could be used to get better spectral matching result.

2.1.5 Color Gamut Differences

Kiran Deshpande et al.[55] defined an approach for matching color gamut of different devices. They compared two color gamut using Gamut Comparison Index (CGI). Intersection and volume of two gamuts are computed by gamut comparison index to

standardize color of source and destination devices. The range of GCI value is from 0 (no match) to 1(exact match). An objective metric is provided by gamut comparison index to compare and quantify the difference between gamut of source and target devices.

Cheol-Hee Lee et al.[56] introduced gamut-based color sampling algorithm to reduce the error in color conversion from device dependent to device independent for printer. They studied the importance of selection of color samples for printer gamut. Three primaries, three secondary and black colors are used to determine the printer gamut volume. For their proposed method, the color sample patches are generated by fixed size of sample points in CIELab color space and by the corresponding CMY control signal. These control signals of uniform color sample points are estimated by multi layered with 3-100-3 structure. The volume of gamut is compared by tetrahedron division method for printer. They compared their proposed method with other color conversion method, such as polynomial regression, neural network and interpolation with three-dimensional lookup tables. They defined that color difference and color error are minimum by using their gamut-based sampling method rather than with other methods. They showed that when regression method is used as color conversion method with their proposed method, gamut-based sampling algorithm then their method effectively performed for printer.

2.2 Literature review on Gravure Printing

2.2.1 Print quality and stability characterization

Akshay V. Joshi and Swati Bandyopadhyay[62] proposed a model to predict print defects or void area on film substrate for gravure printing process. The void area corresponds to the area on substrate where the surrounding is not printed due to the gel in the PVC film by the gravure printing process. The ANOVA was used to study the effect of different parameters of gravure process such as, speed, viscosity, hardness, and line screen frequency on void area. The proposed Regression model is used to predict the void area and to minimize the void area by 65% using their methods for gravure printing process.

Akshay V. Joshi[100] have investigated the printing parameters to identify the printing defects and minimized them for gravure printing process. The effect of different parameters such as, substrate type, ink type, ink viscosity, line screen, printing speed, stylus angle and hardness of impression roller on substrates (PVC and PET-G) has been analyzed using ANOVA. The regression model used to predict the print defect on the

substrates and computed predicted values are close with the press result. For the PVC and PET-G substrates the dot skips were minimized by 90% and 94 % respectively and void area minimized by 90%.

*Mahasweta Mandal and Swati Bandyopadhyay[63]*studied on the properties of water fastness of foil print sample and proposed a kinetic model to evaluate the duration of printed foils when exposed to the water or rain. In the packaging industry to estimate the print stability of package print is important. So, by using their model they predicted accurately the print stability of print on foil substrate against water or rain.

Mahasweta Mandal and Swati Bandyopadhyay[64] defined the print stability using light fastness property of print on blister foil. Different food and medicine packages used blister material to pack products and print on it by gravure printing process. They analyzed the light fastness properties for cyan, magenta, yellow and black inks on blister foil using spectral curves and colorimetric values. The computed color difference ($DeltaE_{00}$) is larger for yellow prints and smaller for black print with time.

Mahasweta Mandal and Swati Bandyopadhyay[65] determined and compared the light fastness properties on plastic films using gravure printers. Due to long time exposure against light, the stability of prints on plastic film is computed using prediction models. They proposed a model with spectrometric values using an Artificial Neural Network (ANN) model to predict the fading rate of prints on the substrate of plastic film. It has been shown that the prediction accuracy is better for ANN model than Regression model for each color (cyan, magenta, yellow, black) printed on plastic film using gravure printers. It might be used for verification and authentication of printed expiry date on package.

Mahasweta Mandal and Swati Bandyopadhyay[66] evaluated the print quality of magenta ink printed on blister foil substrate against water or rain. When the prints are exposed to the water or rain then the waterfastness properties of magenta ink is determined by spectral characteristics and colorimetric values. The durability or stability of magenta prints on blister foil from gravure printers is determined by fading rate with time using an ANN model. Water immersion and water spray methods were applied to compute the waterfastness properties of magenta ink, similar result was also found. The fading rate is significant at blue and red domain of magenta spectrum within visible domain magenta prints. From the comparative study between ANN and regression

model, the optimal result showed that the performance of prediction better for ANN model than Regression model for waterfastness properties on blister foil which might be used for food or medicine packaging for durability purpose.

*Mahasweta Mandal and Swati Bandyopadhyay[67]*proposed a model to predict the fading behavior of packaging prints using an Artificial Neural Network (ANN). Before and after exposure of prints, the spectral curves and colorimetric values of cyan, magenta, yellow and black color on foil substrate printed from gravure printing machine were analyzed and compared with Regression model (assume fast-order kinetic equation). The prediction capability of ANN model is better than Regression model for each color prints on foil from gravure printers which might be used to assess the print stability of food or medicine packages.

Ambrish Pandey et al. [68] analyzed the print quality on different types of substrate in gravure printing. Gravure printing quality is influenced by various factors such as substrate properties, ink chemistry, viscosity, doctor's blade angle, cylinder pressure, rheological behavior, solvent evaporation rate, and drying printing speed etc. They studied of print quality on non-porous substrates, like milky poly, polyester and BOPP. They compared the density and dot gain values for all process colors cyan, magenta, yellow and black for all three types of substrates. They defined that for all substrates the density value of process color black is almost same. The trend of density values for process color C,M,Y are same, and higher for polyester and milky-poly substrates, and almost same density values for BOPP substrate. All process color C, M, Y and K showed almost similar trend from all tint (10%-100%) level with different dot gain values. They showed that process color Y hasleast dot gain while process color K has maximum dot gain value. The print quality is different for different substrates.

Yu-Ju Wu et al.[69] analyzed the quality of gravure spot colors which are used for printing packaging. Ink jet printer is used to analyze the gravure spot colors. Different components like ink jet printer, inks, print media, and printer control software (printer driver and RIP software) with a color management system for inkjet digital proofing is required. They showed that the accuracy of color matching is affected by printer, software, and the choice of substrate. Two RIP software as GMG RIP tends to have better spot color reproduction capability for blue, black, and red spot colors, whereas CGS ORIS RIP has better spot color reproduction capability in yellow spot colors. They defined that the gravure production substrate does not work well in the shadow areas

with the ink jet digital printer because of water based ink and the porosity of substrate. But the result of spot color reproduction is better in highlight and mid-tone zone when the substrate is printed via RIP software. Manufacturer recommended substrate with better spot color reproduction capability for all selected spot colors except for some highly saturated colors. They defined that for using different printer drivers, accurate color prints could be achieved by using RIP software.

2.2.2 Influence of printing parameters

XinguangLv et al.[70] analyzed the variation of gravure printing characterization curve due to different ink cell shapes, ink viscosity, paper types and reducer component. In gravure printing gravure cylinders are engraved with different angles by electro-engraving and the ink of gravure transmits directly from the ink cells to the surfaces of the printing stocks. They stated that the standard ink cells vary with angles from 30^0 to 60^0. They analyzed the gravure characteristics curves for three specific zones including zone of beginning tone, zone of tone jump and zone of density saturation. They stated that in the zone of beginning tone the densities of presswork are close to those papers, due to the small ink cells. Densities of presswork increase with the increased of traverse diagonal length. From the density curve they showed that in the zone of tone jump, tone jump appears, due to the sharp increase of density. In the saturation zone, increases of densities are slowed down with the increase of traverse diagonal length. The printing characteristics curve of ink cell with angle 45^0 (thin ink cell)relatively smooth and minimum contrast. They defined that this ink cells are not suitable for light colors but commonly used for black. Ink cell with angle 45^0 (thick ink cell)used for yellow color and at the begging zone, the ink transfer is poor but ink transfer is better as the increased of density. The transfer of ink cell with an angle of 60° in tinted area is better than theink cell with an angle of 30°. Slope of characteristic curve decrease, the contrast decreases and the color in shaded area become pale, as the increased of proportion of reducer. Contrast varied in different tone of zones for different types of papers in gravure printing.

*J. Kerry [83]*has analyzed different types of aluminum foil for packaging purpose. Different types of aluminum foil can be used, such as metalized film, lamination etc. Since aluminum does not produce any toxic residues or reacted with chemicals, then it is used as packaging material for food, beverage, and pharmaceutical products. The appearance of it is bright, attractive, smooth metallic surface, cleaned and sterilized. The

stability of aluminum against air is better than other materials. Furthermore, the packaged product is prevented with aluminum packaging from oxidation or reaction with any chemicals. For the ability of the crumble it can be used as blister packaging and at low cost aluminum can easily be recycled. The blister pack breaks easily, so this property could be used to pack any medicine and helped to allow the product. The thickness of aluminum foil is less than 150µm. The aluminum is used throughout the packaging industry for numerous beneficial characteristics.

2.2.3 Gravure cylinder printing process

*Donald E. Troxel et al.[71]*described the process of automated engraving of gravure cylinder using a computer-based system. This system was developed and used in a normal production environment. The main focus of this development was to reduce the time and cost required for the gravure cylinder production. The gravure printing quality is maintained by collecting the original copy of image sample from the customer for cylinder engraving. For prepare the input image, low resolution is maintained to engrave the image on gravure cylinder and therefore the gravure output quality is maintained. They showed that 150lines/inch is required to engrave the image per the design and to maintain a betterquality consistency of gravure cylinder.

2.3 Literature review on Anti-Counterfeiting Solutions and Pharmaceutical Packaging

Patel Mitali et al. [85] presented an overview of new packaging technologies and pharmaceutical packages. Technologies, design, marketing, are all included in the packaging area. The pharmaceutical companies mostly rely on their packaging for protection and promotion of their products. They discussed on the good packaging solution and delivered the medicines with the combinations of product quality, tamper evidence, protection, patient comfort and security. For anti-counterfeiting 2-D Barcodes, Mass Encryption Technology, Hologram, Radiofrequency Identification (RFID), technologies developed to identify original product by the packaging. Paper and Board, Rubber Based Components, Glass, Plastic, Films, Foils and Laminations, Metal, Blister Pack, Strip Pack, are latest development of packaging to pack products easily and provide temper resistant and secured packaging.

A. Kailash et al. [84] discussed about the features of anti-counterfeiting and temper evident for pharmaceutical packaging. Medicines ingredients or packaging are

counterfeited and produced duplicate medicines or duplicate packages by counterfeiters. Therefore, different type's health hazard rises in the society. So, to protect medicines from counterfeiters, various technologies have been developed. For tracking purpose Barcodes, Radio frequency identification (RFID), Overt technologies such as Holography, Color shifting security inks and films, Security graphics, Sequential product numbering, On-product numbering and Convert technologies such as Invisible printing, Embedded images, Digital watermarks, Anti-copy or anti scan design, Laser codes have been introduced in the pharmaceutical sector and to identify authentic medicines. But, there is also chance to imitate these technologies and produced duplicate products. Better security is provided by the Convert technologies (invisible to naked eye) than overt technologies (visible to naked eye) in the pharmaceutical industry.

S. Agatonovic-Kustrin and R. Beresford [86] defined the concept of formation and application of an Artificial Neural Network (ANN) in pharmaceutical industry. Large set of data are needed to train the ANN without any knowledge of data source. In the pharmaceutical science an ANN methodology can be applied to analyze the data from drug and dosage form design through bio-pharmacy. The ANN can be used to predict the data and able to reconstructed a pattern which helped to recognize an image. Such ANN methodology could be used as an alternative to conventional response surface methodology, principal component analysis methods in the pharmaceutical science.

Do-Guk Kim et al.[78] proposed a method to identify an original laser printer by using halftone texture fingerprint extraction. To prevent forgery effectively they proposed this method with two procedures like halftone texture fingerprint extraction and correlation-based detection of printer. They used photographed images of printed materials as input image for texture feature extraction in the curve-let transform domain. They defined the method without using any closed lens to capture the printed material and printed it. The RGB image is converted into CMY image and each sub-band is analyzed in the discrete curve-let transform domain. The mean of the absolute coefficient values in the sub-band is higher than 70% of the maximum mean values of all sub-bands. Otherwise, the mean values are set as zero. The halftone texture templates of each CMY color channel is obtained by performing an inverse curve-let transform of the changed values. The most dominant color channel issued to extract the fingerprint from halftone texture template due to different printing angles of each CMY toner in a color laser printer from each other. After extraction the features, the correlation-based detection process is used to

identify the source printer. They analyzed the experimental result and stated that the performance of their proposed method is better than other existing methods. Significant differences are achieved between the methods using scanned image and photographed image.

Soo-Hyeon Lee et al.[79] proposed an algorithm for detecting counterfeited bills due to the scanning and printing technology. They defined a deep learning algorithm which uses a convolution neural network (CNN) model to detect counterfeit bills and their forgery devices. Grey level co-occurrence matrix is used to extract the noise features from printing devices to identify the forgery devices. They analyzed their algorithm using three different laserprinters. The detection accuracy increases with the increase of epochs. They stated that their proposed algorithm could be used to discriminate between original and counterfeit bills and also to identify forgery devices.

*IuliiaTkachenko et al.[80]*analyzed the impact of engraved cylinder for gravure printing on printed patterns for medicine packaging. To identify the original medicine packages and authenticate gravure machines from where the medicine foil is printed, the unique signature of engraved cylinder is used. The impact of signature of engraved cylinder is more than the signature of gravure press on printed pattern on foil substrate. They showed that from chemical etching of engraving process, counterfeiters cannot duplicate the original micro scale shapes which were engraved on cylinder after having original artwork. The analysis was done from the Principal Component Analysis or Non-negative Least Squares with small training samples. Authentic printing cylinder and also the counterfeited blister substrate were identified by using their proposed model.

IuliiaTkachenko et al.[81] proposed a method to authenticate the blister foil packaging using signature of chemical etching engraved printing cylinder. The protection of blister foil packaging is important in the pharmaceutical industry. As text characters are unique, they can be treated as spatial signature of printing cylinder for specific gravure press. To protect all kind of medicines from counterfeiters they used the uniqueness of signature of engraved cylinder and analyzed it based on the Principal Component Analysis or Non-negative Least Squares with classical classifier and small number of training images.

*Das, I et al.[82]*proposed a method to identify the original sample using pattern recognition of printing dot shape. Dots are printed on blister foil using gravure printing

machine. At microscopic scale the printing dot shapes on blister foil substrate are analyzed and used as a fingerprint to detect the duplicate or counterfeited samples.

2.4 Conclusion

Most of the previous papers worked with quality of prints based on the prints of inkjet printers. Previous papers mostly focused on different anti-counterfeit technologies like Hologram, Barcode, Watermark, RFID, etc. to protect the original products(paper documents, bank notes, packages) from counterfeitersand these are accounted with high cost. Few papers studied on the consistency of print quality of gravure printing after scan and print attack, and to authenticate print samples printed by gravure printing machines. In pharmaceutical market, some medicines are packed with blister foil due to the temper evident. In most of the cases, the detail information of product is printed on the blister foil packages used for medicines and it has been printed by gravure printing machines.

In the present work, the focus of the study was on the authentication of gravure printers prints for pharmaceutical packaging with blister foil. Here the main aim of this work is to differentiate between original (print) and duplicate (reprint) samples. If an print (original) gravure output sample has been scanned or captured by digital camera, scanner etc, and produced scanned reprinted samples, then it has been stated that a simple way to identify the original gravure output using some colorimetric values (CIELAB, CIEΔE_{00}), spectral distribution and color gamut of print-reprint color patches on blister foil. Different mathematical models, such as an Artificial Neural Network (ANN), Yule-Nielsen modified Spectral Neugebauer (YNSN) model, have been used in this present research work to predict the reflectance spectrum, CIELAB values of multicolor chart and compared with other gravure print and reprinted samples to get the difference. It can stated that these proposed differences would help to identify an authentic gravure print sample on blister foil substrate (used for medicine packaging). It could be used by manufacturers in pharmaceutical industry to protect their brand quality and their products from counterfeiters.

CHAPTER 3

3. MEDICINE PACKAGINGPRINTING

3.1 Medicine Packaging

Medicine packaging is the process of packages where medicines are kept secured and protected from external damage and as well as biological degradation. In the pharmaceutical industry, different types of materials such as aluminium strips, blister packs, paper/board, plastic films, glass bottles, and ampoules, are used and carefully selected to pack medicines and provide them secure storage until their use. Important information regarding the manufacturing date, expiring date, and ingredients of medicines are needed to disseminate through the medicine packaging. Clear labeling with correct information needs to be disseminated by packages of pharmaceutical products and this information has been printed using different printing processes on packages. This research is mainly focused on the gravure printing process for blister foil medicine packaging.

In the pharmaceutical industry, there are three types of packaging such as primary, secondary, and tertiary.

• *Primary packaging*: The materials used for the primary packaging of medicines are directly in contact with medicines. So, it is very important to choose the proper substrate for medicine packaging which should not interact with the medicines during its entire shelf life. There are different types of medicine packaging like blister packs, strip packaging, ampoules, vial, bottles, and sachet packaging used as primary packaging. The medicine packages are made up of nonreactive substances like PVC and aluminium. Some high-quality materials such as Polyethylene (PE), Polyvinyl Chloride (PVC), Nylon (Polyamide), Polycarbonate, and Polyethylene terephthalate (PET) are used as medicine packaging.

• *Secondary Packaging*: After the process of primary packaging the next layer of packaging is referred to as secondary packaging of pharmaceutical products. The secondary packaging like boxes or cartons is used to pack the medicines and safely transferred them to the destination.

• *Tertiary Packaging*: The main purpose of tertiary packaging is safeguarding the primary and secondary packaging from the external environment. During the storage and transportation, it is very important to protect pharmaceutical products from damage.

3.2 Blister Substrate used for Medicine packaging Printing:

- **Aluminium Blister Foil:**

Secure packaging is an important factor to protect the products from counterfeiters. Aluminium blister foil is suitable for pharmaceutical packaging. To pack any medical and pharmaceutical products such as pills, capsules, and tablets, usually, blister foil is used. The thickness of aluminium foil usually is 25-28micron. Light, gas, and liquid barrier protection properties make the foil material moreuseful for medicine or food packaging. The most important property is the inertness of aluminium foil as a packaging material compared to the other materials. For packaging, aluminium foil does not react with chemicals including medicines, food, and beverages or generate any toxic residues[87]. When the surface of the aluminium is exposed to air, the formation of a thin layer on the metal surface protects the foil material from oxidation. Blister foil is one of the most popular flexible substrates used for medicine and food packaging. Blister packaging forms a bubble or pocket to keep the product safe from external factors such as moisture, humidity, temperature and contamination for an extended period of time. So, due to the resistance factors of blister foil material, it can be used as packaging for pharmaceutical products. Blister foil is tamper evident and it has been used to pack separately each unit of medicines. After using each dosage from the pack, the remaining dosages are sealed intact [87]. If the blister or strip pack materials are tampered, replaced or separated, then they would leave marks of evidence of entry. Any break in the blister packaging, cannot be possible to repair or resealed the tampering place. To provide maximum protection of the product, cold formaluminium blister format is also used for medicine packaging purposes.

Fig3.1: Blister Pack medicines

- **Types of pharmaceutical blister packaging:**
  - ✓ The clear, thermoformed blister foils are used to make cavity and the lid is formed with clear plastic or combination of plastic, paper, or foil.
  - ✓ The other type of medicine blister packaging is formed with foil materials of both sides of packaging.

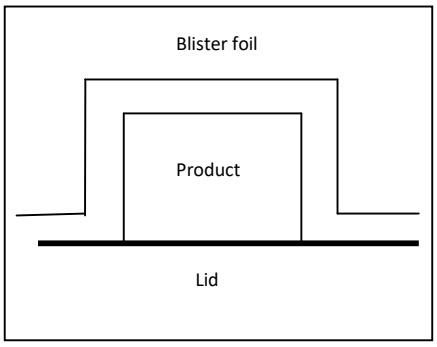

Fig3.2: The basic configuration of blister packaging

- **Pharmaceutical blister Packaging Components:**

  Forming film, lidding material, heat seal coating and printing ink are four basic components of pharmaceutical blister packaging. The selection of proper plastic film or materials is very important for blister packaging. 80% to 85% of blister package is accounted as forming film. Thickness, grade, types, weight, impact resistance, compatibility with product, cost are considered to select the forming film for medicine blister packaging. Aluminium foil, PS(Polystyrene), PVDC(Polyvinylidene chloride), Rigid PVC are example of forming films. Mostly aluminium blister foil has been used as medicine packaging for its high barrier characteristics and chemical resistance.

- ✓ The base structural material on which the final blister packaging has been built is referred as lidding material. It has been selected according to the size, weight, types of medicine and also the design of package to be produced as final blister package. 15% to 20% of total weights of the package are made up with proper lidding material.

- ✓ Heat sealing coating and printability are both essential to produce final medicine package with blister substrate. Due to the different printing processes and use of different inks (water based or solvent based), it is very essential to apply the heat-sealing coating on lidding material to protect the material and printing. To get clarity, good print quality, abrasion resistance of pharmaceutical blister packaging, heat sealing coating has been needed to produce final blister package.

- ✓ By using different printing processes such as letterpress, gravure, flexography, printing inks (cyan, magenta, yellow and black) are used to print the detail information of medicine on substrate. The application of heat-sealing coating on different materials has been resist abrasion, bending, fading the printing and also keep them safe until it is used.

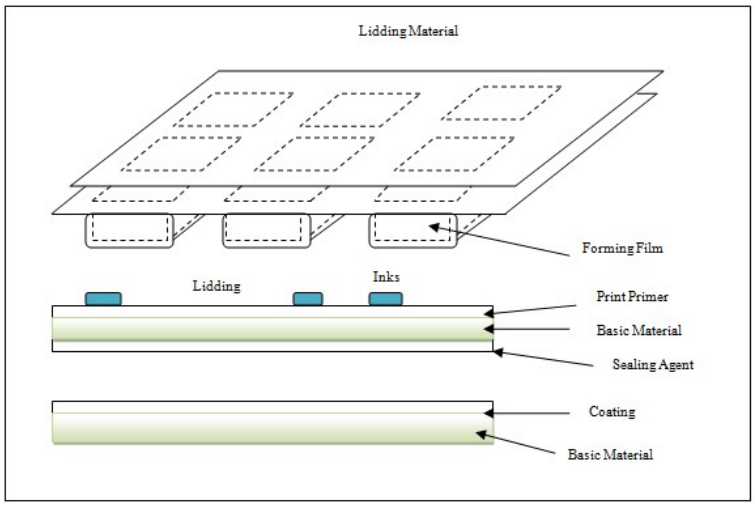

Fig3.3: The basic components of blister packaging

- **Advantages of Blister Packaging:**
  - ✓ **Individual Packaging:**

    Blister packaging is a convenient way of packaging to pack a medicine as an individual dose. The quality of the contents through containment in separate cavities or pockets has been maintained by this type of packaging. If any damage has occurred due to any part of the packaging material then it will not affect the whole packaging.

  - ✓ **Maintaining Product Integrity:**

    According to the sensitivity of the product to external environment like moisture, oxygen, and light the forming films and lidding structures are created to maintain the integrity of products. The packaging components can be laminated with barriers that help to prevent them from penetration of external elements. The product degradation through UV radiation must be blocked for using opaque materials (aluminium) as medicine packaging.

  - ✓ **Tamper Protection:**

    After use of blister packs, it could not be returned to their original form. The lidding to the blister could not be separated for the inherent tamper-evident mechanism of blister packaging without causing visible damage. This type of characteristics of blister packs could help to deter package pilferage in pharmaceuticals Industry.

  - ✓ **Preventing Accidental Drug Misuse:**

    As per the design of blisters and lidding structures, it could not be opened easily without instructions specified by a manufacturer. It is very useful to prevent children, and even seniors, from taking wrong medicine accidentally and the design is referred as child-resistant (CR) packaging.

  - ✓ **Visibility of Product:**

    The design of medicine packaging with blister packs has allowed consumers to see the product through the packaging. In addition, to attract prospective buyers, the lid or backing material is colored and designed.

- ✓ **Minimal Movement Within Packaging:**

  Blister packs can easily be mold according to the shape of the product. A computer-aided machining program has been used to control and creating the mold according to the shape of products (medicines). Therefore, this type of mold can be prepared for minimal movement of product within packaging.

- ➢ **Blister Packaging Process:**

The essential parts and functions of operation of blister foil packaging process include the following steps:

- ✓ The unwinding station: The forming films and the lidding materials are supplied to the unwinding station of the blister packaging machine at corresponding speed.
- ✓ The heating station: The heating station provided the temperature to the forming film and raised the temperature according to the requirement of the materials used for medicine blister packaging.
- ✓ The forming station: The blister cavity is formed in the forming station through compressed air or die plates.
- ✓ The cooling station: After the forming process, the foil is cooled in the cooling station.
- ✓ The feeding machine: The blister cavities are loaded with products (medicines) in the feeding area of the blister packaging machine.
- ✓ The sealing station: When the product is loaded into the cavities then the sealing station heat the lidding material to the forming film for blister packaging.
- ✓ The printing station: The detail information like expiry date, manufacturing date, formulation etc. is printed on substrate in the printing station.
- ✓ The trimming station: In the trimming station blister are cut into specific and individual unit as per requirement.

In this study, blister foil has been used as a substrate for its inertness behavior and print the reference input color chart on it. For the sustainable print on foil substrate, gravure printing machine has been preferable for printing the required artwork on it. The multicolor artwork has been engraved electromechanically on the surface of the gravure cylinder. CMYK foil inks have been used to print the desired color artwork on it with foil ink and the print has not been removed with any external environment

or any chemicals. So, for printing the artwork on blister foil substrate CMYK inks and engraved gravure cylinder are needed for medicine packaging (showed in flow chart). Blister foil has two different sides, one is matt side and another is glossy side. The bright side and the matte side of it are heat seal and print-treat coated respectively.To print the artwork with different gravure printing machines, the same matt side of blister foils has been taken for this experiment. By using three different gravure printers, the consistency of print samples has been examined and analyzed for blister foil substrate used for medicine packaging.

CHAPTER 4

4. GRAVURE PRINTING

A brief description of the gravure printing process has been discussed in this chapter. In this research, a gravure printing machine has been used as an output device to analyze the output sample printed with gravure printers on blister foil substrate.

In the gravure printing process, the image is engraved on the surface of the gravure cylinder in the form of cells and the engraved cylinder has been rotated inside the ink duct for transferring the solvent based ink to the etched cells. The excess ink has been scraped from the surface of the gravure cylinders by using of metal doctors blade [100]. After the transfer of ink to the etched cells, the substrate is passing through the heated drying system to dry the ink by the evaporation and extraction of solvent based ink. To get a succeeding color of printing on substrate, the ink must be dried before printing in the gravure printing process. The gravure printing process is used in the manufacturing of food and non-food packaging, as well as labels, pharmaceutical industry, and transfer printing, and has a variety of further applications in security printing. High print quality and consistency have been achieved by the gravure printing process on the most diverse types of substrates like paper, film, plastic, aluminium foil, coated paper, cellophane, etc. In the gravure process, the printing unit comprises printing cylinders, a doctor blade, an impression roller, and dying system. The engraved gravure cylinders have been used as an image carrier in gravure printing. For long-run durability, gravure printing cylinders can be chromium plated and used repeatedly as per desired for a long time. The Chemical etching, electromechanical engraving, and Laser engraving processes are there to engrave any image on printing cylinders. In the gravure printing process when the printing cylinder rotates on the press, each cylinder catches each color of the gravure ink and all the excess ink has been removed from the surface by doctor blade [75]. So, the inks must be retained on the etched area of the cylinders. When the impression roller has been applied the pressure to the cylinders and substrate, then the inks have been transferred from the intaglio areas to the substrate. The diagram of the printing unit of the gravure process is shown in Fig4.1. The register control system has made it possible to complete the color registration via automatic side and length and therefore it has improved the printing color quality on the substrate. The whole gravure printing cylinder has been used for color separation in industrial rotogravure machines. So for four color gravure printing machines,

four cylinders (Cyan, Magenta, Yellow and Black) have been required to print on the substrate for each new printing job.

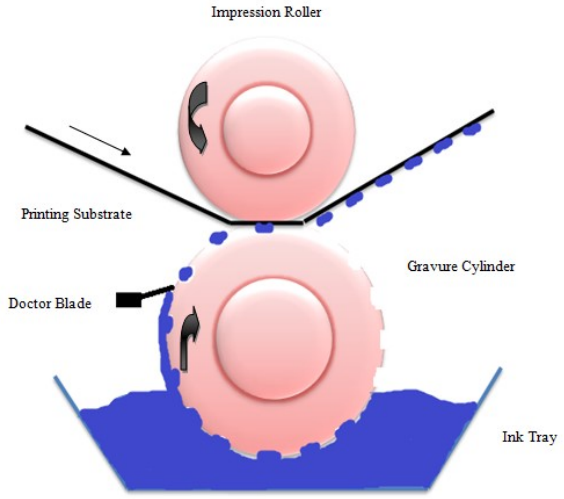

Fig4.1: Printing unit of Gravure Printing Process

The gravure printing process has been provided the color consistency and good printing quality throughout the press run. Several million of printed samples have been produced by the gravure process and so it is a high-volume printing system used in different package printing industries.

4.1 Gravure Cylinder Making:

In the gravure printing process, gravure print samples have been printed from cells or depressions etched in a metal cylinder which are filled with ink and transferred to the substrate. Gravure cylinders are of a metal base that has comprised the engraved image carrier layer. Steel material has mostly been used as a gravure cylinder base and various sizes of cylinders can be used as per the requirement for the gravure printing machines. This steel base, cylindrical, gravure cylinders have been electroplated by copper layer (typically about 2mm) [75]due to the ease enough to electroplate and engrave the image/text. It has provided better predictable, structural, and functional results. After copper plating, polishing has been done to the cylinder base. Then different engraving processes are there such as Chemical etching, Electromechanical engraving process, and Laser engraving process to engrave the image or text on a copper plated cylinder base. A gravure cylinder has a printing design which etched into its nominal surface of broken up into tiny cells. These etched cells of the gravure cylinder rotated into the ink tray and then filled up with

ink. A doctor blade has been used to remove the excess ink from the surface of the cylinder and leave the ink which has been held by the etched cells. As per the requirement of printing the color tone is varied depending on the depth of cells etched on the gravure cylinder. When the cylinder has been pressed by the impression cylinder against the surface of the substrate, then the ink in the cells has been transferred to the surface of the substrate and thus created the printed impression on it. The cylinder has continuously delivered a consistent print quality during the print run and during the repeated print run provided the same ink, same illuminant condition and same gravure cylinder used.

- ***Chemical Etching Engraving Process:*** The Chemical etching engraving process has been developed in the last nineteen century and this process is an indirect exposure of a screen and a positive to a gelatin-coated paper (carbon tissue), or direct exposure of screened images onto a photosensitive coating on the copper cylinder [81,76]. The dilutions of ferric chloride which is helped to etch with differing depths. The carbon tissue has been dependent upon the series of dilutions of ferric chloride for the etching process. Spray etching has been utilized with a constant dilution of ferric chloride for the direct etching process. Although direct exposure increased predictability, a subsequent revision of the cylinder has been required for the uneven etching. The main disadvantage of the chemical etching process is its relatively low uniformity and its inability to pattern small features consistently, due to non-uniformities from the exposure and development steps.

- ***Electromechanical Engraving Process:***Electromechanical engraving process has been used an electronically controlled diamond stylus to cut the cells into the surface of the gravure cylinder as per the printing design. In prepress, the desired data is recorded and the engraving process is controlled directly with the recorded data. At a constant surface speed (approx. 1m/s) the gravure printing cylinder is rotated during the time of the engraving process [75]. Desired line screens and angles have been reproduced by a constant engraving head frequency and variable surface and traverse speeds of the Electromechanical engraving process. The frequency (speed) of Engraving Heads increased over the years and, currently, engraving speeds of 24 kHz are achievable [73]. With different depths, a copper layer of the cylinder has been penetrated by a diamond-stylus to produce cells according to the desired artwork. The development of the engravings has

improved the fidelity and printing process. In this process, different cell depths have been made using different stylus angles. Color density has been made by selecting a more acute engraving stylus angle and the fine screen has been selected for detail that could be made to deliver the cell volume. The engraving head has controlled by the computer and moved across and around the cylinder to engraved cells with varying depths. The cell wall thickness is varied. At 100% depth with a tiny cell wall, the diamond-shaped cells are interlocked with those of the rows on either side of it, and the cells are much reduced in size with higher space between cell walls at 10% depth size of cells.

- ***Laser Engraving Process:*** Laser engraving of gravure cylinders is the latest and most exciting development introduced by the Daetwyler laser engraving system [80]. In the gravure market the Daetwyler Direct Laser System (DLS), is now being used for printing purposes. The galvanic plating of the zinc/chrome layers meets the surface structure and durability requirements for the gravure process. The engraving frequency is at 70kHz for the laser engraving process [75]. The cylinder is engraved by the laser beam and the performance of gravure printing has been enhanced by the Laser engraving process. The advantage of laser processes is the speed. The cells have been made at 30,000 cells per second. The 40-inch wide, 30-inch circumference cylinder would only take about 13 minutes [71]. The Laser engraved cell has several advantages over the Electromechanical engraving process in that the inverted pyramid has been delivered by a diamond stylus, and ink has to be delivered by the laser engraving process more uniformly and economically but the process is still very expensive. The light-sensitive black layer is used for the indirect laser engraving process and is applied onto the surface of the copper layer of the gravure cylinder for engraving purposes [75].
  In gravure cylinder manufacturing companies, hollow cylinders are firstly washed and removed from the chrome or copper layers to reuse the cylinders for engraving and printing purposes. After removing the previously used layers, a thin layer of chrome has been applied to the engraved copper-based cylinder to protect the etched copper surface from the doctor blade during the printing process. Gravure cylinders are extremely long-lasting. After printing, the cylinder can be re-used, but not before the chrome and copper layers are removed and re-plated showed in Fig4.2. The chrome and copper could be removed and the steel base

reused when the cylinder has no longer required for the printing process and the final electromechanically engravedgravure cylinders according to the image for four colors (cyan, magenta, yellow and black) has been shown in Fig4.3.

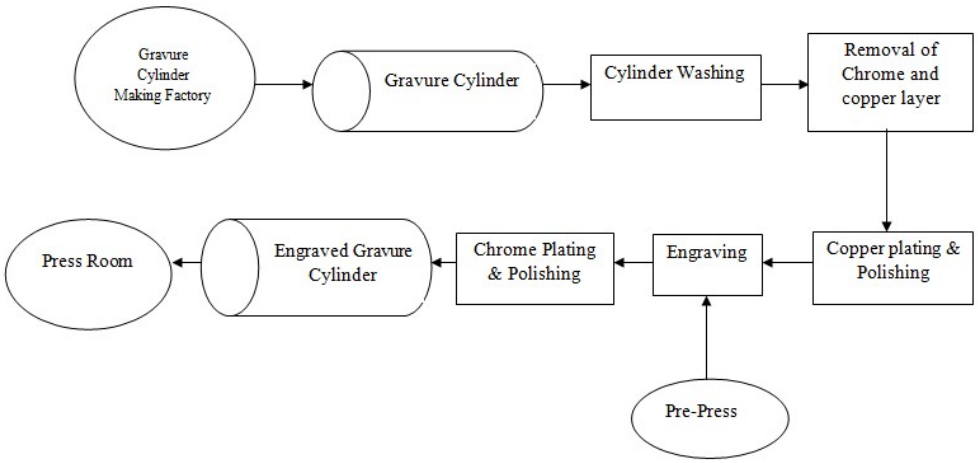

Fig4.2: Flow Chart of Gravure Cylinder Making

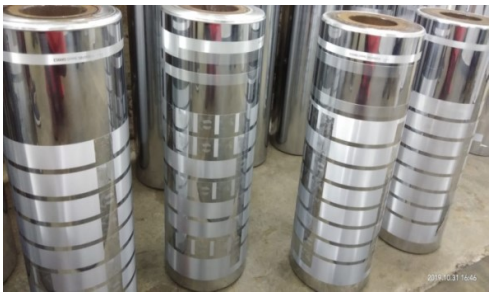

Fig4.3:Gravure Cylinder after engraving

4.2 The Gravure Printing Unit:

In a gravure press each unit consists of an ink duct where engraved gravure printing cylinder is immerged inside the solvent-based ink trays and rotates when the machine is run to begin the printing process. The excess ink has been scraped by the metal doctor blade from the surface of the cylinder. The printing substrate is fed between the engraved printing cylinder and the rubber roller impression cylinder. The in-line arrangement has been followed for the gravure printing process and each unit in the press is installed horizontally. When the gravure machine runs, the solvents are extracted and evaporated through the drying system associated with each printing unit. Different sizes of printing cylinders are used to

print the required dimension of samples and the repeatability of using an engraved printing cylinder has a certain limit.

- **Gravure Cylinder:**
  A gravure cylinder is a form of a tube made of steel and copper plated to engrave the desired artwork on it. Different sizes of printing cylinders are used to print the desired dimension of the image. These cylinders can be reused after removing the previous chrome and copper layers and re-plating and polishing again.

- **Impression Roller:**
  A rubber covering (12-20mm thick) with a steel core (inside) is used as an impression roller in the gravure printing machine [105]. Its primary function of it is to press the printing substrate against the printing cylinder. In gravure machines, to produce the impression on the substrate from engraved printing cylinders the pressure is applied between the impression roller and cylinder during the printing process.

- **Inking System:**
  The enclosed design of the tray is used to hold the solvent-based gravure ink and the printing cylinder is poured into the ink. The ink is supplied to the cylinder from the ink tray and each engraved cell is filled up with supplied ink.

- **Doctor Blade:**
  A metal blade is made from high-carbon flexible steel and generally, its thickness of it is 0.15-0.25 mm [105]. The function of it is to remove excess ink from the surface of the printing cylinder and affect the printing result. The angle of the doctor blade is one of the influencing factors for printing the output sample because it angles with the printing cylinder and helps to remove the excess ink. Otherwise the ink is left in the cells of the printing cylinder. A blunt doctor blade cannot provide a clean wipe of the non-image area.

- **Drying System:**
  When the ink is applied to the substrate the drying chamber is used to dry the printed ink before it has been reached to the next printing unit. The drier capacity is based on the desired printing speed, ink type, and volume of the printing samples. Normally a cold air blower is used as a drying system for some low-speed gravure machines. Sometimes, a steam heated drier may be used to heat the

substrate and then cool it by using a cold chill roller on the exit part of the machine.

Fig4.4: 4-Colors(CMYK) gravure printing machine

4.2.1 Engraved Cell Parameters:

- **Cell Geometry:**

  To hold the ink and its release directly on the surface of the printing substrate is based on the varying cell shape, cell depth, cell size, cell wall, cell opening, screen ruling, etc. For ink transfer, these cell parameters are played a vital role [100,106].

- **Cell Shape:**

  The gravure cells are engraved with a diamond stylus for electromechanical engraving process. These electronic engraved cells have given different shapes with various cell angles (Ranges from 30^{o} to 60^{o}). For 30^{o} cell angle, the vertical width is less than the horizontal width of cell. For 45^{o} cell angle, the vertical width is equal to the horizontal width of cell and vertical width is greater than the horizontal width of the cell for 60^{o} cell angle. The cell angles and formed cell shapes are shown in Fig4.5.

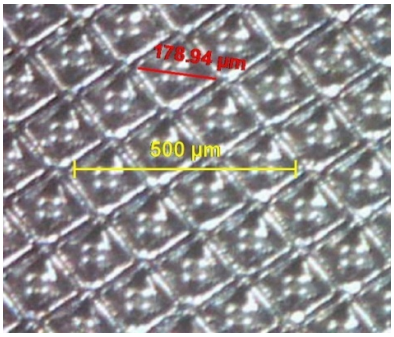

Fig4.5 Pyramidal Electronic Engraved Cell angles [100]

- **Cell Depth:**

  As per the requirement, the desired artwork has been engraved with a diamond stylus on the gravure cylinder for Electromechanical engraving process. Different depth of angle shaped is engraved with stylus angle as shown in Fig4.6. If the stylus angle is decreased, then cell depth is increased. The engraved cell has provided a pyramidal shape approximately.

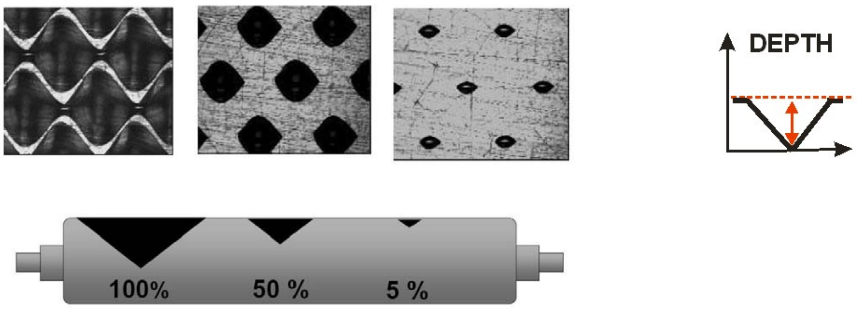

Fig4.6: Varying Cell Depth for Highlight, Middle-tone and Shadow[100]

- **Cell Size:**

  Cell size has a great impact on ink release. For the variation of cell size from 0% to 100%, the range of tonal gradation has been achieved to get different combinations of image on printing substrate. The reduced ink is transferred from a cell with a shallower depth of engraved cell. For full coverage of dots the spacing is lower between dots and spacing is higher between dots for halftone coverage. When the dot coverage is decreased then the spacing is higher.

- **Cell Wall:**

  Each cell is separated from the other by a border known as a wall (Fig4.7). The cell wall is non-printing area and the excess ink is removed from the wall by doctor blade. The shadow or dark region is formed with cells that are surrounded by a thin cell wall and highlighted regions are formed with thick cell walls. The thickness of the cell wall is from 5 to 10 microns.

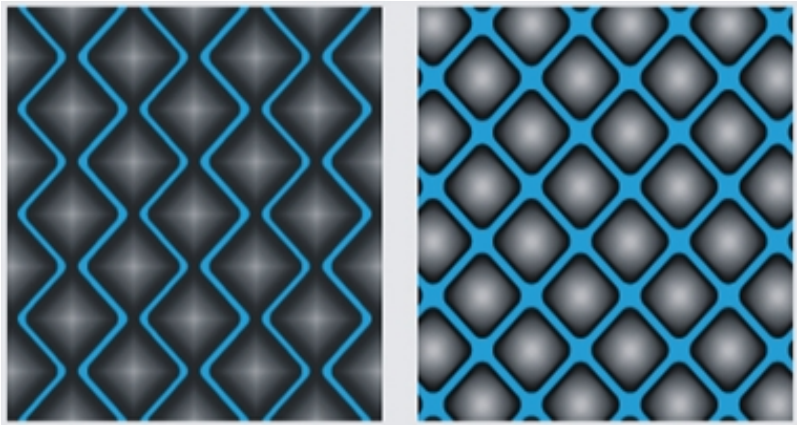

Fig 4.7 Thin cell walls for shadows (L) and thick cell walls for highlights (R)[100]

4.2.2 Gravure Ink

After the printing process, the visual impact is provided by the ink to the substrate. Depending on the printing process, substrates, color, cost, and properties of ink such as gloss, heat and chemical resistance, the composition of ink significantly differs. Colorant, varnish, and additives are the main constituent elements of printing ink. The colorants are insoluble organic and inorganic pigments; soluble dyes and ink are colored with the colorant. Varnish is also known as a vehicle and this liquid part is used as transport medium to carry the pigment and bind them to the substrate.

For the gravure process, the engraved cells are filled with ink and must be transferred the fluid to the substrate for smooth printing. The gravure ink comprises the properties of faster drying, low viscosity, and highly volatile solvent. The gravure ink is generally classified into solvent-based and water-based ink[105]. In gravure printing technology, solvent-based volatile inks have been used to print on substrate. Liquid ink has been needed for gravure printing and so the image forming cells of the gravure cylinders could be filled

by it at high speed. The printing ink must flow quickly from engraved cells on the gravure cylinder into the printing base when the cylinder has contacted the base using the impression cylinder. The distribution of gravure inks has been determined by their Rheological properties in the printing unit and transfer printing ink on the printing base. The non-Newtonian flow behavior of gravure ink is used for the gravure printing process. If the viscosity is too high then transferring the ink has created difficulty to flow into and out of the cells on the cylinder. So, the ink is very low viscosity ink, and the chemical composition of the inks simpler which permitted greater variation in principle due to the direct ink transfer. In this research, four colors such as Cyan(C),Magenta(M),Yellow(Y) and Black(K) inks have been used to print the artwork on blister foil using four color gravure printing machines.

To print any color artwork on foil substrate, gravure printing machines are preferable to get high-quality printing which has been used for packaging purposes. The print could not be removed from the aluminium foil substrate (blister foil) by any external environment.

- **Properties of Ink:**

  Viscosity: Low viscosity of ink has been required for the gravure printing process. During the evaporation process, the gravure ink has been dried with a highly volatile solvent and chemical changes and oxidation have not happened during the drying process. This characteristic is essential to determine the performance of gravure ink. The general range of viscosity of the ink is 15 to 25s Zahn Cup No.2 at 25^{o}C, depending on the condition of the press and also some factors such as evaporation speed, rheological characteristics, the shape of cell depth, nature of substrate, parameters of print design are influenced the viscosity of the ink [105].

  Dispersion: By several manufacturing techniques have been used to produce gravure ink with the process of dispersion of pigments into a vehicle. The selection of dispersion technique [105] has been dependent on the end-use properties and requirements of ink.

  Drying Speed: For the gravure printing process the drying speed is high to dry the ink and therefore some printing faults (trapping, block in the reels, dot skips, etc.) are avoided for high drying speed of gravure printing machines. On the other hand, printability, screening, etc. problems have been occurred due

to the very fast drying speed. The drying speed of ink is dependent on the resin system, selected solvents, and substrates.

Ink Temperature: The solvent-ink consumption is dependent on the ink temperature and the ink consumption is high according to the ink temperature. As increased of ink temperature, some factors such as gloss, and reflection density have decreased. To provide good quality prints the ink temperature has been controlled in the printing press.

- **Raw materials of Ink:**

  The gravure inks contain some major components such as colorant, resins, solvents, and additives. The required color is specified for ink by colorant or pigments. To hold all ingredients together, resins are used as printing ink raw material. The liquid part of the ink has provided the fluidity of ink and it must be any solvent or water depending upon the printing process. To provide specific performance to the printing ink, some additives are added to the ink during the manufacturing of ink[105].

  Pigments: In printing ink formulation, colorants or pigments are a very important ingredient of ink as they provide the visual identity of ink and print it on the substrate according to the requirement. Pigments are basically multi-molecule crystalline structures in different sizes, insoluble, organic, or inorganic particles that are carried through the vehicle and transferred to the substrates. Natural or organic pigments are formed from plants or animals with synthetic formation while inorganic pigments are made from metals or chemicals without the presence of carbon and the size of synthetic particles (organic) is lesser compared to inorganic particles. For organic pigments, the maximum pigmentation at press viscosity is unlikely to exceed 15% and the higher pigmentation level for inorganic pigments (mostly titanium dioxide) is 25%-35%. The color has been given through ink to a substrate by the reflective characteristics of pigments. The specific wavelength of white light has been absorbed by pigments of ink and reflected in the other wavelength. Not only the color of ink, but it also provided specific properties like opacity, transparency, specific gravity, and resistance to heat, water, chemicals, or oils.

  - Color strength: The color strength of pigments has been dependent on the distribution of pigment particles on the substrate and so it must be proportional

to the surface area of pigments present. By any dispersion technique, for varying sizes of pigment particles, it has been defined that the small size of pigment particles has given maximum color strength as narrow distribution of particles.

- Gloss: The reflection of light from the surface has been measured to define the gloss. When the angles of an incident of light and reflection of light are equal then the gloss is high. The choice of raw materials, drying mechanism and dispersion process of the printing press are very much important to achieve a level of gloss on a print.
- Refractive Index: For two mediums, the relationship between incident light and refractive light is defined as the Refractive index and it also described the transparency of ink. It is a constant but depends on the color of the light.
- Resistance: For the chemical nature of pigments, the resistance property is very much needed to protect the print from the external environment like heat, water, soap, alkali, etc.
    - ✓ Lightfastness: Lightfastness is an important resistance property of ink and if it is high then the color became fade after printing on substrate and sometime the color can be disappeared from the substrate. So the lightfastness property has been dependent on the factors such as colorant, exposure time, exposure condition, ink film thickness, substrate etc.
    - ✓ Heat Resistance: For heat-sealing operation, heat resistance property of ink is required to protect the print from the decomposition of colorant of ink thermally. Due to the heat resistance property, the strength of printed color has been maintained on the substrate.
    - ✓ Abrasion Resistance: It is dependent on the dispersion method used for making ink. The abrasion resistance is less for use of better dispersion method. It is also dependent on the ratio of the vehicle to the colorant of printing ink.
    - ✓ Product resistance: Pigments, resins have different resistance properties. For many applications the printing ink has been contacted with the packaging product, so the selection of ink is very much

important to avoid some chemical reaction, odour, etc. with the product.

- ✓ Weathering: When the print sample has been exposed to the weather, then to protect the printed color from external environment, the weathering test with actual condition must be needed during the manufacturing of ink.

Resin: Various types of resins are used as a carrier in printing ink. To bind all ingredients all together in ink, resins are used and form a uniform layer on the substrate. The quality of the selected connection material (resin) is directly affecting the performance of ink during printing. The selection of resins is dependent on the product's use, the function of substrate, type of diluents, printing factors, and cost. The essential properties like adequate adhesion, good solubility in a solvent, gloss, pigment wetting, toughness, and flexibility of final printed material.

Solvent: The largest part of the liquid ink volume (almost 70%) is occupied by solvent. During the manufacturing of ink, the solvent is added to the solvent-based and water-based ink. The solvent has been selected on the base of the resin system, substrate, press speed, cost, and specific ink properties required for a better quality of printing. In the gravure printing process, the solvents in the ink are important properties for using it as a lubrication property to reduce wear on gravure cylinders during printing.

Additives: To enhance the characteristics of ink properties, additives are added to the ink. This solid and liquid material named additives provided some essential properties such as stability, the addition of chemical plasticizing resins, and prevention of ink drying in the engraved cell during printing, adhesion, and flexibility on the substrate used for printing.

- **Foil Ink for Gravure Printing Process:**

  In the packaging industry, aluminium foil is widely used for food and pharmaceutical products. Many colors printed on foil substrate are transparent due to the metallic luster of the aluminum foil. When virgin foil is exposed to the atmosphere, it has been prevented from oxidation by using a primer on the

surface of the foil. Due to the thinnest gauges some hazards have been build-up of ink for a specific area of foil. The use of pigmented nitrocellulose chips and occasionally lightfast dyes is responsible to obtain the transparency of aluminium foil and it is also used for colorant. In the vehicle system the colorant is selected for foil with low odor characteristics.

Foil Laminate: After lamination of foil, it is coated with a wash of nitrocellulose, shellac or vinyl to prevent them from oxidation or any other chemical reaction. If the virgin foil is laminated with hot melt wax, the reasonable degree of heat resistance has been required after lamination of foil.

For the gravure printing process with foil ink, the nitrocellulose is modified with melamine resin to achieve the adhesion and heat seal resistant properties of foil. The adhesion to the surface can be achieved with plasticized nitrocellulose modified with polyvinyl butyral. The formulation of ink for Aluminium foil is nitrocellulose pigmented chip(60%), Maleic or Shellac Varnish, Alcohol-soluble polyamide, Nitrocellulose Varnish, Micronized polyethylene wax, Plasticizer, n-propyl alcohol, Ethanol n-propyl Acetate. Foil Ink Formulation [105]:

50% of pigmented nitrocellulose chip	25.0
Polyvinyl butyral	4.0
Dioctyl phthalate	4.0
Wax dispersion	3.0
Ethanol	54.0
Isopropyl acetate	10.0
	100.0

Therefore, for medicine printing packaging, the gravure printing process and foil ink are very much needful to get color printing stability on blister foil substrate. Unlike other printing processes, the printed part on blister foil could not be easily removed by any external environment (air, water, heat, etc.). Because of the good print stability on blister foil, the medicine packages can easily be stored in the deep freezer or any other place according to the requirement. Therefore, in this study, to determine the stability or consistency of color of the print and reprint samples different gravure printing process has been used with two different gravure engraved cylinders.

CHAPTER 5

5. CONSISTENCY OF GRAVUREPRINTING PARAMETERS

In the printing industry, for a variety of printing processes, inks, printing parameters, and different types of substrates, getting the same consistency of prints is a real challenge. For product packaging, printing and designing parts are very important to achieve consistent and desired product packaging as per the requirement. For design and brand value color is a key element. It is always a difficult task to keep the same color consistent during printing. Different printing processes offset, flexography, gravure, letterpress, digital, and screen, all process can use different types of inks and colorants; some are water-based, some are petroleum-based, the curing methods and gloss levels, various types material of substrates, all variables that could given an impact to the final color area printed on the substrate.

In this study, the color consistency has been analyzed for the gravure printing process using specific ink and blister foil substrate used for Medicine packaging. The gravure printing process has been taken as an output device to print the color chart on blister foil.

5.1 Color Consistency

Color is the key element of visual experience. For printing and packaging, maintaining color throughout the process is required to get the same result as the original. Since the consistency of color plays a vital role in brand identification and also the protection of the product, so the variation of color of printed samples on a selective substrate has affected the brand value. Consumers could be lost their trust in the brand for the inconsistency of printed color on product packaging and query about the authenticity of the product. So, maintaining color consistency is very important to get accurate results during printing processes and for using various printing devices and substrates it is very much needed to ensure that the colors will remain unchanged when the device is changed and maintain color consistency. CMYK color stands for cyan (C), magenta (M), yellow (Y), and black (K for "key"), processed colors have been used for printing on the desired substrate. Different properties such as colorimetric values, spectral reflectance of color, color difference, and color gamut have been used to analyze the color consistency on the substrate after printing using CMYK colors for specific ink

substrate combinations and printing processes. Using the same printing process, same ink, substrate, and same printing parameters under standard illuminant conditions if the color variation has happened then the variation between colors may be used to identify the authentic printed sample in medicine printing packaging.

In this study, the Gravure printing process has been taken as an output device to print the color chart on blister foil. To authenticate product packaging by manufacturer, color can be used at low cost instead of using existing high-cost methods such as Hologram, RFID, Barcode, etc. For medicine packaging, authentication is much more important to identify original medicines product packaging. By using the color properties while a desired image or text is printed on blister foil substrate used for medicine packaging with the gravure printer process, counterfeited samples could be identified. After printing, using some color properties like Spectral reflectance, CIELAB, Color gamut, and Color difference of C(Cyan), M(Magenta), Y(Yellow), and K(Black)on aluminium foil substrate with gravure printing process has been discussed in this study to authenticate the medicine packaging after print scan attack. Devices are calibrated using the standard color chart and generate profiles to achieve color consistency[32,33].

5.2 Color Basics:

Color is associated with the electromagnetic radiation of a specific range of wavelength visible to the human eye. Color is based on the stimulus based on the visible response to the light. Visible radiation is a form of energy, when electron moved from higher energy level to lower energy level, then light is formed and energy is emitted by this process. In terms of hue, lightness, saturation the color of an object is defined. Hue refers to the dominant wavelength, lightness is measured with the amount of white or black mixed with the color and saturation refers to the color intensity. The Range of all colors are represented by a structured system called color models such as RGB, CMYK, LAB, HSV etc. and these color models are used to specify and represent the color spaces for different application.

- RGB Color Space: The additive colors are red, green, and blue also known as RGB. The mixing two or more colored light sources together has created the Additive colors. The RGB color system is an example of additive color, as

it combines the primary colors, red, green and blue, in various degrees to create a variety of different colors. When all three of the colors are combined with their equal proportion, they have produced pure white. However, when they are combined to the lowest degree, they have produced black. The RGB color system is device independent color system. Different digital devices have used RGB additive color system for display and each element of these colors are known as ‘pixel’. These pixels are formed to create pictures on LCD,LED screens etc.

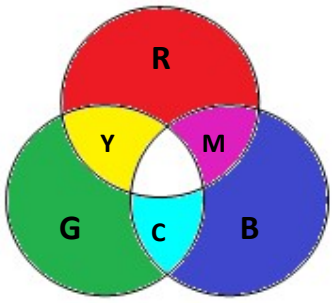

Fig5.1.RGB Color Model

- CMYK Color Model: In the subtractive color model, cyan, magenta, and yellow are used. CMYK color stands for cyan (C), magenta (M), yellow (Y), and black (K for "key"), and the subtractive color model is used by commercial printing equipment to create full-color graphics and images. In the subtractive color model, color is produced using reflected light when color pigments are added to a substrate used for printing. The printing process involves combining varying amounts of the different color inks to produce a full spectrum of color. The production of primary colors of red, green, and blue from subtractive colors has been shown in Fig5.2. CMYKcolor is also called process color, or four-color process and it is mostlyused for printing purposes.

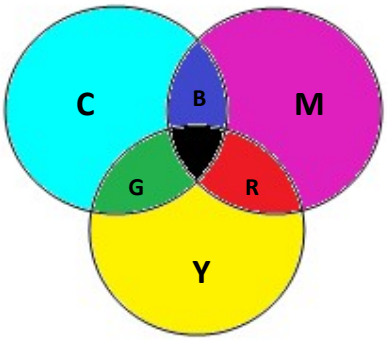

Fig 5.2: CMYK Color Model

- L*a*b* Color Model: The standard color system CIELAB or CIEL* a* b* has been used as a device-independent color space to easily visualize the color of the object with human vision [50]. The three-dimensional CIELAB color space has quantified by three axes: L* axis has defined the lightness values and the a* and b* defined the chromaticity coordinates. On the CIELAB color space diagram, the L* is represented on a vertical axis with values from 0 (black) to 100 (white). The red and green components are represented on the* axis as +a* (positive) and -a* (negative) values, respectively. The b* value is indicated the yellow-blue component of a color, where +b* (positive) and -b* (negative) indicate yellow and blue values, respectively. The plane is neutral or achromatic at the center. The L*a*b* color space diagram is shown below (Fig5.3).

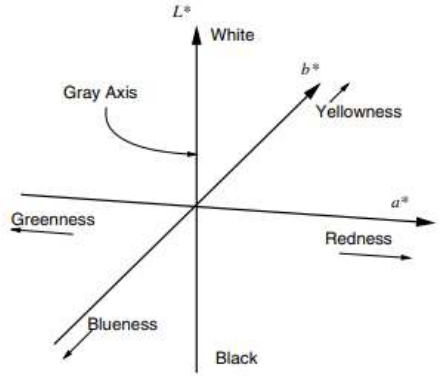

Fig 5.3: Three dimensional CIELAB color coordinates [101]

The equations of the CIELAB color coordinates has been computed from the tristimulus values X, Y and Z is expressed below with Eq.(5.1),(5.2),(5.3). The distance from the central axis represented as the chroma (C*), or saturation of

the color. The angle on the chromaticity axes has represented as the hue (h^o). Chroma and hue are defined by the equations of Eq. (5.4) & Eq.(5.5) [101].

$$L^* = 116\,(Y/Yn)^{1/3} - 16 \quad \text{Eq. (5.1)}$$

$$a^* = 500\,[(X/Xn)^{1/3} - (Y/Yn)^{1/3}] \quad \text{Eq. (5.2)}$$

$$b^* = 200\,[(Y/Yn)^{(1/3)} - (Z/Zn)^{1/3}] \quad \text{Eq. (5.3)}$$

$$C^* = \sqrt{a^{*2} + b^{*2}} \quad \text{Eq. (5.4)}$$

$$h^* = \tan^{-1}(b*/a*) \quad \text{Eq. (5.5)}$$

In this study, colorimetric properties of the color of the L*a*b* values of CMYK color patches of IT8.7/3 standard color chart [52] have been collected from printed (Original) and scanned reprinted (counterfeited) samples for different gravure printers and also predicted the L*a*b* values for different color patches of the color chart by using a mathematical model (Artificial Neural Network). Color difference (ΔE_{00}) [49,51,52] has been used to compute the difference between original and scanned reprinted samples and established a range to identify the authentic samples using color values.

HSV Color Model: The HSV is represented Hue (H), Saturation(S) and V(Value) of color in HSV color space. The hexagon boundary (Fig 5.4) is denoted as hues and the range of hue angle is from 0^o (red) to 360^o. Saturation is measured along the horizontal axis and it varies from 0 to 1. Value is measured along the vertical axis of the HSV color space and range of it from 0 to 1. Pure hue is represented at V is 1 and S is 1 and white point represented as V is 1 and S is 0 in HSV color space.

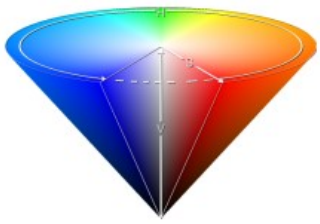

Fig 5.4: HSV Color Model[106]

5.2.1 The CIE Color System

In 1931 The CIE (Commission Internationaled'Eclairage or International Commission on Illumination) is a scientific body formed by color scientists and they introduced the element of standardization of source and fundamental color knowledge. The system has provided the methodology to derive numbers that provide a measure of a color seen under a standard source of illumination by a standard observer. The CIE system has initiated several standardized color ordering systems based on objectively specifying the light source, the observer, and the relationship among colors, or color matching [43,43].

5.2.2 Spectral Reflectance

Color is the human eye's perception of reflected radiation in the visible region of the electromagnetic spectrum (400–700 nm)[35,46]. At each wavelength, the spectral reflectance function of a surface specifies the fraction of the illumination reflected by it. Light reflected from the material is collected in an integration sphere, normalized to the source light of the reflectance, and calibrated with the measurement of a pure white standard (100% reflection) and a black box (zero reflection) over the entire wavelength spectrum of visible light (Fig5.5). For material studies, the spectral range of near-ultraviolet and near-infrared are (250–400 nm) and (700–850 nm) respectively. The nature reflectance spectrum of color is unique and used as a signature to a specific color. In this study, within the visible range of color the spectral signature of single processed printing inks such as cyan (C), magenta(M), yellow(Y), and black(K) or their combinations of color have been used as unique properties of color to authenticate original (printed) sample from scanned reprinted samples.

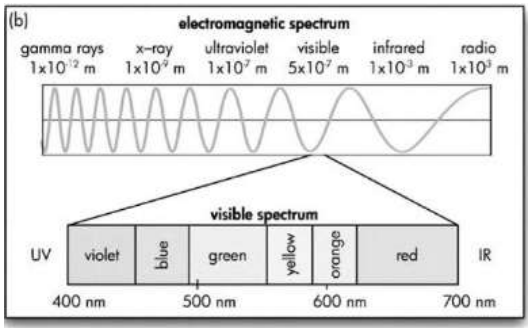

Fig 5.5: Reflectance Spectrum within visible range [107]

5.2.3 Color Gamut

A color gamut is a range of a set of colors that can generate by a particular device. For printers, displays, or other imaging devices the color gamut can generate under specific illuminant conditions. It is usually illustrated by the enclosed area of primary colors (RGB) or processed colors (CMY) on the Chromaticity diagram for a particular device. The appearance of color is dependent on the same perceptual attributes such as hue, chroma, and lightness which affect the color gamut. To reproduce the desired color appearance for a specific device, the color gamut helps to define it. By using an ICC color profile color gamut can be generated for particular devices in an XYZ or L*a*b* color space. Gamut mapping is a technique used to transform them from one color space to another and reproduced the required color appearance of a device.

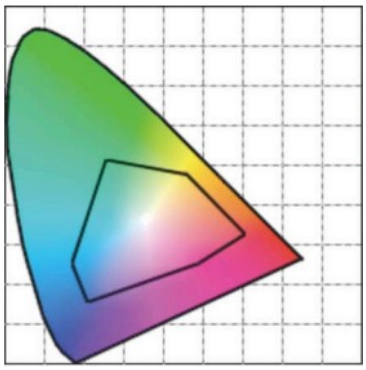

Fig5.6: Color Gamut[103]

5.2.4 Color Difference

The color difference is the difference between two colors designated as two points in the Lab color space. The color difference has been computed by using the values of the L, a, and b attributes of two colors in the Lab color space and it has been denoted as Delta E or ΔE [51,52]. In this research, the color difference formula CIEΔE2000 (ΔE_{00}) has been used to assess if color differences between original (print) and tested (scanned reprint) are noticeable, or not, for a human observer and also defined a range of print and reprint samples to identify the difference between print (original)-scanned reprinted samples. ΔE_{00} is the color difference between two points in Lab three-dimensional spaces and it is defined as follows by Eq.(5.6)[101]:

$$\Delta E_{00} = \sqrt{\left(\frac{\Delta L'}{k_L S_L}\right)^2 + \left(\frac{\Delta C'}{k_C S_C}\right)^2 + \left(\frac{\Delta H'}{k_H S_H}\right)^2 + R_T \frac{\Delta C'}{k_C S_C}\frac{\Delta H'}{k_H S_H}} \quad \text{Eq. (5.6)}$$

Where,

$$\Delta L' = L_2^* - L_1^*$$

$$\bar{L} = \frac{L_1^* + L_2^*}{2} \bar{C} = \frac{C_1^* + C_2^*}{2}$$

$$a_1' = a_1^* + \frac{a_1^*}{2}\left(1 - \sqrt{\frac{\bar{C}^7}{\bar{C}^7 + C^{25}}}\right) a_2' = a_2^* + \frac{a_2^*}{2}\left(1 - \sqrt{\frac{\bar{C}^7}{\bar{C}^7 + C^{25}}}\right)$$

$$\bar{C}' = \frac{C_1' + C_2'}{2} \Delta C' = C_2' - C_1' \text{where,} C_1' = \sqrt{a_1' + b_1^*} C_2' = \sqrt{a_2' + b_2^*}$$

$$h_1' = \text{atan2}(b_1^*, a_1') \bmod 360° \quad h_2' = \text{atan2}(b_2^*, a_2') \bmod 360°$$

$$\Delta h' = \begin{cases} h_2' - h_1' & |h_1' - h_2'| \le 180° \\ h_2' - h_1' + 360° & |h_1' - h_2'| > 180°, h_2' \le h_1' \\ h_2' - h_1' - 360° & |h_1' - h_2'| > 180°, h_2' > h_1' \end{cases}$$

$$\Delta H' = 2\sqrt{C_1' C_2'} \sin(\Delta h/2) \; \bar{H}' = \begin{cases} (h_1' + h_2' + 360°)/2, & |h_1' - h_2'| > 180° \\ (h_1' + h_2')/2, & |h_1' - h_2'| \le 180° \end{cases}$$

$$T = 1 - 0.17\cos(\bar{H}' - 30°) + 0.24\cos(2\bar{H}') + 0.32\cos(3\bar{H}' + 6°) - 0.20\cos(4\bar{H}' - 63°)$$

$$S_L = 1 + \frac{0.015(\bar{L} - 50)^2}{\sqrt{20 + (\bar{L} - 50)^2}} \qquad S_C = 1 + 0.045\bar{C}' S_H = 1 + 0.015\bar{C}' T$$

$$R_T = -2\sqrt{\frac{\bar{C}^7}{\bar{C}^7 + C^{25}}} sin\left[60°.exp\left(-\left[\frac{\bar{H}' - 275°}{25°}\right]^2\right)\right]$$

5.2.5 Calibration & Characterization:

Device calibration is the process of maintaining the device with a fixed known characteristic color response and is a precursor to characterization[43]. Calibration of any device is necessary to guarantee the stability of systems over time and to ensure similar behavior between different display brands and types.

The characterization process derives the relationship between device-dependent and device-independent color representations for a calibrated device[108]. Correct representation of colors is very important with different devices to understand the originality. So, for printing devices color consistency of printed substrates is more desirable and the requirement is fulfilled by the device profile characterization [101]. The use of ICC profiles for achieving good color reproduction across devices with various standard color charts is possible to achieve good color reproducibility. The profile is used to communicate color between the display and other devices. In this study, IT8.7/3 standard color chart has been used to characterize and make a profile of gravure printing machines for blister foil substrate.

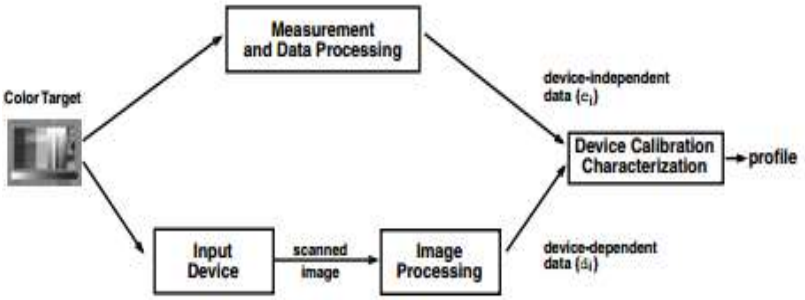

Fig 5.7: Workflow diagram of Device Characterization [101]

- **Profile Making**

  A profile is a set of data that describes the properties of a color space, the range of colors (gamut) that a monitor can display or a printer can output. To reproduce the color in the same manner from scanner to monitor to printer devices, a profile is necessary for each device[101]. An ICC device profile is the collection of information related to the transformation of color data between device data and device-independent CIE-based color space. For printing, press profiling is a very important task to get similar or accurate output printed results as an original sample on a specific substrate. Different standard color charts are used to make a profile for a particular device. In this study, the IT8.7/3 color chart has been used to make a profile of the gravure printer's output sample for blister foil substrate. GretagmacbethSpectroscan device has been used to collect reflectance spectrum and L*a*b* values of printed color patches on blister foil substrate from print and reprint samples

for different dot areas. ProfileMaker software has been used to make profiles for printed output samples of gravure printing machines.

5.2.6 The Neugebauer Equation &Yule-Nielsen modified Model

- **Neugebauer model**

In color halftone prints, the halftone process inks have been deposited according to a specific binary pattern whose surface coverage has determined the amount of ink per unit area and therefore the spectral absorbance of the print surface of the substrate. Many different phenomena have influenced the reflection spectrum of a color halftone patch printed on different substrates. The prediction of color from the halftone separations is not trivial, but the Neugebauer model [49] has been successfully used mostly to predict the color of halftone systems for various printing systems on paper. This predictive model has also been used in different substrates [87]. In the halftone, process ink is deposited on the substrate in small dots. The halftone color patches have been formed by a different number of elementary colors, denoted with "colorants" but also often called "Neugebauer primaries" [6,31], are limited and depend only on the number of inks.

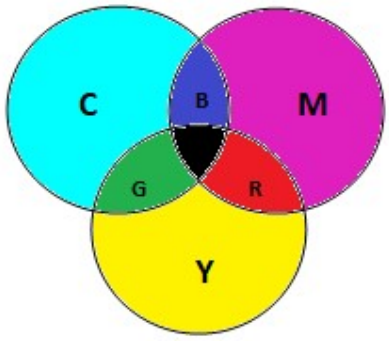

Fig5.8:Schematic illustration of the generation of eight Neugebauer Primaries from the overlap of Cyan, Magenta, and Yellow halftone dots

It predicts reflectance spectrum of the area covered by multiple colorants by summing the reflection spectra of its individual colorants weighted by their fractional area coverage's a_i:

$$R'_{\lambda} = \sum a_i R_{\lambda,i,max} \qquad \text{Eq. (5.7)}$$

Where, the number of colorants, i, equals 2^k, where k is the number of inks, thus in the case of a four-ink printer, the summation is done over i=16 Neugebauer primaries [34] (bare substrate plus inks with all possible overlaps), a_i is the fractional area coverage of each spectral reflectance of each i^{th} primary at full colorant coverage $R_{\lambda,i,\ max}$. For example,CMY halftones contain $2^3 = 8$ colorants. For respective coverage of c, m, y patches, when cyan, magenta, and yellow inks have been used to print independently, then the Demichel equations have used to get the fractional area coverage of the individual colorants [29]. The Demichel equation has given the respective surface coverage of the colorants as a function of the surface coverage of the individual inks. White, cyan, magenta, yellow, red (magenta + yellow), green (yellow + cyan), blue (cyan + magenta), and black (cyan +magenta+ yellow) are respective fractional areas of colorants and they are defined below respectively.

white: $a_w = (1-c).\ (1-m).(1-y)$

cyan: $a_c = c.\ (1-m).\ (1-y)$

magenta: $a_m = (1-c).\ m.\ (1-y)$

yellow: $a_y = (1-c).\ (1-m).\ y$

red: $a_r = (1-c).\ m.\ y$

green: $a_g = c.\ (1-m).\ y$

blue: $a_b = c\ .m\ .\ (1-y)$

black: $a_k = c.m.y$

The Neugebauer is a relatively straightforward multi-color extension of the monochrome Murray-Davies. It also makes the same assumptions as the Murray-Davis model [29].The Neugebauer model is a generalization of the Murray-Davis model whose colorants are formed by only one ink and the paper white.

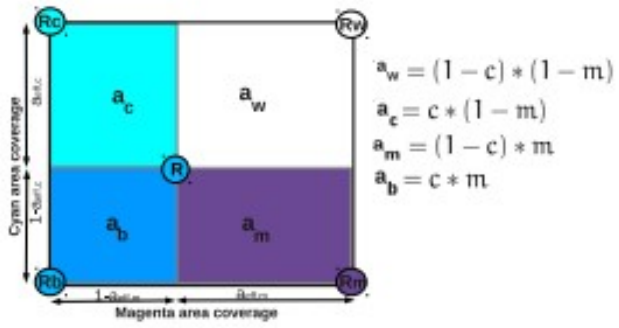

Fig5.9: Demichel equations for 2 inks: cyan (c) and magenta (m)

5.2.7Spectral Neugebauer model

The simplest model considers that the contribution of each colorant i to the spectral reflectance R(λ) of a halftone color is proportional to its surface coverage a_j:

$$R(\lambda) = \sum_{j=1}^{2^k} a_j R_j(\lambda) \qquad \text{Eq.(5.8)}$$

Where k denotes the number of primary inks and Rj(λ) is the individual spectral reflectance of colorant i printed alone on the surface of the substrate. This model is accurate only if the majority of photons traverse [34] at most one colorant along their path across the print. If specular reflectors (mirrors, non-scattering films) have been used to print the halftone color patches then the transition of photons from one colorant to another one is limited and with the help of printing support photons are scattered. In some special cases, these conditions have been satisfied. Most of the time, it has been difficult to predict accurate data with the linear equation (5.8).

5.2.8Yule-Nielsen modified spectral Neugebauer model

Yule-Nielsen spectral modified Neugebauer has been applied the Yule-Nielsen relationship to the spectral Neugebauer equations resulting in the Yule-Nielsen modified Spectral Neugebauer model (YNSN). The reflectance of halftones and the reflectance of the individual solid colorants have established the non-linear relationship by Yule and Nielsen and this empirical law has been used

as a correction of the Neugebauer equation by Viggiano [38,45]. The equation (5.9) showed the Yule-Nielsen modified spectral Neugebauer equation and the following is:

$$R(\lambda) = \left[\sum_{j=1}^{2^k} a_j R_j^{1/n}(\lambda)\right]^n \quad \text{Eq.(5.9)}$$

where n is a scalar parameter related to the proportion of photon paths going through different colorant areas. It has dependent on the printing support, the halftone screen frequency, and the absorbance of the inks. In equation (Eq.5.9), n=1 [38] has also been assumed to compute the Neugebauer equation. The n value has been increased when the halftone screen frequency increased, or equivalently, the size of the ink dots has been decreased, or when the printing support is more scattering. It has been experimentally determined when calibrating the model. Since the spectral reflectance of the colorants has been measured at certain illumination and observation geometries, the spectral reflectance of halftones predicted by equation (5.9) has been valid for the same illumination and observation geometries.

5.3 Consistency/Inconsistency of Prints and Reprints

In this research, to authenticate the original print sample of blister foil Yule-Nielsen spectral modified Neugebauer has been applied with different dot areas of the printed color chart and computed the spectral difference between predicted and measured reflectance spectrums of different colors combined color patches such as red (magenta & yellow), green (cyan & yellow) and blue (cyan & magenta) for different gravure printing machines. The range has been established between print and reprinted samples to identify the authentic print sample.

To identify original gravure output prints using different color combination patches with YNSN model.

In this study, different combinations (two colors) of dots of cyan(C), magenta (M), and yellow(Y) colors, from patches of reference IT8.7/3 color chart were used to analyze and detect authentic print samples and reprint samples using gravure printing machines. For these experiment different combinations of color, patches have been taken to predict the reflectance spectrum of these patches using solid

color patches. For example, the double color combination of cyan and magenta creates a red(CM), cyan and yellow creates a green(CY),and magenta and yellow creates a blue(CM). The following color patches,A5(MY100%),A17(MY20%),A12(MY40%),A10(MY70%),A6(CY100%), A9(CY70%),A14 (CY40%), A16(CY20%), A4(CM100%), A15(CM20%), A11(CM40%) and A8(CM70%) have been taken from reference color chart for this experiment to predict spectral data from CMYK values and to detect original printed samples from reprints. By using solid (100%) and 20%, 40%, and 70% of cyan, magenta, and yellow, red, green, and blue color patches of the color chart, spectral data were predicted. The prediction was completed by Yule-Nielsen spectral modified Neugebauer prediction model(YNSN). To predict the color accurately due to the scattering of light on the substrate the Yule-Nielson transform has been applied to the Spectral Neugebauer equation, where n is the real number and dependent on the scattering strength of the printed substrate. In this study, it has been assumed that n=1 to predict the reflectance spectrum of color patches from the YNSN prediction model. Within the visible domain (from 380nm to 730 nm), reflected spectrums were computed for different dot combinations. The comparison was done between predicted spectrum, measured spectrum of printed and reprinted samples to analyze the accuracy of the spectral distribution. From the experiment it has been observed that for a double color combination patches (CM/CY/MY), the predicted reflectance spectrums are mostly matched with the reflectance spectrum of printed samples than the reprinted samples. So, this difference could be used to identify an original print sample among print reprint samples. Comparison between authentic and scanned reprinted samples has been done by using color differences. Ranges of color differences were empirically estimated to define both print and reprint samples. In this experiment, if the range is from 0.0 to 9.0 (approx.) then it can be considered an authentic print sample and when the range is from 11.0 to 26.0 (approx..) then it can be considered a reprint sample. In this study, we analyzed the prediction accuracy with print samples using graphical representation and showed that it is difficult to match the reflected spectrum of authentic print samples with a reflected spectrum of scanned reprinted samples within the visible range. It is therefore difficult for counterfeiters to predict and duplicate printed samples on blister foil by the gravure printing machine. In gravure printing process, to imitate printed samples on blister foil, the gravure cylinder must be duplicated by

counterfeiters. In this study the same procedure has been followed to produce counterfeited samples. From the experiments it has been observed from the obtained result that the color differences are lesser when samples are printed with different printers using the same cylinders, but on the other hand, color differences are higher when samples are printed with different cylinders using the same gravure printer.

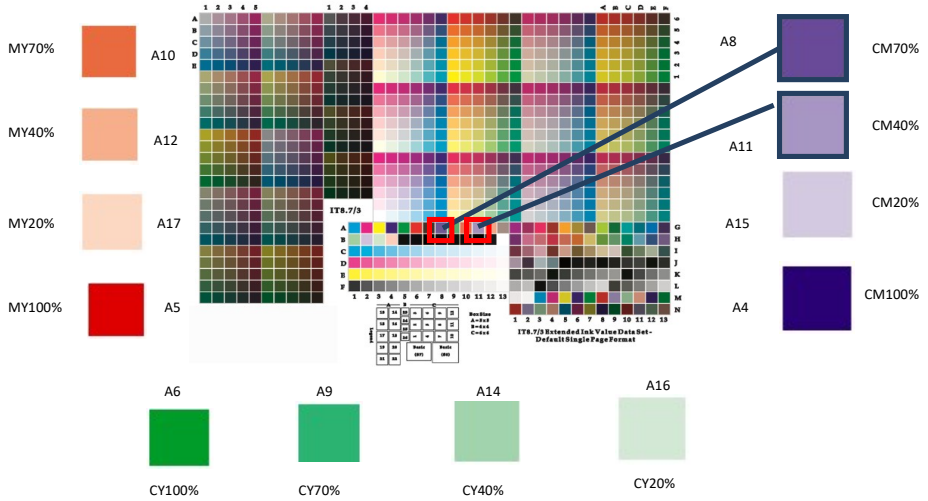

Fig.5.10: Selection of color patches from IT8.7/3 color chart

From the above experiments with different procedures, it has been observed that if gravure printers are used to print with different color combinations on blister foil substrate, then it would be difficult to duplicate the print samples, but possible to determine an original gravure print (output) sample among different print or reprint(duplicate) samples. Experimental results have been discussed in Chapter 8.

Chapter 6

6. EXPERIMENTAL PROCEDURE

This chapter presents the collection of data and experimental procedure developed during this study. Different methods relevant to this research are discussed in this chapter.

6.1 Procedure

6.1.1 Source of Data

In this study, the artwork IT8.7/3 color chart has been engraved as reference image on a gravure cylinder using an Electro-mechanical engraved process. In general, test targets represent known values from an object or in a digital file. Different test target charts have been used to compare the relationship between source target and their reproduction by any device. For printer profiling IT8.7/3 color chart (Fig6.1) has been used and this color chart has total 928 color patches with different color combinations of cyan (C), magenta (M), yellow (Y), and black (k). Various combinations of color patches of cyan, magenta, yellow and black of the color chart were used as input data and used to compute the profiles (as output data)for three different gravure printers(output devices).

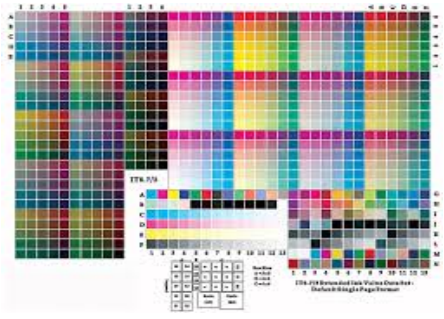

Fig 6.1: IT8.7/3 Color Chart

6.1.2 Cylinder Making

- Pre-Press: After selection of color chart (IT 8.7/3), it has been given to the pre-press section of the gravure cylinder making company before engraved the desired image. In this study, ArtPro software has been used to set the desired

parameters (Table 6.1). During the time of cylinder engraving process different parameters such as line per inch (LPI), cell angles, stylus angles (cell depth) etc. have been required to engrave electromechanically the desired image into four cylinders for cyan, magenta, yellow and black colors.

Table 6.1: Set parameters for engraving on gravure cylinder

Color	LPI	Angle	Stylus	Channel	Wall	Volume
Magenta	150	30^o	130	35	8	12.2bcm
Cyan	150	60^o	110	4	8	12.0bcm
Yellow	150	45^o	130	27	8	12.4bcm
Black	150	30^o	110	30	8	11.2bcm

- Gravure Cylinder Engraving**:** In this research, 300x534 mm cylinder size has been maintained for four colors (c, m, y, k) engraving process. Theelectromechanicalengraving process has been used to engrave the color chart according to the set parameters using HELL engraving machine (Fig 6.2).

Fig 6.2: Gravure Cylinder Making by electromechanical engraving process

6.1.3 Gravure Printing

✓ Gravure Printers: In this experiment three different gravure printing machines has been taken to analyze the output samples collected from gravure printing machines. These three gravure printing machines have been represented in this study as P1, P2 and P3. During the printing some parameters such as cylinder speed, gravure printing speed, doctor blade angle and pressure, pressure of

rubber roller, humidity 75%, temperature 31^{o}C, have been maintained to get consistent print output from different gravure printing machines (Table 6.2).

Table 6.2: Set parameters for Gravure printing

Parameters	**Specification**
Cylinder size	300X534 mm
Gravure speed	17MPM
Angle of doctor blade	30^{o}
pressure of rubber roller:	2.5 kg/cm^{2} (for each unit)
pressure of doctor's blade:	1kg/cm^{2} (for each unit)

- ✓ Substrate: In this study, blister foil has been used as substrate to get print the desired multicolor chart on it using three gravure machines. It has two sides, matte and glossy side. Print has been done on matte side of blister foil and the thickness of the blister foil is 25µ. To analyze the color consistency of blister foil used for medicine packaging. In Fig 6.3 has shown the gravure printing on blister foil using engraved gravure cylinder with one color.

Fig 6.3: Engraved Gravure Cylinder during printing on blister foil

- ✓ Printing Ink: To print the image on blister, foil ink has been used and the specification of foil inks for cyan, magenta, yellow and black colors has been given in Table 6.3. The samples have been printed with foil ink.

Table 6.3: Set parameters for foil ink

SAP Code	Description	Viscosity, Ford Cup 4@30°C	Unit of Measure
120000003599	DK0020-AL GV FOIL YELLOW	28 ± 5	Second
120000003587	DK0020-AL GV NEW MAGENTA	32 ± 5	Second
120000003560	DK0020-GR. FOIL BLUE	27 ± 5	Second
120000003538	DK0020-GR. FOIL BLACK	25 ± 5	Second

The same conditions have been maintained for the printing and reprinting process to neglect the effect of change of these parameters on the results. The reference image has been printed on blister foils with CMYK colors, next a set of samples (i.e. of color patches) from the printed image were analyzed.For a single patch, the measurement has been taken five times and ten separate sheets were used to check the repeatability.Different input device (digital camera, mobile camera, scanner) were used to capture an image of each print sample selected, for the three different gravure printing machines used, to get the color values of the reprint samples. Within controlled illumination condition, the printed samplehas captured with different cameras like Sony alpha 350, Vivo 1716, Redmi 7 mobile cameras in a lighting booth. ISO color light meter has been used during calibration. Exposure has done inside viewing booth. In this experiment, the color temperature of the illuminant has been set to 6500k, the focal length to 3.5F, the exposure time to 1s, the ISO (International Organization for Standardization) to 400, to capture the print image and to produce the scanned-reprint patch samples. For all kinds of measurements an organization sets international standard and this ISO standard has been referred here the camera's sensitivity to light whenever an image is captured by the camera.

After capturing the image, output data were converted from RGB mode to CMYK mode. The color channels were separated for prepress process in order to engrave color data on another set of 4 gravure cylinders (C,M,Y,K) using an electro-mechanical engraved process for reprint. The set of printed and reprinted samples have beenmeasured and analyzed using the GretagmacbethSpectroscan[53]. The spectrum and CIE L*a*b* values of the samples have been obtained using this device. The framework of the experimental procedure has been illustrated in Fig.6.4. It also

used to make a color profile for each print and reprint samples using ProfileMaker software and analyze the difference of color gamut between them.

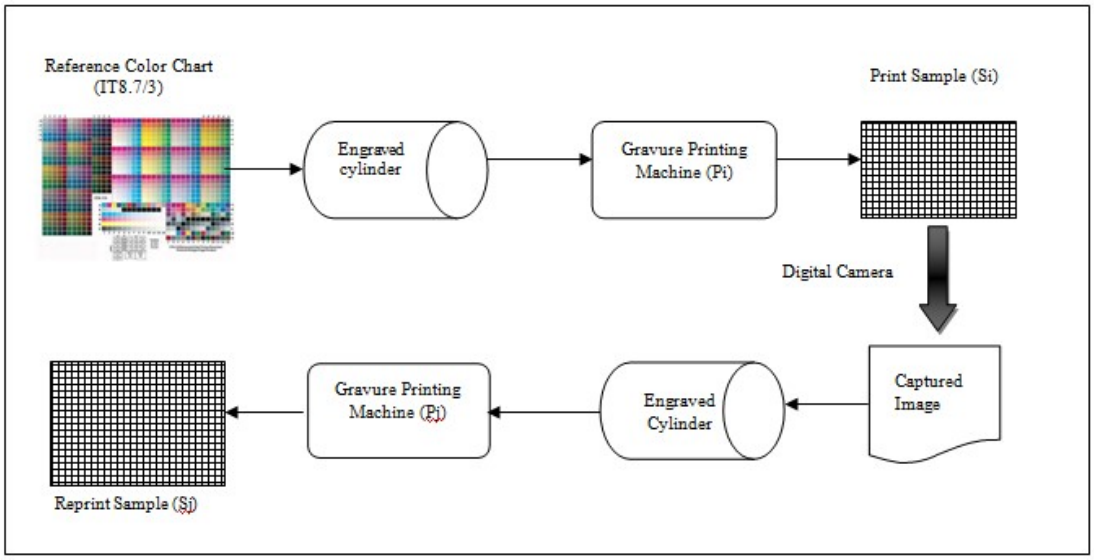

Fig.6.4: Flow chart diagram of the experimental process

- Camera Calibration: Camera calibration has been needed to determine the relationship between the input scene radiance and response of camera. Under known illumination condition a target has been illuminated with known spectral reflectance measurements of gray patches. The luminance Y has been obtained from the illuminant and reflectance data for each patch. The opto-electronic conversion function has been generated using the correspondence between input luminance Y and output RGB display.

6.2 Measurement

6.2.1GretagmacbethSpectroscan Device:

A spectrophotometer instrument has been used for measuring the spectral reflectance of the object. To calibrate printers or scanners, the spectrophotometer has been used and helps to characterize the different devices. It has its own light source that illuminates the samples under measurement. The lens of spectrophotometer has been used to collimate the light and decomposed into its spectrum. The spectrum of measured samples is recorded with a single or multiple detectors. The output of detectors is usually interpolated to determine the final spectrum reflectance of sample and grating is used for diffraction of element at given wavelength. Even though CCD

(Charge Couple Device) has a linear relationship, but the spectral sensitivity is not uniform. So, linear response has been needed to simplify the calibration procedure. The geometries of sensors or illuminant combinations are different for different application. For color imaging application, in the spectrophotometer device the sensors are setup with $45^o/0^o$ condition to record the reflectance spectrum of color samples (Fig.6.5).

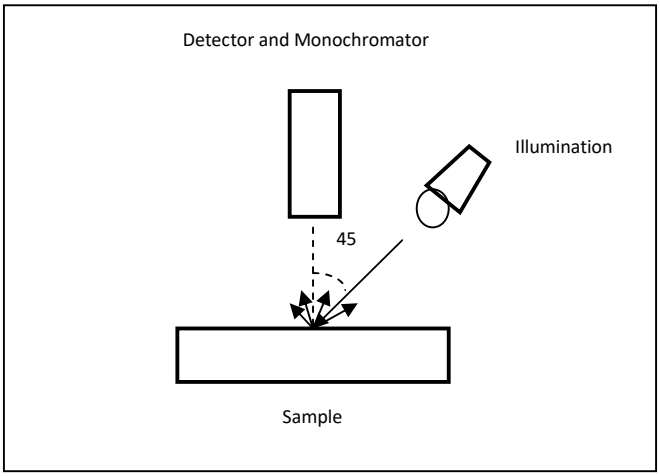

Fig.6.5: 45^o-0^o measurement geometry

Most of the spectrophotometers have reported the reflectance spectrum of color samples with higher intervals at 5nm, 10 nm, 20 nm. In color application, spectrophotometer mostly work with spectrum range of 380-780nm. The measurement of spectrophotometer has been shown in Fig6.6. The ratio of the two spectral measurements has been obtained by the spectrophotometer system. The known or standard reflectance and test sample reflectance are represented as $r_s(\lambda)$ and $r_o(\lambda)$. The SPD of light source is denoted as $I(\lambda)$. At $\Delta\lambda$ wavelength intervals, If the spectrophotometer device has made a K measurements in the region of $[\lambda_0,\lambda_0+(K-1)\Delta\lambda]$ and d_k is denoted as spectral sensitivity of detector at $(\lambda_0+ k\Delta\lambda)$, then the spectral measurement of reference sample $[m_s(k)]$ and test sample $[m_o(k)]$ are represented by the given Eq. (6.1) and (6.2).

$$m_s(k) = d_k I((\lambda_0+ k\Delta\lambda)\, r_s\, (\lambda_0+ k\Delta\lambda), \quad 0 \le k \le (K-1) \qquad \text{Eq. (6.1)}$$

$$m_0(k) = d_k I((\lambda_0+ k\Delta\lambda)\, r_0\, (\lambda_0+ k\Delta\lambda), \quad 0 \le k \le (K-1) \qquad \text{Eq. (6.2)}$$

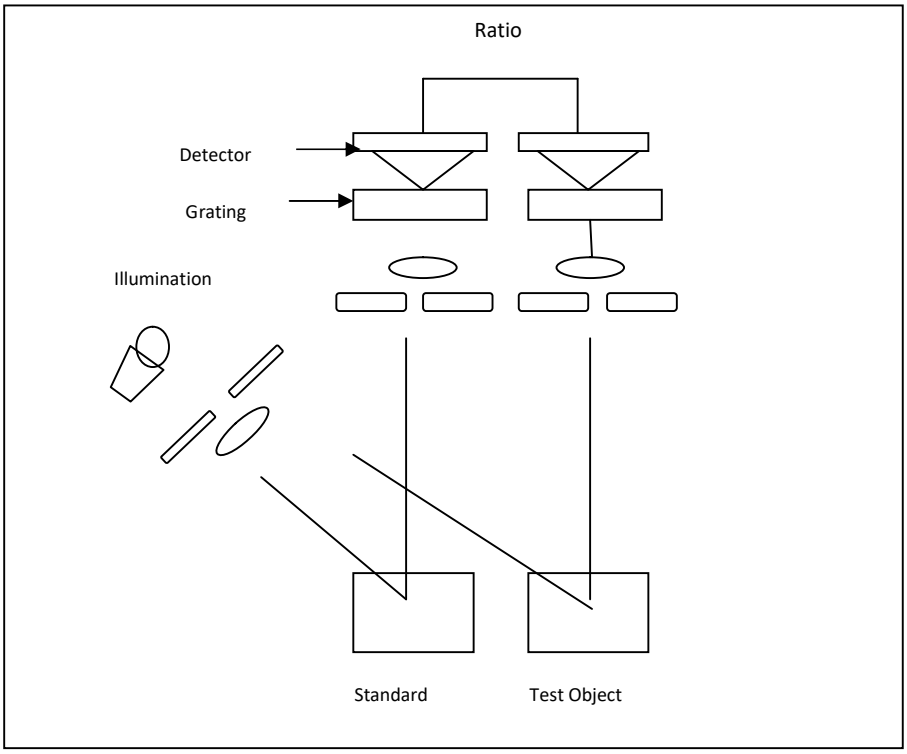

Fig 6.6: Measurement of Spectrophotometer

The GretagmacbethSpectroscan Device is an automated type of spectrophotometer system that can be used to read and measured thousands of data, without human intervention [53]. TheCIE L*a*b* color values of patch samples of the printed color chart weremeasured by a GretagmacbethSpectroscan device in a dark room, without any other light source illuminating the experimented sample.

The GretagmacbethSpectroscan probe named Spectrolino (Fig 6.7) is used to measure the reflectance spectrum of color samples and recorded the spectrum from 380 to 730 nm of visible spectral range at 10nm intervals. Different filters are allowed to use with it to measure the variety of measurements under different lighting conditions. D50,D65, UV filters are used and changed the spectral output of measured sample. The light source of the Spectroscan probe corresponds to the CIE D65 standard illuminant used to illuminate the measured sample. The tungsten-halogen light source is used as an inbuilt light source for GretagmacbethSpectroscan device. The measurements have been performed under the$0^{o}/45^{o}$geometry.

Fig.6.7: GretagmacbethSpectrolino

In CIELAB color space L*, a* and b* represents the lightness, redness/greenness and yellowness/blueness, respectively. The lightness of the substrate (on which color patches were printed) has been measured to identify the significance of color differences induced by aluminum foils. The colorimetric values of bare foil and the respective color differences are enclosed in the below mentioned tables (Table 6.4 & Table 6.5).

Table 6.4: The L*a*b* values of different bare foil

Samples	L*	a*	b*
Foil 1	82.65	0.51	3.63
Foil 2	82.45	-0.68	1.60
Foil 3	87.83	-1.13	1.05

Table 6.5: Color, Lightness & Chroma differences between various bare foils

Samples	Foil 1_ Foil 2	Foil 1_Foil 3	Foil 2_Foil 3
ΔE_{00}	1.63	3.80	3.59
ΔL^*	0.2	5.18	5.38
ΔC_{ab}	1.77	1.67	0.25

From the above table (Table 6.5), all these $\Delta E_{00}$are lower than 5.0, all ΔL^* are lower than 5.5, all ΔC_{ab} are lower than 2.0.This demonstrates that neither the reflectance of the substrates(foil samples),nor their lightness and their chromaticity, have an impact on the color measurements of color patches, and thus these can be neglected for this experiment.

In this research work, different gravure printer profiles have been computed by using the profile maker software associated with the GretagmacbethSpectroscan device. The color profile of three different gravure printers has been computed from color values of color patches of both printed and reprinted sampleson blister foils (Fig.6.9).

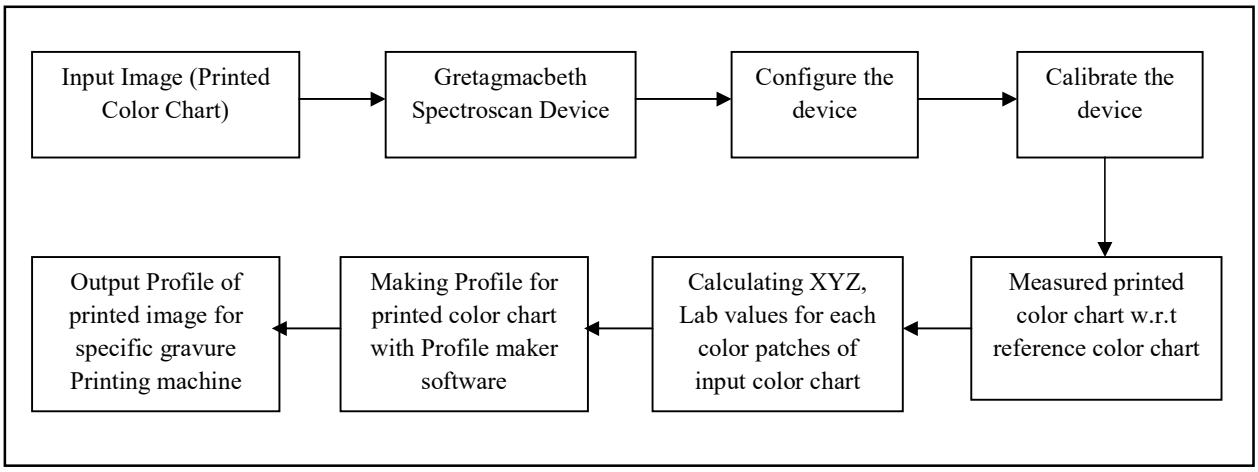

Fig.6.8: Block diagram ofGretagmacbethSpectroscan device for measuring the inputimage

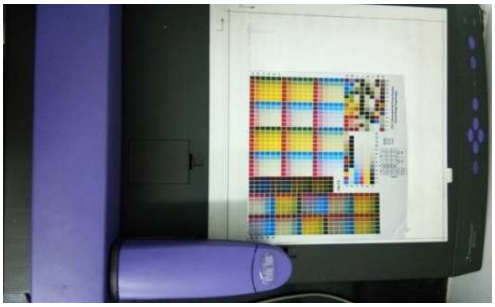

Fig.6.9: Data collection from GretagmacbethSpectroscan device

- Viewing Booth:

  The look of color is changed due the different lighting condition. So controlled of light source is needed to evaluate the color values. To get consistent and accurate evaluation of color values the proper illumination condition has been applied by using the viewing booth. The viewing booths are designed to control the amount of selected light source which is interacted with the specified sample. Different light sources (incandescent, daylight source, cool white fluorescent etc.) are puts into the light booth and same intensity of light (Lux or foot candles) is illuminated on the sample from the selected light source. In this research work, to take a picture of printed multicolor color chart sample with different devices like digital camera, mobile camera etc under controlled light source, and theXrite Macbeth Judge II viewing booth has been used and the daylight source (D65) has been illuminated on the measured printed sample to capture the sample.

Fig 6.10: Viewing booth

- ISO Color Light Meter:

  ISO Color Light Meter has been used to hold the test chart safely and it's for sensors measured the illumination brightness, uniformity, color. The LCD screen has displayed the parameters of lighting conditions to measure the color test sample under specific light source in viewing booth.

Fig 6.11: ISO Color Light Meter

6.3Analyze of results

To identify the original gravure output prints using different methods:

In comparison to the original printed sample, the effect of the scan and reprint process were analyzed on the basis of reflectance spectrum and colorimetric values. To analyze the effect of different printers, CMYK color print and reprint samples were compared for three different gravure printers.The Root Mean Square Error (RMSE) was used to analyze the inequality between reflectance spectrums of solid colors (Cyan (C), Magenta (M), Yellow (Y) and Black (K)) within the visible domain (380nm to 730nm) for different gravure printers. If a print results from a scanned and reprinted, it can easily be demonstrated whether it was printed by an original printer or not. It has also been shown

that between print and reprinted samples, the RMSE values are different for different printers, especially in the red spectral domain (380nm-490nm), green spectral domain (500nm-600nm) and blue spectral domain (610nm-730nm) regions of the visible domain. The other statistical measurements, like SAM (Spectral Angle Mapper), GFC (Goodness of fit Coefficient) are performed for comparison purpose between print and reprint process and the result has been discussed in Chapter 8. As RMSE provided better result than other comparison measures between print and reprinted samples, itcould be used to authenticate the printer for blister foil substrate used for medicine packaging. Other spectral or color difference metrics could also be used additionally with the RMSE metric, but in this preliminary study the RMSE values of spectral differences have been sufficient to identify the original printer.In this study, an Artificial Neural Network (ANN) model and Yule-Nielsen spectral modified Neugebauer prediction model(YNSN) have beenused for predicting colorimetric values (CIE L*a*b*) resulting from a mixture of color inks (cyan, magenta, yellow, black) printed on blister foil using gravure printing machines and compared between predicted and measure color values of other print-reprint samples for differentiation to identify the original gravure output prints. The experimental results of two different models have been discussed in Chapter 8.

CHAPTER 7

7. ARTIFICIAL NEURAL NETWORK (ANN) MODEL

An Artificial Neural Network (ANN) [98.99] is an information-processing model that is inspired by the way biological nervous systems such as the brain, process information, and this computational model formed from hundreds of single units, artificial neurons, connected with coefficients (weights) which have been constituted the neural structure. Self-learning, adaptivity, fault tolerance, nonlinearity, and advancement in input to an output mapping are excellent properties of ANN [101] and therefore it has been used in many domains as a data analysis method to solve the nonlinear problem. The main advantage of using artificial neural networks is that it has predicted the data from full use of some unknown information hidden in the data set. A conventional ANN configuration (Fig7.1) based on a multilayer feed-forward architecture has been used to make a prediction model and provided more accuracy for complex natural systems with large inputs. In Feed-Forward Neural Network (FFNN) [96] each node in a layer is related to all the other nodes in the layers. These layer's connections with nodes are not all equal because each connection can have a different weight or strength. The potential amount of knowledge of the network is measured by the weights of the network connections measured. An Artificial Neural Network consists of one input layer, one hidden layer, and one output layer. In FFNN, information is transmitted only in one direction, first from the input nodes to the hidden nodes, and then from hidden nodes to output nodes[97]. The input variables have been inserted into the input layer. One or more hidden neurons in the hidden layer are used to help the nonlinearity in the system. Finally, the output of the last hidden layer is sent to the output layer. A convergence criterion is used for the training step[106]. It described the set of weights learned during the supervised training, as the network learns the values needed to produce the correct response within some margin of error.

The signal flow (f) from inputs $x_1,\dots,x_n$ are considered to be unidirectional and the corresponding neuron's output signal flow (O) is given by[96]:

$$O=f(\sum^{n}_{j=1} w_j x_j) \qquad \text{Eq. (7.1)}$$

Where w_j is the weight vector associated to the variable x_j.

To train, the network different training algorithms have been used to obtain the output of the neural network. When inputs are faded to the neural network topology then the corresponding output is evaluated, and after that, the difference between the network output and the expected output is used for adjustment of the network's synaptic weights. If it exists any differences, then weights (w) are associated with each layer to connect the layers and adjust the error between the network output and the expected or predicted output. Different weight values have provided a potential amount of knowledge of the network. Each layer of the neural network is independent of another and arbitrary numbers of nodes called bias (b) are present in each specified node. The bias parameter set as equal to one [95] and defined as has been used to shift the activation function either to the left or to the right and helped to increase the successful training of ANN. The w and b are represented as a matrix of dimensionality (SxR) and (Sx1) respectively, where R is the number of elements in the input vector and S is the number of neurons in the layer to adjust (training) weights and biases values of its neurons in the neural network. Mean square error (MSE) is commonly used as a mathematical computational training error between targets and outputs [94] and the training process has been performed till the minimum mean square error (MSE) is achieved. One way to measure how well the neural network fits is to compute for all data the correlation coefficient (R).

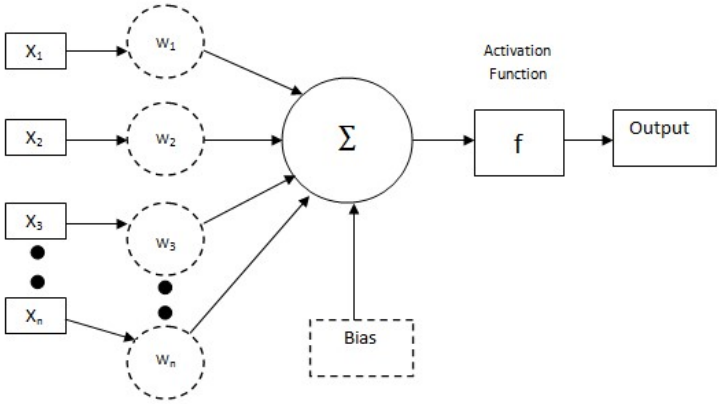

Fig7.1: A Schematic Representation of Neuron in a Neural Network

7.1ANN Model Development to predict Colorimetric values from printed Color patches on blister foil

7.1.1 Development of the Artificial Neural Network

To develop an Artificial Neural Network (ANN) the parent database must be partitioned into three subsets after data collection [92]. The three subsets are training,

testing, and validation. The data belonging to the problem domain called input parameters included in the training dataset are fed to the network. In the training phase, the training dataset is used to update the weights of the network. During the learning process, the test dataset is used to check the network from the untrained dataset. The test dataset should be distinct from the training dataset but lied within the training data boundaries [15]. Several training cycles must be applied based on the performance of the ANN on the test dataset. This can also help to improve the accuracy of the network. The third phase is the validation phase where the validation subset is different from the training and test datasets. This validation dataset is used to improve the network accuracy and to provide better prediction accuracy before implementing it in the neural network system.

In this study, an Artificial Neural Network (ANN) model has been used for predicting colorimetric values (L*a*b*) resulting from a mixture of color inks (cyan, magenta, yellow, black) printed on blister foil. The framework of this network is drawn and shown in Fig7.2. The input (target) data of the network are the CMYK values of the color chart. After an experiment with different numbers of hidden neurons [22, 94, 97], 10 hidden neurons have selected based on the regression coefficient result. The architecture of this ANN is based on 10 hidden neurons, 4 inputs, and 3 outputs; it has been implemented in MATLAB. The network architecture has been tested to predict, next to validate, the colorimetric values of printed color patches. The output data of the network are the colorimetric values (L*a*b*) of the printed color chart on blister foil.

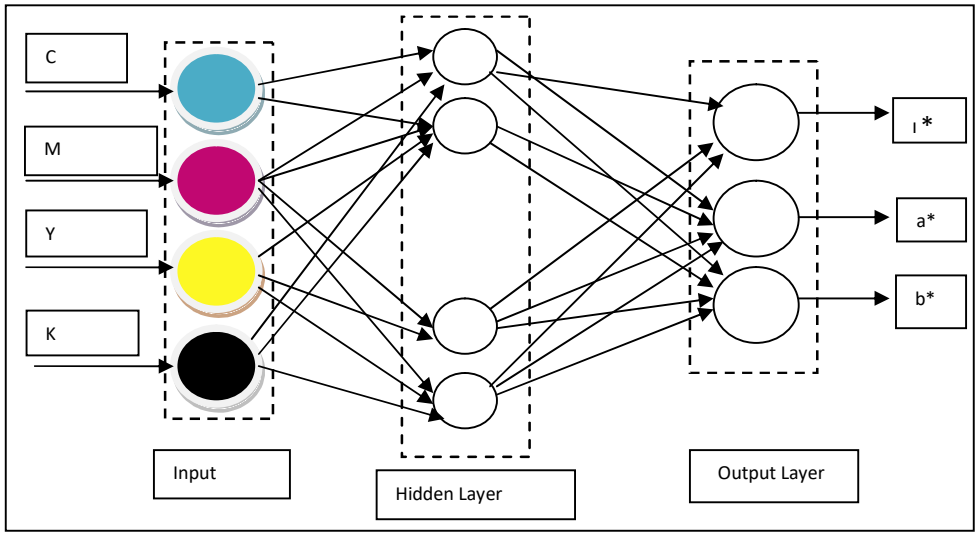

Fig.7.2: Artificial Neural Network Configuration

7.1.2 Training and Testing Network

- **Input Parameters:**

  A standard color chart has been taken to collect the data of percentages of inks of cyan, magenta, yellow and black from different color patches printed on blister foil by gravure printing machines. The data collection process has been discussed in Chapter 6. In this research, different mixtures of dot percentage values of color patches (IT8.7/3 color chart) printed with cyan, magenta, yellow, and black processed colors have been fed to the network as input parameters. Here, a total 4 inputs per patch have been used to develop the artificial neural network.

- **Output Parameters:**

  The colorimetric values L*a*b* have been predicted by the Artificial Neural Network. L* values are numerical output reflecting the lightness/darkness value of printed color patches meanwhile a* and b* values reflect the redness/greenness and yellowness/blueness of the printed color patches on blister foil. Next, it has been computed the color difference between the estimated values and the measured colorimetric values of scanned reprinted or counterfeited (scanned reprinted) samples.

- **Training of Neural Network**

  To train the network, the Levenberg-Marquardt (LM) [98] training algorithm ('trainlm' MATLAB function) has been used. The Levenberg-Marquardt method is an optimization method, based on back propagation, developed to solve data fitting problems using a mean squared normalized error performance function. For non-linear least-square problems, this LM algorithm has become a standard iterative technique and is widely used in data fitting applications. One way to measure how well the neural network fits is to compute the regression coefficient (R) for all samples[98]. If the network learns to fit the data well, the linear fit to this output-target relationship should closely intersect the bottom-left and top-right corners of the regression plot (plot of input vs. output values) and the regression coefficient should be close to 1, then the intersection between output-target relationship and regression plot is good. If this is not the case then further training, or training a network with more hidden neurons, would be necessary. In this study, this network was first tested for the set of color samples printed using

the first printer (P1, taken as reference). The R-value was 0.988 (Fig 7.3). This score confirmed that the network can predict accurately the CIE L*a*b* colorimetric values from the CMYK input values of the color chart. In all cases, the network can predict accurately the CIE L*a*b* values from the CMYK input values of the color chart printed on blister foil. In this research different mixtures of color and values have been included in the training set and 70% of training data has been selected to train the neural network. For cross-validation, 15% of data has been used during training and test set. Another 15% of data has been used to verify the accuracy of the neural network and compared the performance of other networks.

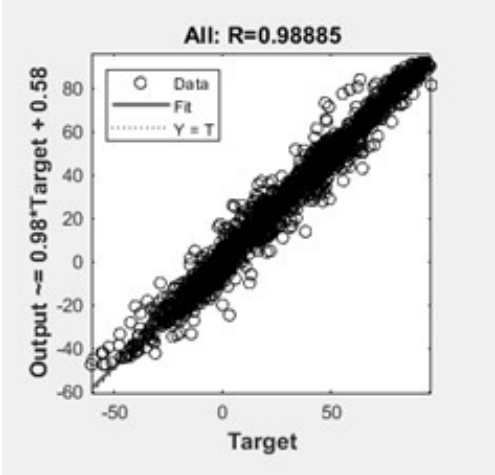

Fig.7.3: Correlation Coefficient (R) values for Target vs. Output

7.1.3 Building the Neural Network Architecture

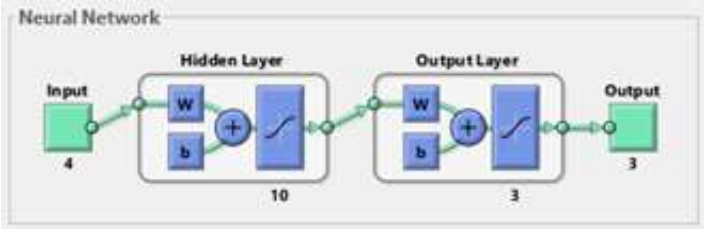

Fig7.4: Architecture of the ANN implemented in MATLAB

To build the Artificial neural Network architecture input dataset, target dataset, hidden layers, output layers, and training functions, weight/bias learning function, training algorithms have been required and implemented in MATLAB. In this study, the architecture of the ANN was built by using four inputs, ten hidden layers, and

three outputs as it has been shown in Fig7.4. The Neural Network toolbox of MATLAB R2018a has been used to develop the network for this experiment [98]. The mixture of C,M,Y,K (Cyan, Magenta, Yellow, and Black) has been taken from printed color patches as input and fed to the network, and colorimetric values (L*a*b*) were collected as predicted output from the network.

7.1.4 Evaluation Criteria

After the process of training, testing, and validation of the network, the obtained data have been evaluated by usingthe Mean Square Error (MSE) [98] and Regression Coefficient (R^2) values. In this research, the network has been first tested for the set of color samples printed with a first printer (P1, taken as reference). The R-value was 0.988. This score confirms that the network can predict accurately the L*a*b* colorimetric values from the CMYK input values of the printed color chart. Similar R values have been obtained for two other printers and print and reprint samples. In all cases, the network can predict accurately the L*a*b* colorimetric values from the CMYK input values of the used printed color chart.

7.1.5 Implementation

In this study, the developed ANN model predicted the colorimetric values (L*a*b*) from the different percentages of CMYK color patches printed on blister foil by gravure press. Different gravure printing machines were used to compute the variations between printed samples, as well as to compute differences with counterfeited (scanned reprint) samples. The predicted L*a*b* values (computed from the reference printer P1) have been compared with the measured L*a*b* values of two other printers (P2, P3) and also with the measured L*a*b* of reprint samples. From these comparisons, we made the hypothesis that the predicted L*a*b* values can be used as a tool to identify an original (print) sample from a scanned reprinted sample. The methods have been discussed in chapter 8 and these comparisons are based on the color difference (ΔE_{00}), chroma difference (ΔC_{ab}), hue difference (ΔH_{ab}), and lightness difference (ΔL), between two print color charts (e.g. P1 vs. P2) or between a print and a reprint.

CHAPTER 8

8. EXPERIMENTAL RESULTS& DISCUSSION

8.1 Introduction

This Chapter presents the results of the experiments done in study. The graphs illustrated below have showed the difference of color using reflectance spectrum, CIELab colorimetric values and gamut volume between printed and reprinted output samples on blister foil for three different gravure printers. The IT8.7/3 color chart has been printed with one reference printer P1 and also with other printers such as P2 and P3. After printing, the samples were scanned and reprinted with same gravure machines and mentioned as reprint samples. Then using the spectrophotometer device the spectral and L*a*b* color values for solid colors (C,M,Y,K) and two solid colors combinations(CM,MY,CY) of color patches of print and reprint samples have been obtained to observe the differences of spectrums. CIEL*a*b* color value and color difference values between printed and scanned reprinted output samples within visible range are obtained. The Artificial Neural Network (ANN) model has been used to predict the CIELab colorimetric values from print sample collected from reference printer P1 and then compared with the other print samples and scanned reprinted sample. The comparison has been done using color difference (ΔE_{00}). The reflectance spectrum of solid color patches of reference print samples have been taken to predict the spectrum of different dot percentages of color patches printed on blister foil using Yule-Nielsen spectral modified Neugebauer prediction (YNSN) model. Then the spectral comparison have been observed between predicted and measured spectral values of print and scanned reprinted samples for different percentage of dot areas. To assess the difference between print (original) and scanned reprinted samples, the color gamut volume also demonstrated in this chapter and the difference between them have been identified to authenticate the gravure output samples.

8.2 Experimental results obtained

- **Comparison of reflectance spectrums of Solid Cyan patches for Printer1, Printer2 & Printer3 (Figures 8.1 to 8.3).**

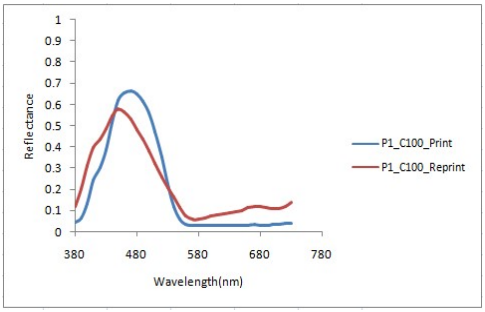

Fig 8.1: Reflectance Spectrum of Solid Cyan for Printer1 (P1)

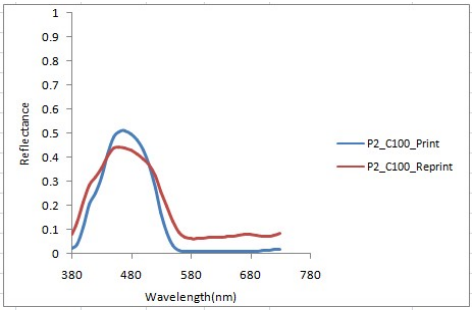

Fig 8.2: Reflectance Spectrum of Solid Cyan for Printer2 (P2)

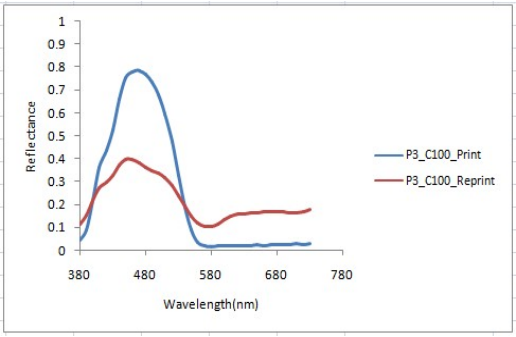

Fig 8.3: Reflectance Spectrum of Solid Cyan for Printer3 (P3)

These spectrums have been measured from cyan (solid) patch of different printed and reprinted sample of blister foil using GretagmacbethSpectroscan device. It has beenobserved that the spectrums have a similar shape, with a peak at around 470 nm. The intensity of this peak is higher for the original print than for the reprint sample for all three printers. This peak is also a little bit shifted between print and reprint samples. These deviations could be used as a first indicator whether a print is original or not and might be used to identify an original printer used to print a reference sample.

- **Comparison of reflectance spectrums of solid magenta patches for Printer1, Printer2 & Printer3 (Figures 8.4 to 8.6).**

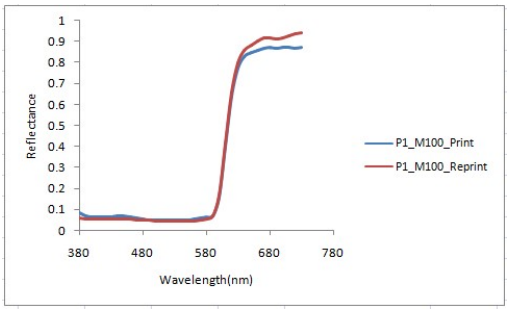

Fig 8.4: Reflectance Spectrum of Solid Magenta for Printer1 (P1)

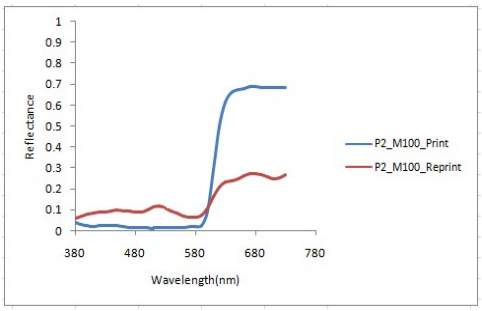

Fig 8.5: Reflectance Spectrum of Solid Magenta for Printer2 (P2)

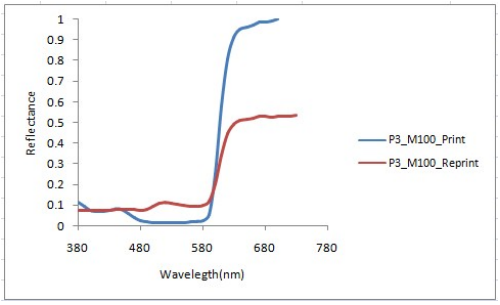

Fig8.6: Reflectance Spectrum of Solid Magenta for Printer3 (P3)

The spectral differences have beenplottedfor magenta (solid) patch between print (original) and reprint (duplicate) sample. It has been observed that the spectrums have similar shapefor all printers, but differences of amplitude (i.e. reflectance values) are significantly high for printers 2 and 3,meanwhile they are very low for printer P1. For the two printers P2 & P3, in the red region, the reflectance values of the magenta color are clearly higher for print than forreprint. Even if this spectrum shift can be modeled, it may be assumed that while grabbing the magenta patch through the image acquisition device, its color may be changed (shifted a little bit). These deviations could be used as a second indicator whether a print is original or not, and maybe used to identify an original printer used to print a reference sample.

- **Comparison of reflectance spectrums of solid yellow patches for Printer1, Printer2 & Printer3 (Figures 8.7 to 8.9).**

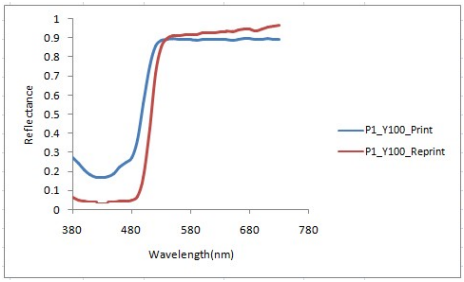

Fig8.7: Reflectance Spectrum of Solid Yellow for Printer1 (P1)

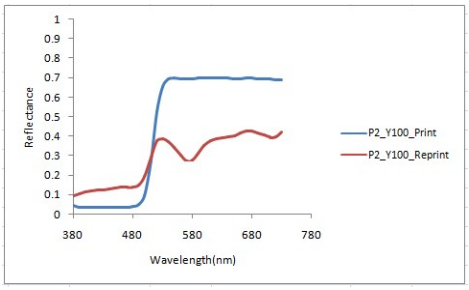

Fig8.8: Reflectance Spectrum of Solid Yellow for Printer2 (P2)

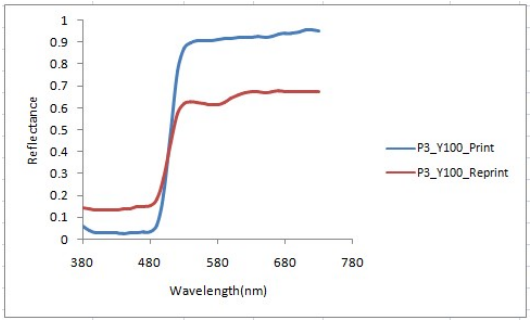

Fig8.9: Reflectance Spectrum of Solid Yellow for Printer3 (P3)

Figure 8.7 to 8.9 show the reflectance spectrums ofyellow patchesof printed and reprinted sample for three different printers. It has been observed that for printers P1 & P3, the overall shape of the spectral curve for print and reprint yellow samples is similar, meanwhile for printer P2 the curves are rather dissimilar. On the other hand, for printers P2 & P3, in the green region, the reflectance values of the yellow color forthe print are higher than for the reprint. Once again this cannot be compensated by any color post processing. These deviations could be used as a third indicator whether a print is original or not and might be used to identify an original printer used to print a reference sample.

❖ **Comparison of reflectance spectrums of solid black patches for Printer1, Printer2& Printer3 (Figures 8.10 to 8.12).**

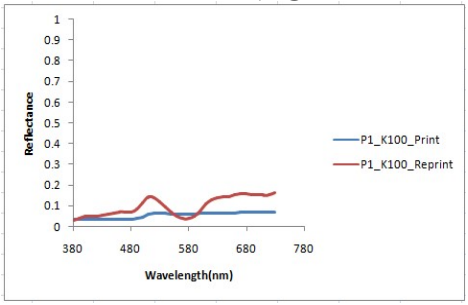

Fig8.10: Reflectance Spectrum of Solid Black for Printer1 (P1)

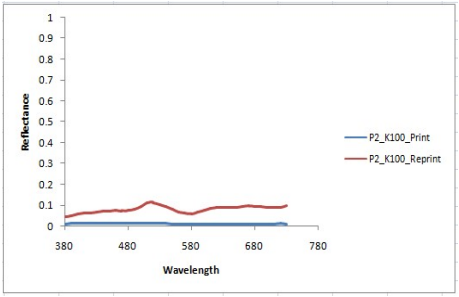

Fig8.11: Reflectance Spectrum of Solid Black for Printer2 (P2)

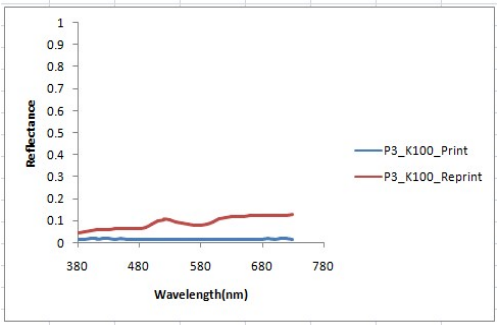

Fig8.12: Reflectance Spectrum of Solid Black for Printer3 (P3)

For black (solid) patch it has been observed for all printers that the shape of the spectral curve ofprint black samples is more homogeneous than for the reprint. Moreover, for all printers, in the red and blue regions, the reflectance values of the black color forthe reprint area little bit higher than the print. On the other hand, for printer P1, the curves are rather dissimilar. One again this could not be compensated by any color post processing. These deviations could be used as a fourth indicator whether a print is original or not and might be used to identify an original printer used to print a reference sample.

From the spectral representations of C, M, Y and K inks, it has been showed that the unique nature of spectrum of reference samples could be used to identify authentic printed samples and also could contribute to recognize an original printer by which original samples are printed.

❖ **Comparison of reflectance spectrums of solid Blue(CM)patches for Printer1, Printer2& Printer3 (Figures 8.13 to 8.15).**

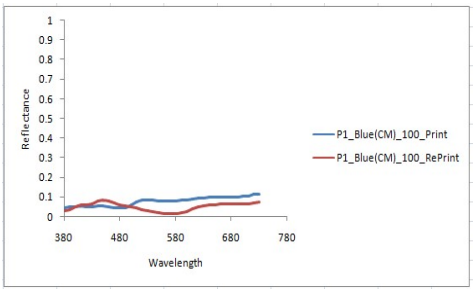

Fig 8.13: Reflectance Spectrum of Solid Blue(CM) for Printer1 (P1)

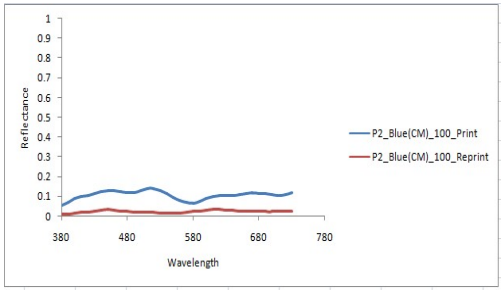

Fig 8.14: Reflectance Spectrum of Solid Blue(CM) for Printer2 (P2)

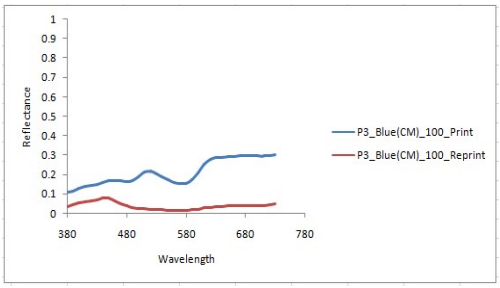

Fig 8.15: Reflectance Spectrum of Solid Blue (CM) for Printer3 (P3)

❖ **Comparison of reflectance spectrums of solid Green(CY)patches for Printer1, Printer2& Printer3 (Figures 8.16 to 8.18).**

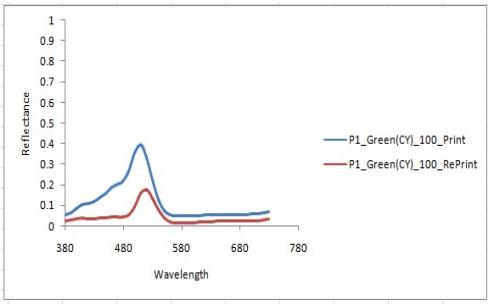

Fig 8.16: Reflectance Spectrum of Solid Green(CY) for Printer1 (P1)

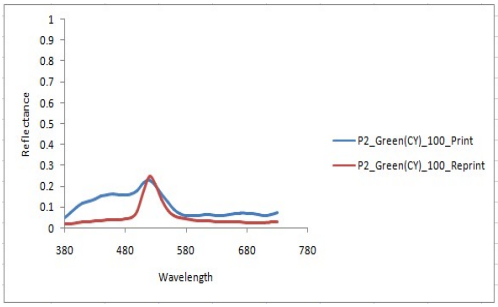

Fig 8.17: Reflectance Spectrum of Solid Green(CY) for Printer2 (P2)

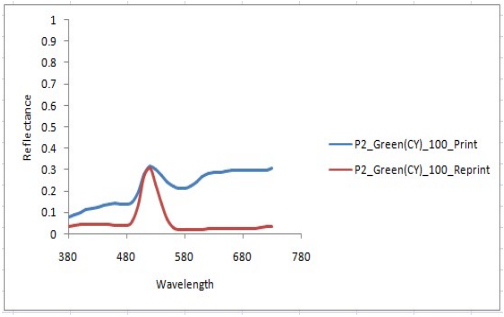

Fig 8.18: Reflectance Spectrum of Solid Green (CY) for Printer3 (P3)

❖ **Comparison of reflectance spectrums of solid Red(MY)patches for Printer1, Printer2& Printer3 (Figures 8.19 to 8.21).**

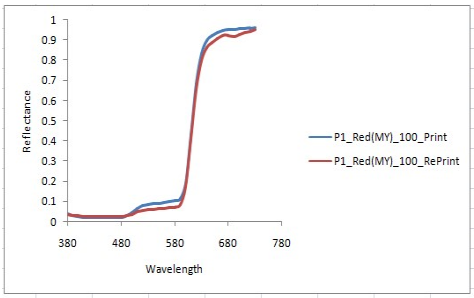

Fig 8.19: Reflectance Spectrum of Solid Red(MY) for Printer1 (P1)

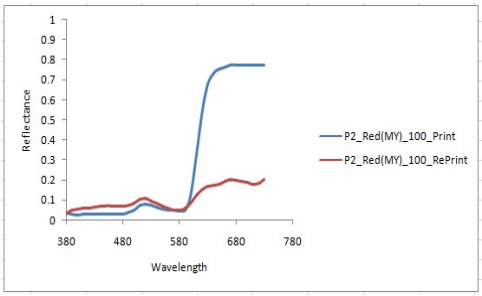

Fig 8.20: Reflectance Spectrum of Solid Red(MY) for Printer2 (P2)

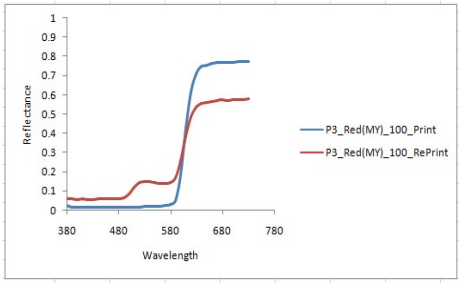

Fig 8.21: Reflectance Spectrum of Solid Red (MY) for Printer3 (P3)

From Fig 8.13to 8.21, the inequality of reflectance spectrum of two color combinations of color patches has been observed between print and scanned reprinted samples. The nature of spectrum also different for two color combinations and the higher intensity value difference observed in red domain. The intensity value is higher for print sample than the reprint samples and this could be used as indicator to differentiate between print and reprinted samples.It has been observed that the differences in spectral characteristics of two color combinations are more distinct in comparison to single color cyan, magenta, yellow or black.

❖ Comparison of Color difference (ΔE_{00})values of solid colors for Printer1, Printer2 & Printer3 (Table 8.1).

Most of spectral differences observed in previous plots correspond to noticeable color differences for human observers between printed samples and print-reprint samples for solid colors (C,M,Y,K)for three gravure machines used in this experiment. From the Table8.1,it has been shown that the printer P1 has been taken as reference printer and then compute the color difference with other print samples taken from P2 and P3 gravure printing machines and also compared with the reprinted samples (R1, R2,R3)from same three gravure machines.

Table8.1: ΔE_{00}(Color Difference) of reflectance spectrum of solid C, M, Y, Kinks (100% of surface coverage) for three different printers between prints and print-reprint samples.

Solid Patches	P1-P2	P1-P3	P1-R1	P1-R2	P1-R3
$\Delta E_{00}(C_{100\%})$	5.65	0.86	15.17	13.79	12.84
$\Delta E_{00}(M_{100\%})$	4.77	2.11	24.18	20.64	11.54
$\Delta E_{00}(Y_{100\%})$	6.42	5.49	13.42	26.43	11.98
$\Delta E_{00}(K_{100\%})$	10.84	8.92	22.47	12.06	10.63

From table 8.1, it has been analyzed that for solid C,M,Y,K , the color difference is lower between printed samples than the print-reprint samples. The color differences are greater than 10 between reference and other reprinted samples, where as the color difference is lower between reference and other printed samples for three gravure printing machines. Therefore, it could be used as indicator to differentiate between original printed and scanned reprinted sample and also authenticate the printing machine.

- **Comparison of RMSE values of solid colors for Printer1, Printer2 & Printer3 (Table 8.2).**

As mentioned above, most of spectral differences observed in previous plots correspond to noticeable color differences. For the Black color and Printer 1, only two RMSE values are lower than 0.045 (for B and G regions), meanwhile theΔE_{00} value is equal to 7.76, that means that the color difference corresponding to this spectral difference is visually noticeable. Similarly, for Printer 3, only one RMSE value was lower than 0.045 (for B region) for Magenta and Black color patches, meanwhile the ΔE_{00} value was equal to 10.66 and 18.45 respectively, that means that the color differences corresponding to these spectral differences are visually noticeable. The RMSE values reported in Table 8.2 (and in Figures 8.22 to 8.25) confirm the observations done in previous section based on the analysis of reflectance spectrum curves.

Table 8.2: RMSE (Root Mean Square Error) of reflectance spectrum of solid C, M, Y, K inks (100% of surface coverage) for three different printers between print and reprint. Highest RMSE values are in bold. Lowest significant RMSE values (i.e. lower than 0.045) are surrounded by a cell.

RMSE	**P1**				**P2**				**P3**			
Spectrum	C100	M100	Y100	K100	C100	M100	Y100	K100	C100	M100	Y100	K100
Region(nm) Blue(380-490)	0.128	0.013	0.186	0.027	0.067	0.065	0.089	0.275	0.275	0.029	0.108	0.043
Green(500-610)	0.082	0.006	0.159	0.046	0.068	0.073	0.317	0.163	0.163	0.081	0.248	0.075
Red (620-730)	0.075	0.045	0.050	0.080	0.062	0.395	0.293	0.140	0.140	0.435	0.264	0.104

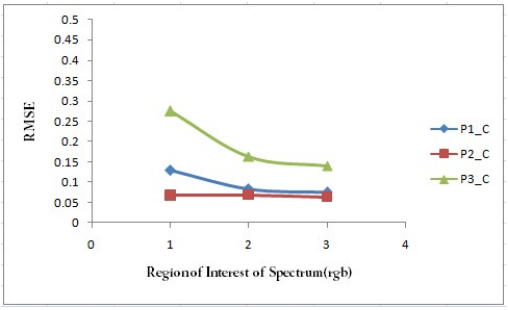

Fig8.22: RMSE values of Solid Cyan in R, G, B regions for printers P1, P2 and P3

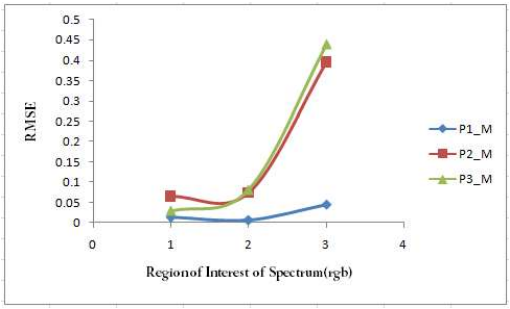

Fig8.23: RMSE values of Solid Magenta inR, G, B regions for printers P1, P2 and P3

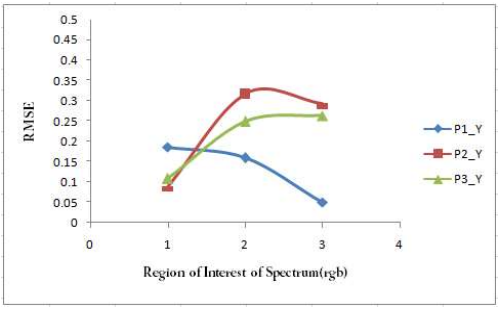

Fig8.24: RMSE values of Solid Yellow in R, G, B Regionsfor printers P1, P2 and P3

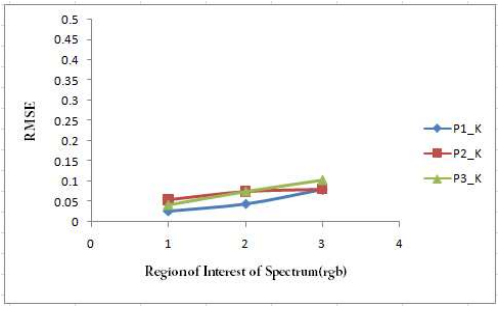

Fig8.25: RMSE values of Solid Black in R, G,B regions for printers P1, P2 and P3

All observations mentioned above can be also observed in Figures 8.26 to 8.29.These graphs summarize, for the three different printers used, the inequality of errors between reference (print) and test (reprint) samples for different color regions. For Cyan ink printed on blister foil, RMSE values are higher in the blue range (380nm to 490nm) than

for green range (500nm to 600nm) and red range (610 nm to 730nm). For Magenta ink, RMSE values are higher for red range for P1 and P2 printers than for the two other regions. No significant tendency can be drawn for Yellow and Black inks.

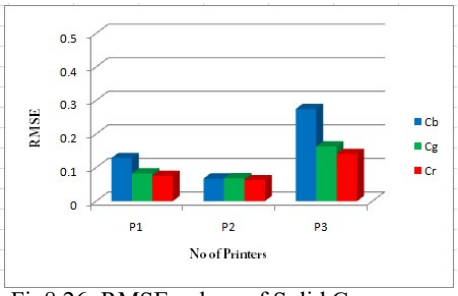

Fig8.26: RMSE values of Solid Cyan (between reference and test samples) for the three Printers

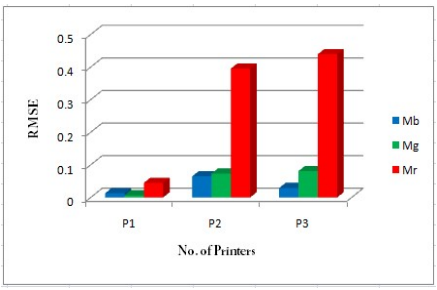

Fig8.27: RMSE values of Solid Magenta (between reference and test samples) for thethree Printers

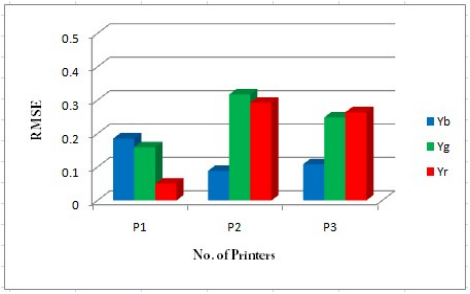

Fig8.28: RMSE values of Solid Yellow (between reference and test samples) for the three Printers

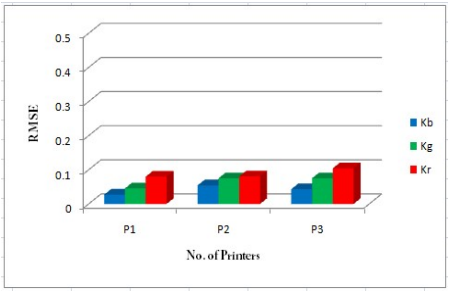

Fig8.29: RMSE values of Solid Black (between reference and test samples) for the three Printers

❖ **Comparison of GFC values of Solid colors for Printer1, Printer2 & Printer3 (Table 8.3).**

In this study, the Goodness-of-Fit Coefficient (GFC) values were computed and compared between print and reprint samples, for the blue, green and red regions of the visible domain, and for the three different printers used. The highest GFC values (higher than 0.995), for R, G and B regions, are for the solid color Magenta for Printer 1. As the corresponding color difference is acceptable for human observers, we could assume that GFC values higher than 0.995 correspond to non-significant spectral differences.

That is, results shown in Table 8.3 are not all coherent with results reported in Table 8.2, for example RMSE value for Black color and Printer 3 is acceptable for blue region but the opposite happens for GFC, inversely RMSE values for Black color and Printer 3 are significant for green and blue regions but the opposite happens for GFC. Likewise, a result reported in Table 8.3 is not all coherent with Fig8.1 to 8.12.

Therefore, it may be mentioned that to analyze print and reprint samples, RMSE values are preferred to GFC values.

Table 8.3: GFC (Goodness-of-Fit Coefficient) of reflectance spectrum of solid C, M, Y, Kinks (100% of surface coverage) for three different printers between print and reprint. Lowest GFC values (i.e. lower than 0.995) are in bold. Highest GFC values (i.e. higher than 0.995, means good match between spectral curves) are surrounded by a ▭ cell.

GFC	**P1**				**P2**				**P3**			
Spectrum Region(nm)	C100	M100	Y100	K100	C100	M100	Y100	K100	C100	M100	Y100	K100
Blue(380-490)	0.9617	0.9967	0.9949	0.9717	0.9832	**0.9187**	0.9863	0.9896	0.9799	**0.9234**	0.9664	0.9907
Green(500-610)	0.9706	0.9961	0.9826	**0.9057**	0.9537	**0.7073**	0.9659	0.9802	**0.9168**	**0.7219**	0.9959	0.9950
Red (620-730)	0.9966	0.9999	0.9999	0.9972	0.9888	0.9977	0.9993	0.9985	0.9929	0.9998	0.9999	0.9979

❖ **Comparison of SAM values of Solid colors for Printer1, Printer2 & Printer3 (Table 8.4).**

In this study, the Spectral Angle Mapper (SAM) values were computed and compared between print and reprint samples, for the blue, green and red regions of the visible domain, and for the three different gravure printers used. For the solid color Magenta,the lowest SAM values (lower than 0.1) has been reported for all R,G,B spectral regionsfor Printer 1. As the corresponding color difference is acceptable for human observers, we could assume that SAM values lower than 0.1 correspond to non-significant spectral differences.

That is, results shown in Table 8.4 are not all coherent with results report in Table 8.2, for example RMSE value for K color and Printer 3 is acceptable for B region, but the opposite happens for SAM, inversely RMSE values for K color and Printer 3 are significant for G and B regions, but the opposite happens for SAM. Likewise, results report in Table 8.4 is not all coherent with Figures 8.2 to 8.13. Therefore, to analyze print and reprint samples, RMSE values should be used preferably to SAM values.

Table8.4: SAM (Spectral Angle Mapper) of reflectance spectrum of solid C, M, Y, Kinks (100% of surface coverage) for three different printers, between print and reprint. Highest SAM values (i.e. lower than 0.1) are surrounded by a ▭ cell.

SAM	P1				P2				P3			
Spectrum Region(nm)	C100	M100	Y100	K100	C100	M100	Y100	K100	C100	M100	Y100	K100
Blue(380-490)	0.278	0.081	0.101	0.238	0.183	**0.406**	0.166	0.144	0.201	**0.394**	0.260	0.137
Green(500-610)	0.257	0.049	0.179	**0.438**	0.314	**0.857**	0.247	0.199	**0.451**	**0.583**	0.085	0.100
Red (620-730)	0.007	0.015	0.011	0.075	0.153	0.038	0.033	0.055	0.119	0.012	0.013	0.063

❖ **Comparison of RMSE values between reference print (P1) and other print and reprint samples (P2,P3,R1,R2,R3) in red(R) visible region**

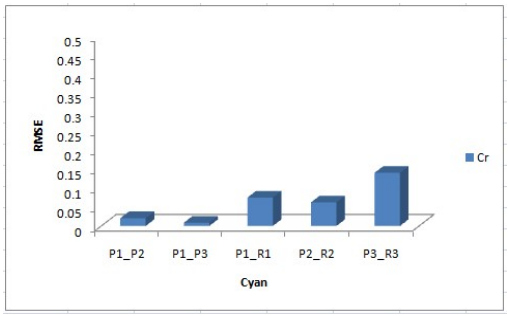

Fig8.30: RMSE values of Solid Cyan between reference (P1) and test samples in red visible region

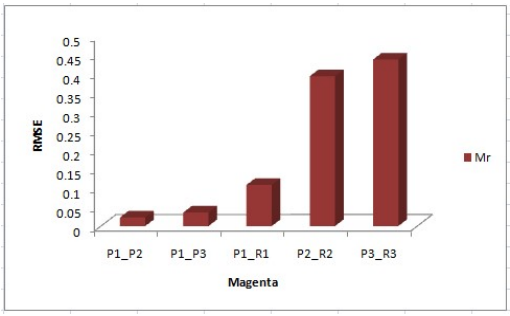

Fig8.31: RMSE values of Solid Magenta between reference (P1)and test samples in red visibleregion

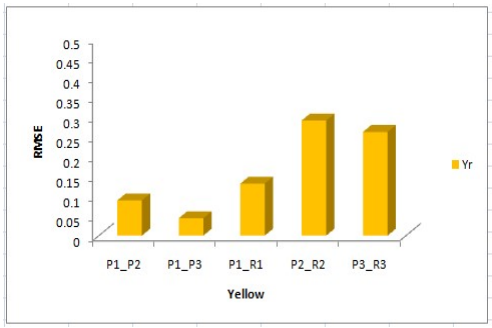

Fig8.32: RMSE values of Solid Yellow between reference (P1)and test samples in red visible region

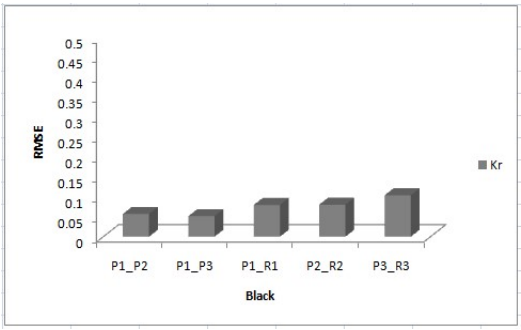

Fig8.33: RMSE values of Solid Black between reference (P1)and test samples in red visible region

The above graphs (Fig8.30 to Fig8.33)summarize the differences between reference print sample printed from Printer1 and other printer-reprint samples for solid cyan, magenta, yellow and black color patches within the red visible region. From these graphical representations, we can observe that the difference is higher between reference printer(P1) and reprint samples (R1,R2,R3) than with print samples. For solid cyan, magenta and yellow, the higher difference is observed within red region. From these comparisons we can draw the hypothesis that these colors could be used to provide better security and protect medicine packaging from counterfeiters, and could be used to identify original print samples.

Application of Artificial Neural Network to predict Lightness and color difference for different color patches printed in different printers

To analyze the effect of the print process and of the reprint process on color values, and to analyze the effect of different printers and gravure cylinders (print & reprint), we perform the following comparisons. For these comparisons only few CMYK color print and reprint samples have been used.In order to do these analyses, we perform the following comparisons using an Artificial Neural Network (ANN) prediction model. Artificial Neural Network (ANN) model is used to predict the CIELAB color values of a print sample printed from a printer. In this study, 70% of color patches (total 928) have been used to train the network, 15% of the data used as cross-validation and 15% of the data is used to verify the accuracy of the network. Then the predicted color values of one printer are compared with other print and scanned reprint sample to assess the differences.

- **Comparison of Predicted value L* (for reference printer P1) and Measured values L* for color patches printed by printers P1, P2 and P3. Plots shown in Fig8.34 correspond to print samples, meanwhile Fig8.35 corresponds to reprint samples.**

Fig8.34 showed that the measured L* values of print samples are closer to predicted L* values when samples are printed with same gravure printing machine (i.e. same printing cylinder). Same for reprint samples when samples are printed with same gravure printing machine but with different printing cylinder, that is the variations of L* values between predicted and measured samples are higher for reprint than for print samples(Fig8.35 vs. Fig 8.34).

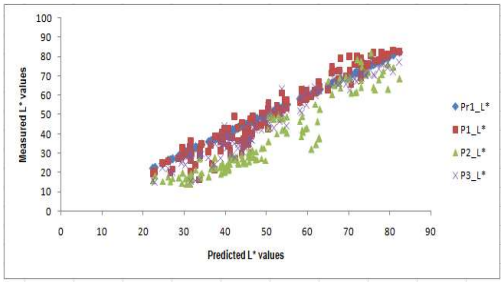

Fig8.34: Predicted (Pr1 for reference printer P1) vs. Measured L* values for print samples (for printers printers P1,P2 &P3)

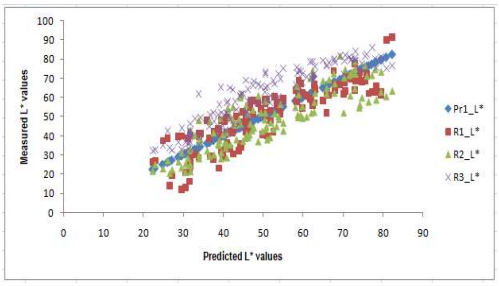

Fig 8.35: Predicted (Pr1 for reference printer P1) vs. Measured L* values of reprint samples (for P1, P2& P3)

❖ **Comparison of Predicted L* values (for reference printer P1) and Measured values L* of samples printed by printer Pi (P1, P2 or P3) and samples reprinted (R1, R2, R3) by same printer Pi(Figures 8.36 to 8.38).**

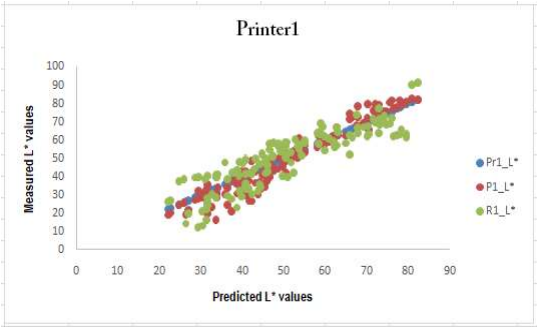

Fig 8.36: Predicted (Pr1 for reference printer P1) vs. Measured L* values (P1 for print and R1 for reprint samples).

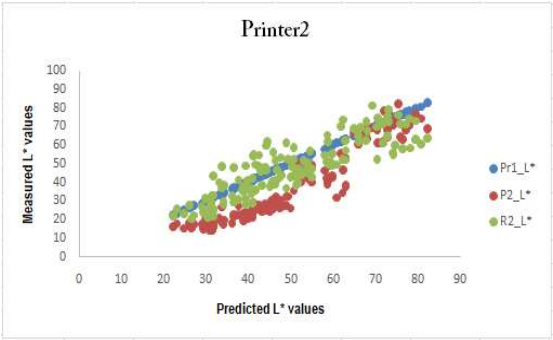

Fig8.37: Predicted (Pr1 for reference printer P1) vs. Measured L* values (P2 for print and R2 for reprint samples)

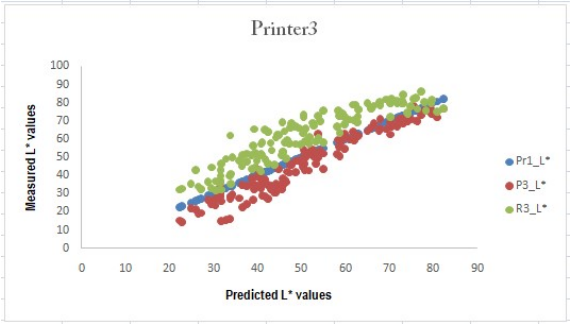

Fig 8.38: Predicted (Pr1 for reference printer P1) vs. Measured L* values(P3 for print and R3 reprint samples).

These L* values of tested color patches has been measured from different printed foil papers and the color patches mostly tested with three-four color (CMYK) combinations.

Table 8.5: Regression Coefficient(RCi) Values for Printand ReprintSamples for the Three Printers.

Samples	**Printer1**	**Printer2**	**Printer3**
RCi(Print)	0.94	0.89	0.94
RCi(Reprint)	0.77	0.74	0.83

These L* values of tested color patches have measured from different printed foil papers. In the above graphs it has been observed that, for all printers (Pi, with i = 1, 2 or 3), the measured L* values of print samples (Pi_L*) are closer to the predicted L* values (Pri_L*) than the measured L* values of reprint samples (Ri_L*). Although the printing machines were identical for print and reprint, these differences are due to the different printing cylinders used. For each printer (Pi, with i = 1, 2 or 3), we plotted the regression graphs of Predicted vs. Measured L* values, next we compute the corresponding Regression Coefficients (RCi). For print samples, all RCi values are higher than 0.89 (Table 8.5). For reprint samples, all RCi values are lower. The all regression coefficients (RCi) for print and reprint samples are in Table 8.5.

Another way to compare the measured L* values of print samples (Pi_L*) with the measured L* values of reprint samples (Ri_L*) is touse bar plots, such as illustrated in Fig8.39. In average the L* values of reprint samples are higher than the L* values of print samples. This difference of L* values could be used as in indicator to identify an original from a scanned reprinted sample. These differences are not due to a calibration problem, as camera and print devices werecalibrated before doing these experiments.

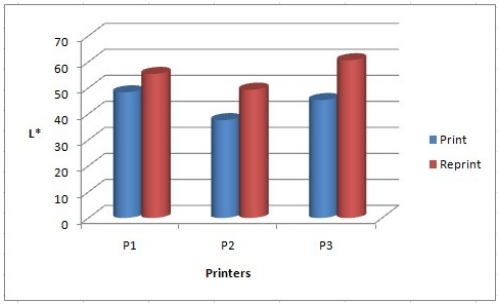

Fig 8.39: Measured L* values of print samples vs. measured L* values of reprint samples (for Printers P1, P2 and P3)

In the following Tables 8.6 and 8.7, lightness and color difference values between predicted L*a*b* and measured L*a*b* values, werecomputed fromtotal 928 patches of color chart.

*Table8.6: Comparison of lightnessand color differences between Predicted L*a*b* and Measured L*a*b* Values for a Set of Print Samples (For Printers P1, P2 and P3).*

Print Samples			
Parameters	*P1*	*P2*	*P3*
ΔL^*_{avg}	3.99	6.36	5.15
ΔE_{00}	5.41	7.76	5.81

*Table8.7: Comparison of lightness and color differences between Predicted L*a*b* and Measured L*a*b* values for a set of Reprint Samples (for Printers P1, P2 and P3)*

Reprint Samples			
Parameters	*R1*	*R2*	*R3*
ΔL^*_{avg}	11.35	8.22	10.91
ΔE_{00}	11.87	11.28	11.49

First for the prints (original prints, Table8.6), next for the reprints ("scanned reprinted sample" prints, Table 8.7), lightness and color differences were compared. It is important to remind that P1, P2 and P3correspond to the three different printing machines used, meanwhile Pi and Ri correspond to the same printing machine (i = 1, 2 or 3) but different printing cylinders were used for print (on Pi) and reprint (on Ri). As lightness differences are significantly upper than chroma and hue differences, only lightness differences are reported in Tables 8.6 and 8.7.

From these Tables (8.6 and 8.7), it can be observed that lightness and color average differences for all reprint samples are higher than for each print samples. For reprint samples, the color average difference is significantly higher than the print samples and in all cases upper than 10.0.So, we can hypothesis that a color average difference upper than 10.0 is characterized for a reprint sample.Fig8.40 and Fig8.41show again that the color differences between predicted L*a*b* and measured L*a*b* values are in average higher for reprint samples than print samples for all three gravure printing machines. It has been confirmed that when an original print sample is copied (reprint) then the color average difference between predicted L*a*b* and measured L*a*b* values is not only high (upper than 10.0) but also significantly upper than the original print.

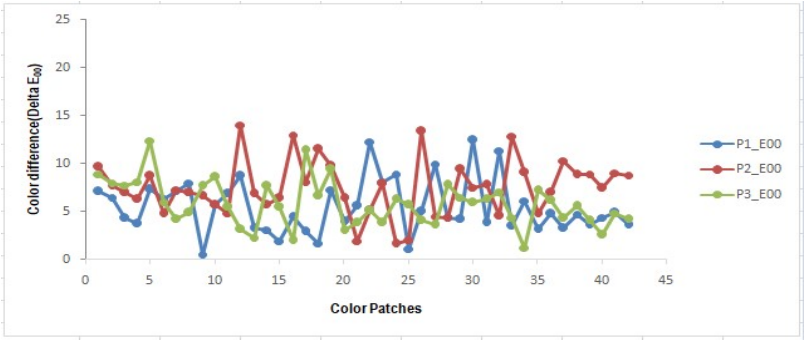

Fig8.40: Color average difference (ΔE_{00}), between predicted L*a*b* and measured L*a*b* values of print samples for each of the three gravure printers.

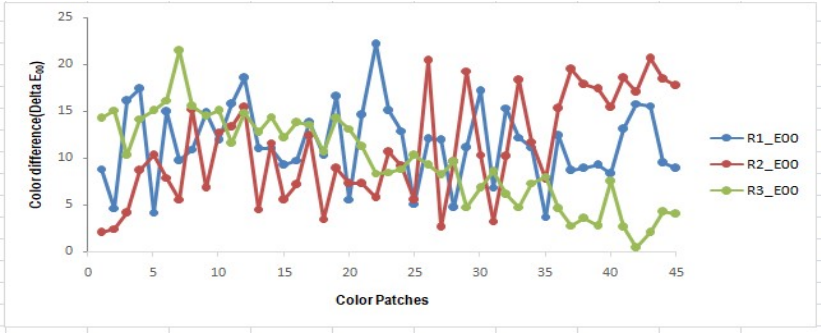

Fig8.41: Color difference (ΔE_{00}),between predicted L*a*b* and measured L*a*b* values of reprint samples for each of the three gravure printers.

- **Comparison of lightness contrast values of print samples for reference printer P1 with lightness contrast values for printers P2 and P3, and contrast values of reprint samples printed with printers P1, P2 and P3.**

The lightness contrast is defined as the ratio of maximum and minimum lightness values of predicted and measured L* values.

$$\text{Contrast} = \frac{L^*_{max(measured)} - L^*_{min(measured)}}{L^*_{max(predicted)} + L^*_{min(predicted)}}$$

The lightness contrast of the prints, with respect to predicted values for reference printer P1, is higher for the prints than for the reprints. The lightness contrast, computed from the predicted values, for the printer P1 is of 1.16. The lightness contrast for all three prints, computed from the measured values, is within the range 1.09 to 1.18. On the other hand, the lightness contrast values of the reprints, with respect to predicted values for reference printer P1, are all within the range 0.84 to 0.90. Colors samples were also compared by observers. They reported that the samples printed from an original artwork had better lightness contrast, higher saturation, and were much cleaner than reprint sample.

- Analysis of Reflectance spectrum of two-color combinations of patches with 70%,40%,20% dot areas, and of predicted color differences using Yule-Nielsen spectral modified Neugebauer (YNSN) model, and comparisons between print and reprint samples to identify an original print sample.

❖ **Comparison of reflectance of predicted, print and reprint samples for three printers for different dot areas.**

- Comparison of reflectance of **Blue(CM)** color patch with70% dot area coverage using printers P1,P2 & P3

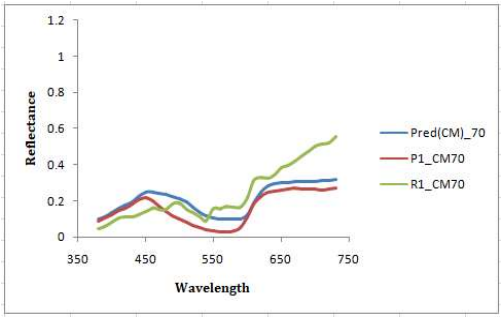

Fig 8.42: CM_70% Reflectance Spectrum of Predicted,P1 & R1

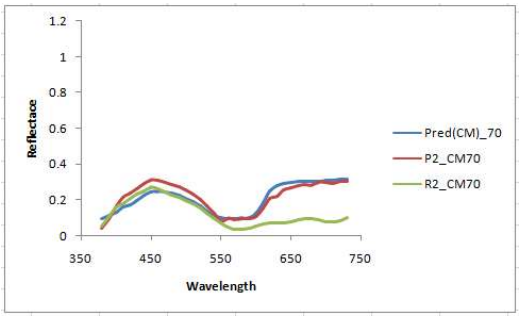

Fig 8.43: CM_70% Reflectance Spectrum of Predicted,P2 & R2

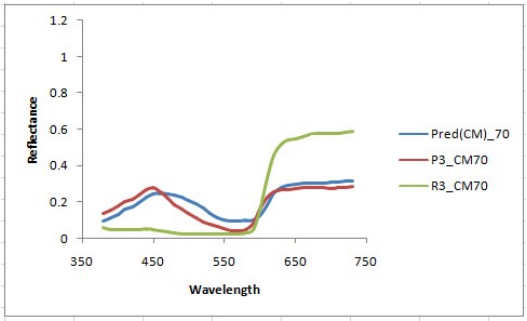

Fig 8.44: CM_70%Reflectance Spectrum of Predicted, P3 & R3

These spectrums have been measured from different print and reprint samples printed on foil papers, using GretagmacbethSpectroscan device. Yule-Nielsen modified Spectral Neugebauer model (YNSN) was used to predict the reflectance spectrum for different dot area coverage (70%,40%,20%) of blue patch using reflectance of solid cyan, solid magenta, solid blue and bare foil for different printers. In the above graphs(from Fig8.42 to Fig 8.44) blue line, red line and green line represented the reflectance spectrum predicted, and the reflectance spectrum of measured print and measured reprint, respectively. In case of 70% of dot area coverage, it has been observed that the spectrums are similar in nature, but the spectral difference between predicted and measured print are less than the spectral difference between predicted and measured reprint. Moreover, the reprint sample has a peak at 650 nm (in the red domain) with a higher intensity value than the predicted and measured print samples for P3 & P1 printers and lower intensity for printer P2 within the visible spectrum region.

- Comparison of reflectance of **Blue(CM)** color patch with 40% dot area coverage using printers P1,P2 & P3

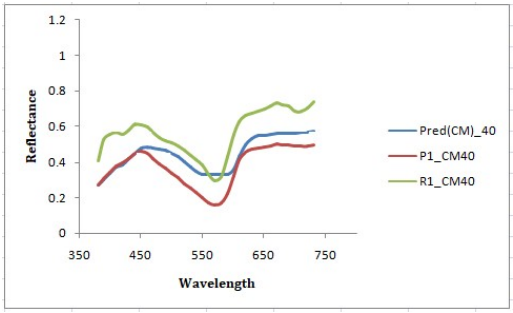

Fig 8.45: CM_40%Reflectance Spectrum of Predicted, P1 & R1

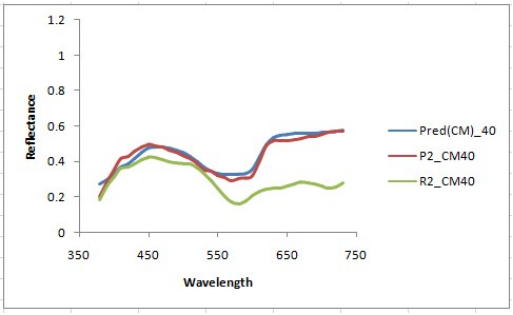

Fig 8.46: CM_40%Reflectance Spectrum of Predicted, P2 & R2

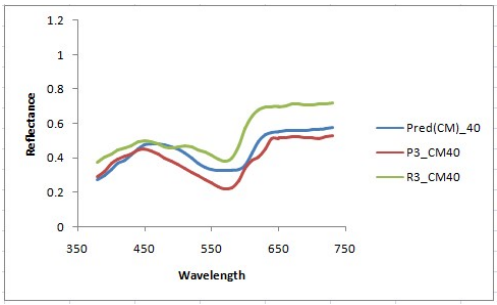

Fig 8.47: CM_40% Reflectance Spectrum of Predicted, P3 & R3

Once again, these spectrums were measured from different color patches printed on foil substrate and measured again after reprint. From the Fig 8.45 to Fig 8.47, it has been observed that the differences for 40% of dot area coverage of blue patch for print, reprint and predicted reflectance spectrums. The overall shape of the spectrum is similar for the three printers, but there are some spectrum differences between the reprint and the predicted value, mostly in the red zone within the visible range, for all printers. Moreover, the spectrum intensity of reprint is low in red zone for P2 printer device.

- Comparison of reflectance of **Blue(CM)** color patch with 20% dot area coverage using printers P1,P2 & P3

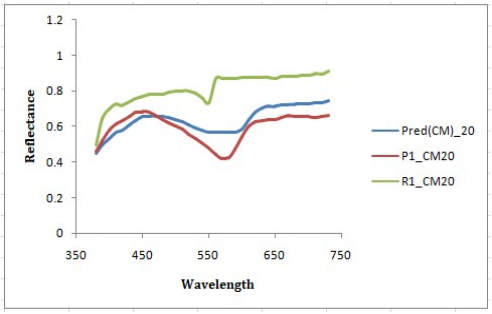

Fig 8.48: CM_20%Reflectance Spectrum of Predicted,P1 & R1

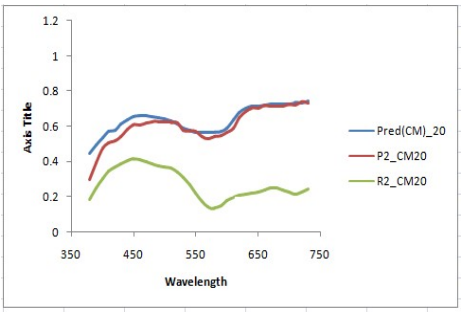

Fig 8.49: CM_20%Reflectance Spectrum of Predicted, P2 & R2

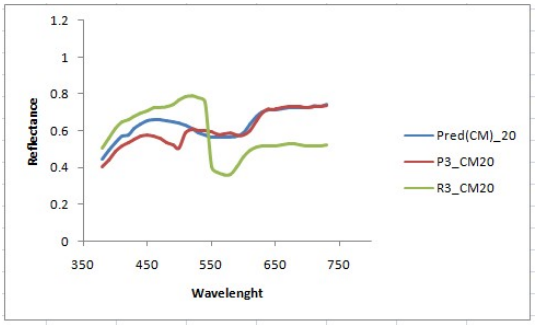

Fig 8.50: CM_20% Reflectance Spectrum of Predicted, P3 & R3

Similarly, from Fig 8.48 to Fig 8.50, it can be observed that some differences between reflectance spectrums for 20% dot area coverage of blue patch for print, reprint and

predicted data. For three printers the global shape of the reprint spectrum is dissimilar to all other printers. On the other hand, the spectrum intensity is higher for reprint sample for printer P1 and P3, but lower for printer P2 within the visible spectrum region. The spectrum of theprint is closer to the spectrum of the predicted for 20% area coverage of blue patch on printed foil substrate for three different gravure printer machines.

- Comparison of reflectance of **Red(MY)** color patch with 70% dot area coverage usingP1,P2 & P3

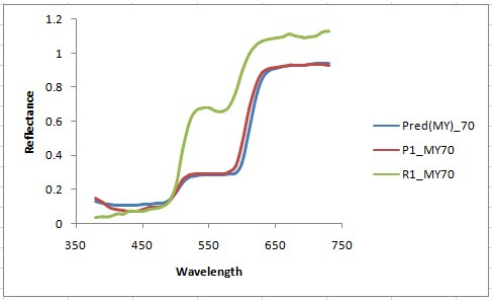

Fig 8.51: MY_70%Reflectance Spectrum of, Predicted P1 & R1

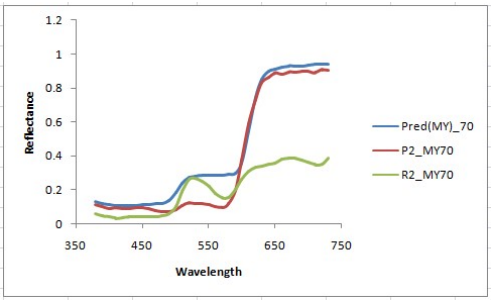

Fig 8.52: MY_70%Reflectance Spectrum of Predicted, P2 & R2

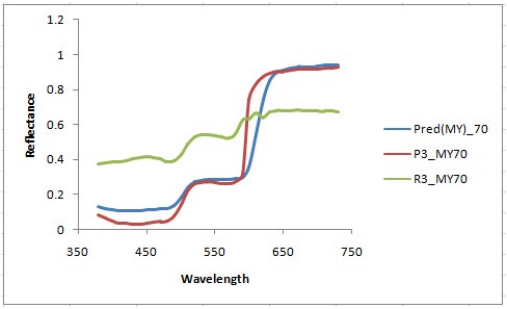

Fig 8.53: MY_70% Reflectance Spectrum of Predicted, P3 & R3

The red patch used corresponds to a combination of Magenta (M) and Yellow(Y) solid colors that were printed and reprinted on foil substrate. The spectral graphs for red patch for print and reprint foil samples are shown in Fig 8.51to Fig 8.53. The data were predicted from the solid magenta, solid yellow, solid red patch and bare foil using the YNSN model for different percentages of dot area coverage. For MY patch (70% dot area) the predicted spectrum is closer to the measured printed spectrum for all three printers. It has been observed that the shape of the spectrum of the measured reprint is dissimilar from the spectrum predicted for all three printers. Moreover, predicted and printed samples have higher intensity values in the red zone for P1, and lower intensity value than other spectrum in red visible range.

- Comparison of reflectance of **Red(MY)** color patch with40% dot areacoverage usingP1,P2 & P3

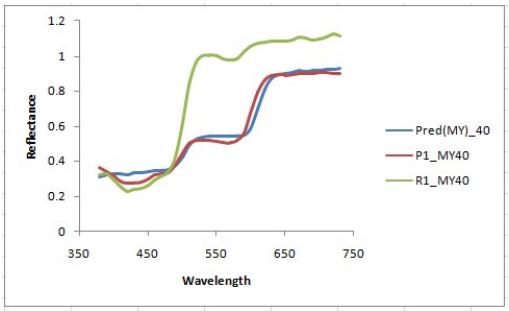

Fig. 8.54: MY_40%Reflectance Spectrum of Predicted,P1&R1

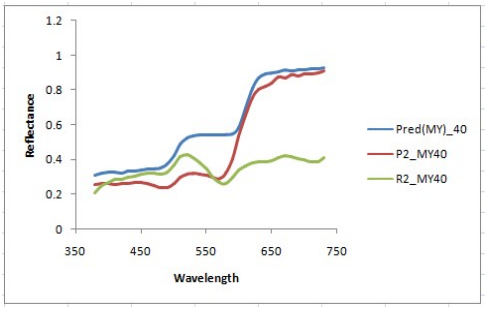

Fig.8.55: MY_40%Reflectance Spectrum of Predicted,P2 & R2

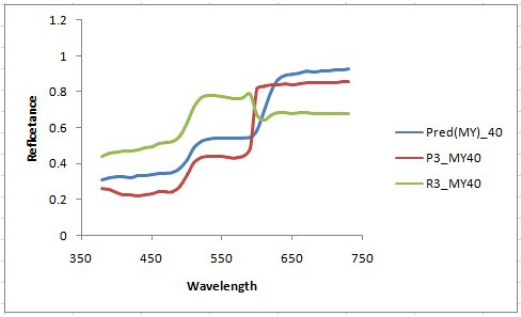

Fig. 8.56: MY_40% Reflectance Spectrum of Predicted, P3 & R3

For MY patch (40% dot area) the shape of thespectrum of the reprint is dissimilarfrom other spectrums ofmeasured print and predicted,for all three gravure printers, as reported in Fig. 8.54 to Fig 8.56. For printer P1, the spectrum of the reprint has ahigher intensity value in green andred visible range.On the other hand, the spectrum of the reprint has alower intensity value in red zone for printer P2 & P3.

- Comparison of reflectance of **Red(MY)** color patch with20% dot area coverage using P1,P2 & P3

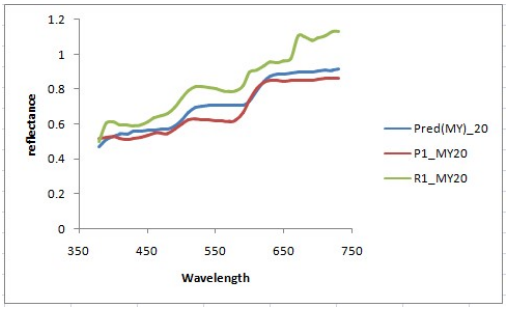

Fig 8.57: MY_20%Reflectance Spectrum of Predicted,P1 & R1

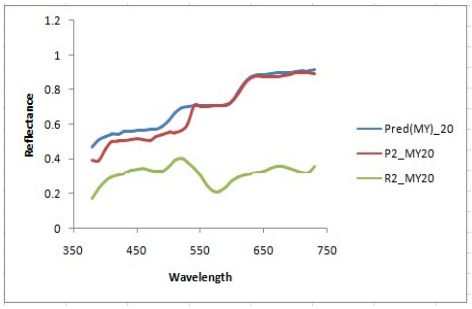

Fig 8.58: MY_20%Reflectance Spectrum of Predicted,P2 & R2

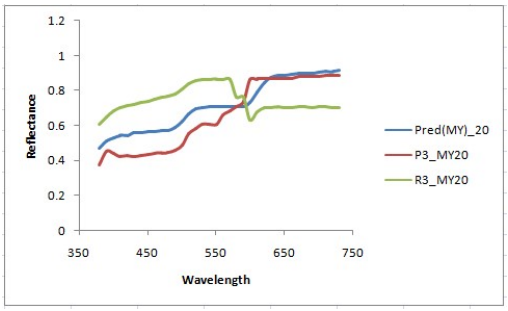

Fig 8.59: MY_20% Reflectance Spectrum of Predicted, P3 & R3

For MY patch (20% dot area), the same shape of spectrum can be observed(from Fig 8.57 to Fig 8.59) for predicted and measured printed spectrum,oppositely to the spectrum of the measured reprinted, for all three gravure printer machines. It can also be observed thatthe spectrum of the reprint has lower intensity value in the red visible range for printer P2 than for other spectrums.

- Comparison of reflectance of **Green(CY)** color patch with70% dot area coverage using P1,P2 & P3

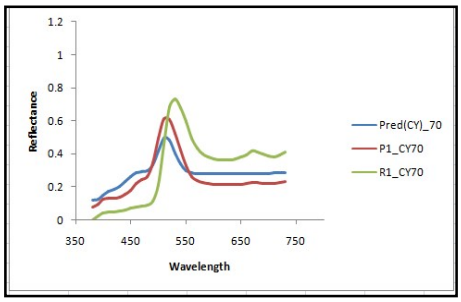

Fig 8.60: CY_70%Reflectance Spectrum of Predicted,P1 & R1

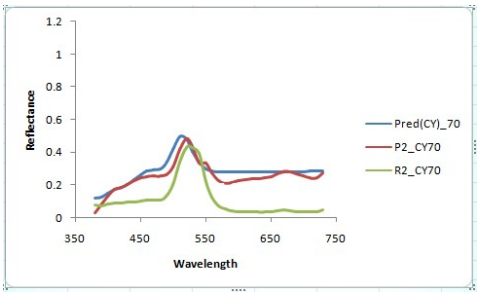

Fig 8.61: CY_70%Reflectance Spectrum of Predicted, P2 & R2

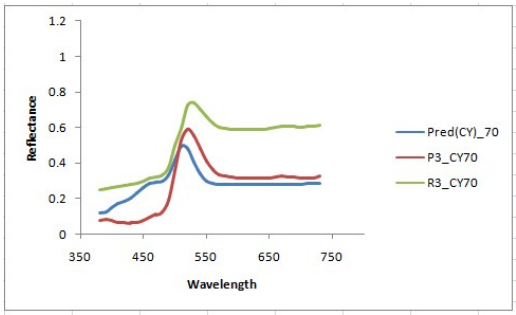

Fig 8.62: CY_70% Reflectance Spectrum of Predicted, P3 & R3

The shape of the spectrums of the green patch can be compared for different dot area coverage on blister foil substrate from Fig 8.60 to Fig 8.62. The color chart was printed and reprinted using three gravure printer machines. Then, measured and predicted

spectrum from print and reprint samples for all three printers can be compared on the basis of different percentages of dot areas. The combination of cyan(C) and yellow(Y) solid colors produced the green patch. For printer P1, it has been observed that, for the reprint, the peak of higher intensity of the spectrum is shifted and has a higher intensity value in red visible range, for printer P3. The peak is higher in the green range than for other measured print and predicted spectrums for 70% dot area coverage of green patch on blister foil.

- Comparison of reflectance of **Green(CY)** color patch with40% dot area coverage using P1,P2 & P3

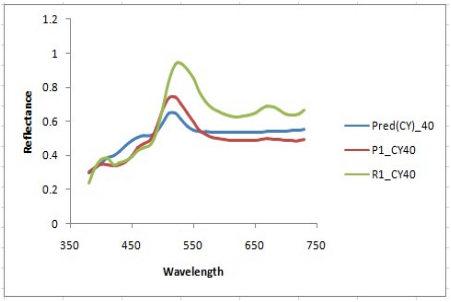

Fig 8.63: CY_40%Reflectance Spectrum of Predicted,P1 & R1

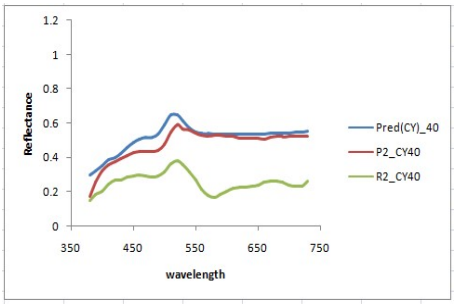

Fig 8.64: CY_40%Reflectance Spectrum of Predicted,P2 & R2

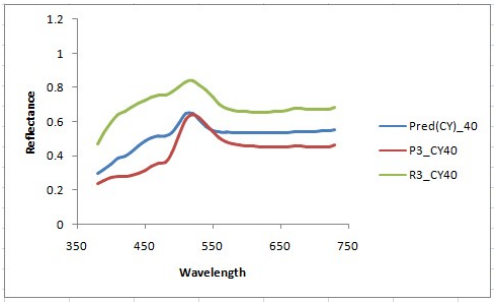

Fig 8.65: CY_40% Reflectance Spectrum of Predicted, P3 & R3

We can observe that, for printer P1, for the CY patch (40% dot area), in the green visible range, the peak of the spectrum for the reprint is higher than for other measured and predicted. On the other hand, lower (higher intensity) value can be observed for printer P2 (P3, respectively), as showed in Fig 8.63 to Fig 8.65.

➢ Comparison of reflectance of **Green(CY)** color patch with20% dot area coverage using P1,P2 & P3

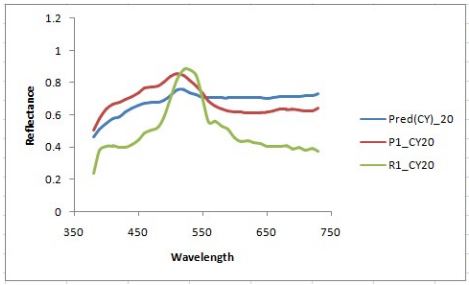

Fig.8.66: CY_20%Reflectance Spectrum, of Predicted, P1 & R1

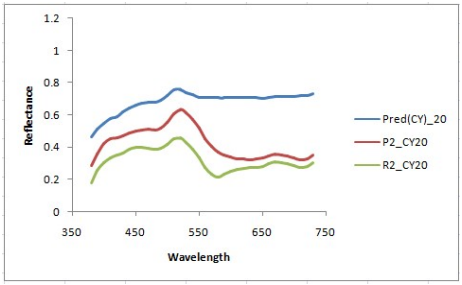

Fig8.67: CY_20%Reflectance Spectrum of Predicted, P2 & R2

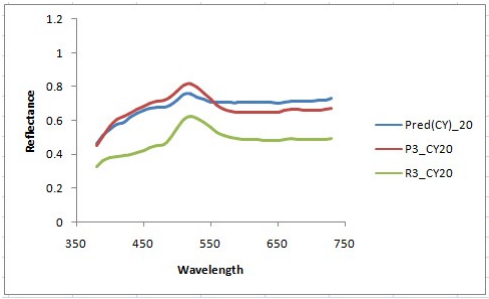

Fig. 8.68: CY_20% Reflectance Spectrum of Predicted, P3 & R3

InFig8.66 to Fig8.68, it has been observed that for CY patch (20% of dot area coverage), in green range, the peak of the spectrum is shifted a little bit for the reprint in comparison to the other measured and predicted spectrums. On the other hand, its intensity is lower for printer P1 than for the two other printers. For printer P2 and P3, the intensity of the spectrum is lower than for the predicted and measured print, for 20% dot area coverage of green (CY) patch.

8.3 Main observations

For two solid colors combination patches, the deviation of reflectance spectrum of reprint samples from predicted and printed samples could be used as an indicator to identify an original sample (print) among a set of print and reprint samples, for blister foil as substrate and gravure printing machines. These deviations could not be compensated by any color post processing.

This study has demonstrated that under same illuminant and printing condition, whenwe use the same printer but different printing cylinders, then the difference between print color patches is higher than when we use same cylinders but different printers. This

higher difference comes fromthe acquisition (scan or capture) and reprint process used to duplicate (imitate)original print samples.

In this study, P1 (gravure Printer) was used as a reference printer. The Tables (8.8, 8.9 and 8.10) summarize the color differences computed for different percentages of dot area coverage (100%,70%,40%,20%) of two-color combinations (red(MY), green(CY) and blue(CM)). Red color results from the combination of magenta (M) & yellow (Y), green from the combination of cyan(C) and yellow (Y), and blue from the combination of cyan (C) & magenta(M).

*Table 8.8: Calculation of Color Differences (ΔE_{00}) of **Blue patch**(CM) between Print samples and Print-Reprint Samples for different Dot Area Coverage*

CM	P1-P2	P1-P3	P1-R1	P1-R2	P1-R3
$\Delta E_{00}(CM_{100\%})$	2.39	5.68	14.16	15.63	**27.03**
$\Delta E_{00}(CM_{70\%})$	2.41	4.24	15.86	21.65	15.70
$\Delta E_{00}(CM_{40\%})$	4.51	4.49	11.86	19.28	17.60
$\Delta E_{00}(CM_{20\%})$	5.25	2.26	11.08	18.39	**10.45**

*Table 8.9: Calculation of Color Differences (ΔE_{00}) of **Red patch**(MY) between Print samples and Print-Reprint Samples for different Dot Area Coverage*

MY	P1-P2	P1-P3	P1-R1	P1-R2	P1-R3
$\Delta E_{00}(MY_{100\%})$	6.76	6.70	22.95	26.08	12.90
$\Delta E_{00}(MY_{70\%})$	4.57	7.28	15.48	18.30	11.26
$\Delta E_{00}(MY_{40\%})$	5.77	5.29	18.77	15.32	12.97
$\Delta E_{00}(MY_{20\%})$	6.62	7.97	17.27	18.14	15.57

*Table 8.10: Calculation of Color Differences (ΔE_{00}) of **Green patch (CY)**betweenPrint samples and Print-ReprintSamples for different Dot Area Coverage*

CY	P1-P2	P1-P3	P1-R1	P1-R2	P1-R3
$\Delta E_{00}(CY_{100\%})$	5.97	4.01	11.44	11.19	25.29
$\Delta E_{00}(CY_{70\%})$	6.34	3.16	16.31	11.38	13.28
$\Delta E_{00}(CY_{40\%})$	7.84	4.14	12.98	20.31	11.68
$\Delta E_{00}(CY_{20\%})$	8.96	5.55	18.55	16.78	15.00

From these Table 8.8, Table 8.9 and Table 8.10, related to the use of different gravure printing machines (P1, P2, P3) to print same sample (color chart on blister foil) under

same printing (parameters) condition, and different dot area coverage, we can observe that the range of color differences between a reference printer (P1) and other printers (P2, P3) is within 2.0 to 9.0 (approx.) when using ΔE_{00} for 2-colors combinations. A digital camera (Sony alpha 350) has been used to capture the print sample and to reprint it with same three printers (P1, P2, P3). In these Tables, reprint samples correspond to R1,R2, R3 depending of the printer used (P1, P2, P3, respectively). The minimum (maximum)color difference value for blue (CM) patch is2.26 (5.68, respectively)between printers (P1 vs. P2, P1 vs. P3) and between print-reprint is 10.45 (27.03, respectively) (ie. for P1 vs. R1, P1 vs. R2, and P1 vs. R3). The maximum values are for 100% of dot area coverage. The minimum values were obtained for blue patches. For red (MY) patch, the minimum (maximum)color differencevalue is of 4.56 (7.97, respectively), between printed samples for 70% (20%, respectively) of dot area coverage of red patches.Between print-reprint samples,minimum (maximum) color difference value is of 11.26 (26.08, respectively), for 70% (100%, respectively) of dot area coverage of red patches. For green (CY) patch,the minimum (maximum) color difference value is of 3.15 (8.96, respectively), for70%(20%, respectively) of dot area coverage of green patch, for the three printed samples. The minimum (maximum) color difference value is of 11.19 (25.29, respectively)for 100% (100%, respectively) of dot area coverage of green patch,forprint-reprint samples.

From these Tables, it can also observe that, for every dot area coverage, the color differences increase after reprint of the original printed samples, for three printers. Color differences between reference printer (P1) and other printers (R1, R2, R3) vary within the range from 10.5 to 27.0 (approx.) for two-color combinations of color patches printed on blister foil substrate. From the prediction data computed by YNSN model, the spectrums of the printed samples are closer to the spectrum of the original print sample than to the spectrum of the reprint samples, for the three gravure printers. Therefore, we claim that it will be challenging for counterfeiters to predict the data after scan and reprinted data.

- Comparison of the gamut volume of printed and reprinted samples on blister foils is done for three different gravure 4-color printers.

❖ **Comparison of gamut volumes for Printer1, Printer2 & Printer3 (Figures 8.69 to 8.74).**

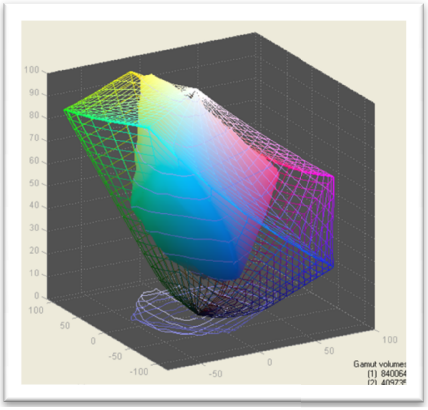

Fig.8.69: Gamut volume of printed sample for Printer1(P1)

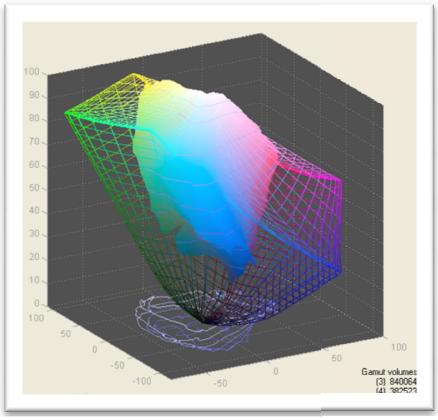

Fig.8.70: Gamut volume of reprinted samplefor Printer1(P1)

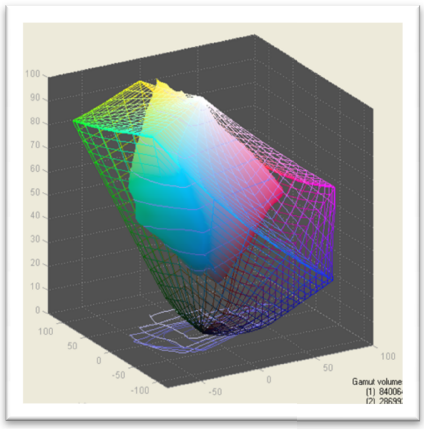

Fig.8.71: Gamut volume of printed sample for Printer2(P2)

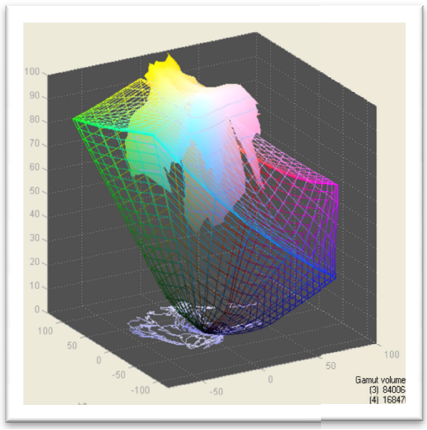

Fig.8.72: Gamut volume of reprinted sample for Printer2(P2)

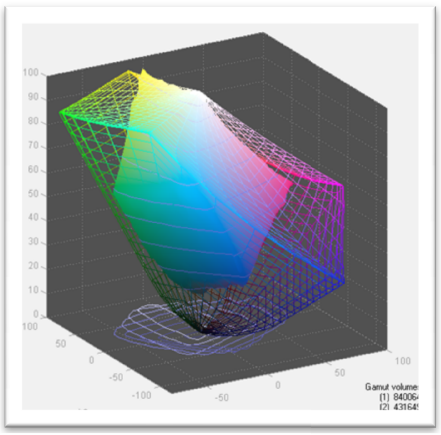

Fig.8.73: Gamut volume of printed sample for Printer3(P3)

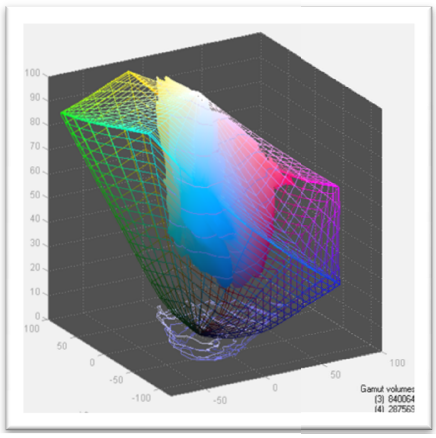

Fig.8.74: Gamut volume of reprinted sample for Printer3(P3)

In the above Figures(8.69 to 8.74), each print and reprint color gamut is represented as solid gamut, meanwhile the sRGB color gamut is used as standard color gamut with wider color volume. It has been observed that the volume of the color gamut of the print sample is more compact and bigger (in L*a*b* color space) than the color gamut volume of scanned and reprinted samples for the three gravure printers. Same ink and same blister foil substrate were used for each print. The color gamut volume of printed and reprinted samples for different gravure printers are reported in Table8.11.From these results we can draw the assumption that color gamut differences can be used as an indicator whether a print is original or not, and could be used to identify an original printer used to print a reference sample.

Table 8.11: Comparison of color gamut volumes of printed and reprinted samples for three different printers

Samples	Print (Gamut Volume)	Reprint (Gamut Volume)	Remarks
Printer1(P1)	**409735**	382523	When a sample is printed with different press, even if ink and foil are same, then the gamut volume is lower for reprinted sample than printed sample
Printer2(P2)	**286992**	168470	
Printer3(P3)	**431649**	287569	

❖ **Comparison of gamut volumes for two different inks printed with Printer3.**

Table8.12: Comparisons of color gamut volume of printed and reprinted samples for Ink1 & Ink2 for one gravure printer

Samples	P3&Ink1(Gamut Volume)	P3&Ink2(Gamut Volume)
Print Sample	**431649**	368792
Reprint Sample	**287569**	104236

As reported in Table8.12,some difference between color gamut volumescan be observed. Under the same illuminant condition and same printing procedure, when substrate and press are same but inks are different, then differencesbetween color gamut can be observed (Fig 8.75). To print the artwork with a 4-color gravure printing machine four cylinders (cyan, magenta, yellow and black) were needed. After scanning the printed artwork, four cylinders were required to engrave the scanned artwork on four new cylinders and reprint it. So after reprint process (with different ink than the first print, but

same press),the volume color gamut has decreased in comparison with the volume of the color gamut of the oringinal printed artwork which was printed with same press.

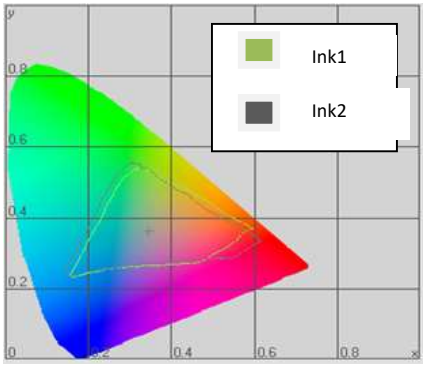

Fig.8.75**:** 2D gamut volume (in xy chromaticity diagram) of print artwork printed with Printer3 and with Ink1& Ink2.

❖ **Comparison of reflectance spectrum of solid colors (cyan, magenta, yellow and black) of two different inks printed with Printer3.**

➢ Comparison of reflectance spectrums of solid color Cyan between Ink1 & Ink2 printed and reprinted withPrinter3 (Figures 8.76 to 8.77).

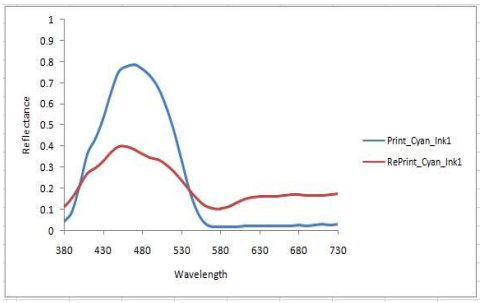

Fig.8.76: Reflectance spectrum of solid color Cyan of Ink1for Printer3

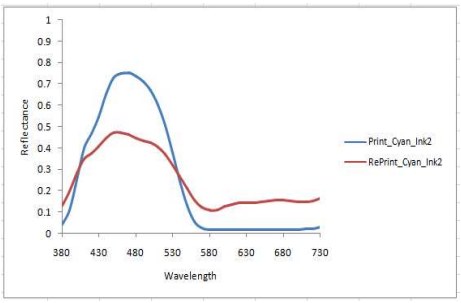

Fig. 8.77: Reflectance spectrum of solid color Cyan of Ink2for Printer3

➢ Comparison of reflectance spectrums of solid color Magenta between Ink1 & Ink2 printed and reprinted with Printer3 (Figures 8.78 to 8.79).

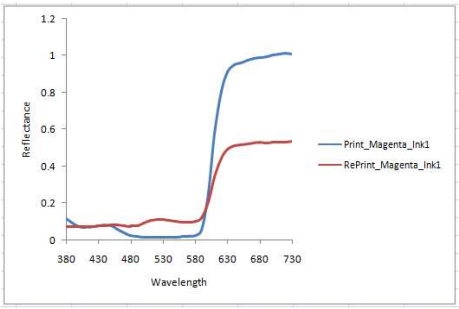

Fig.8.78: Reflectance spectrum of solid color Magentaof Ink1for Printer3

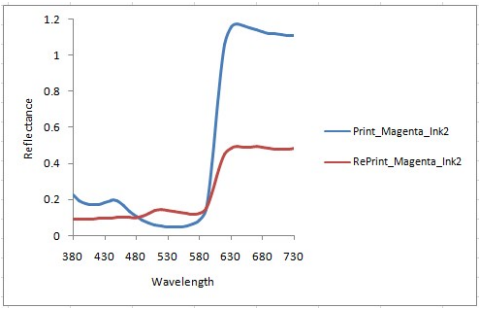

Fig.8.79: Reflectance spectrum of solid color Magentaof Ink2for Printer3

- Comparison of reflectance spectrums of solid color Yellow between Ink1 & Ink2 printed and reprinted with Printer3 (Figures 8.80 to 8.81).

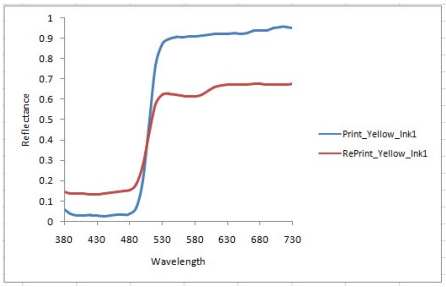

Fig.8.80: Reflectance spectrum of solid color Yellowof Ink1 for Printer3

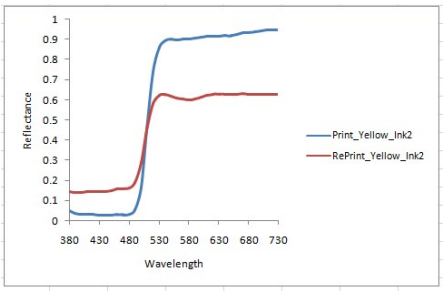

Fig.8.81: Reflectance spectrum of solid color Yellow of Ink2 for Printer3

- Comparison of reflectance spectrums of solid color Black between Ink1 & Ink2 printed and reprinted with Printer3 (Figures 8.82 to 8.83).

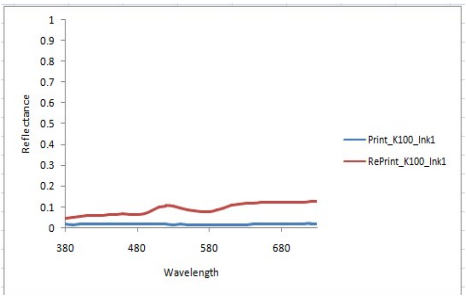

Fig.8.82: Reflectance spectrum of solid color Black of Ink1for Printer3 (P3)

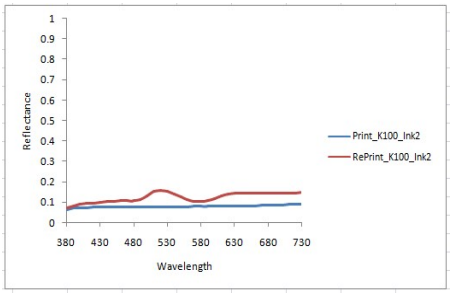

Fig.8.83: Reflectance spectrum of solid color Blackof Ink2 for Printer3 (P3)

- Comparison of reflectance spectrums of solid color Blue (CM) between Ink1 & Ink2 printed and reprinted with Printer3 (Figures 8.84 to 8.85).

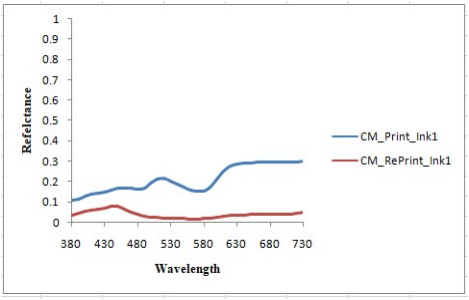

Fig.8.84: Reflectance spectrum of solid color Blue(CM) of Ink1for Printer3 (P3)

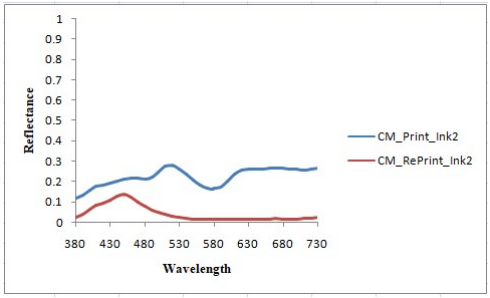

Fig 8.85: Reflectance spectrum of solid color Blue(CM)of Ink2 for Printer3 (P3)

- Comparison of reflectance spectrums of solid color Green (CY) between Ink1 & Ink2 printed and reprinted with Printer3 (Figures 8.86 to 8.87).

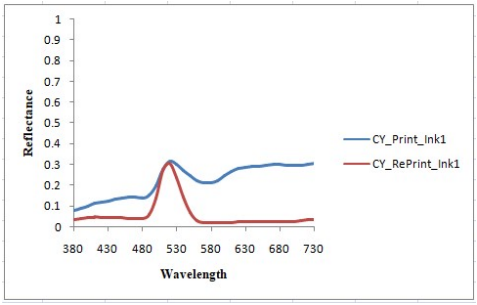

Fig 8.86: Reflectance spectrum of solid color Green(CY) of Ink1for Printer3 (P3)

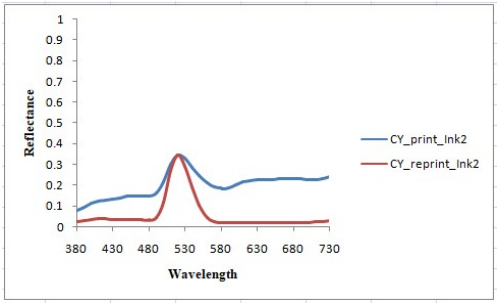

Fig.8.87: Reflectance spectrum of solid color Green(CY)of Ink2 for Printer3 (P3)

- Comparison of reflectance spectrums of solid color Red (MY) between Ink1 & Ink2 printed and reprinted with Printer3 (Figures 8.88 to 8.89).

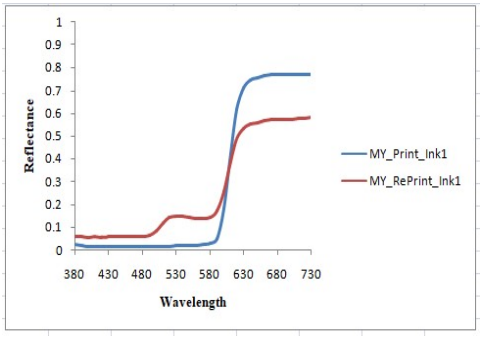

Fig 8.88: Reflectance spectrum of solid color Red(MY) of Ink1for Printer3 (P3)

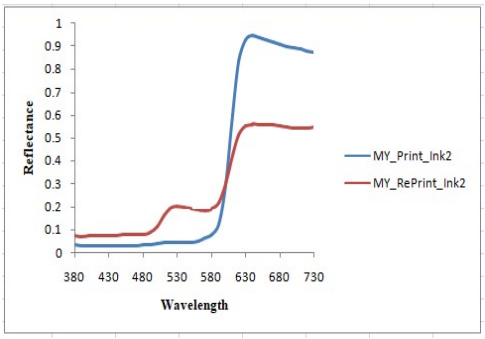

Fig 8.89: Reflectance spectrum of solid color Red(MY)of Ink2 for Printer3 (P3)

- Comparison of reflectance spectrums of solid color CMY between Ink1 & Ink2 printed and reprinted with Printer3 (Figures 8.90 to 8.91).

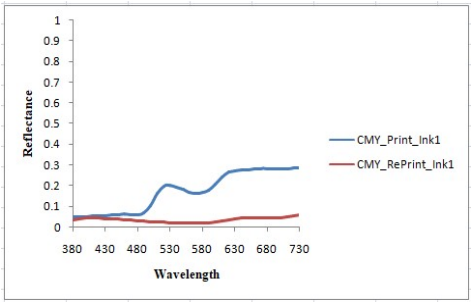

Fig 8.90: Reflectance spectrum of solid color CMY of Ink1for Printer3 (P3)

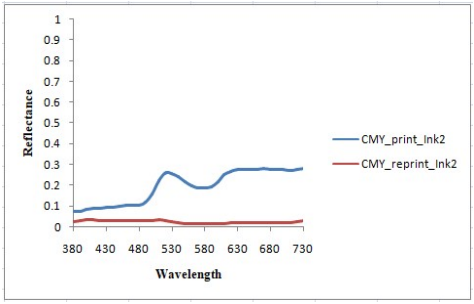

Fig.8.91: Reflectance spectrum of solid color CMY of Ink2 for Printer3 (P3)

- Comparison of reflectance spectrums of solid color CMYK between Ink1 & Ink2 printed and reprinted with Printer3 (Figures 8.92 to 8.93).

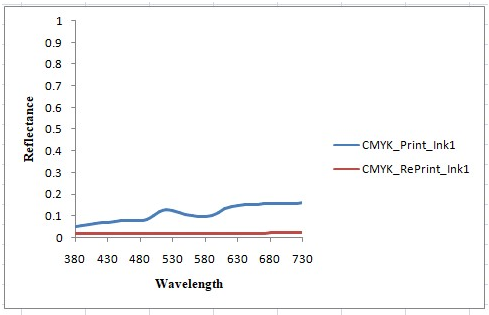

Fig.8.92: Reflectance spectrum of solid color CMYK of Ink1for Printer3 (P3)

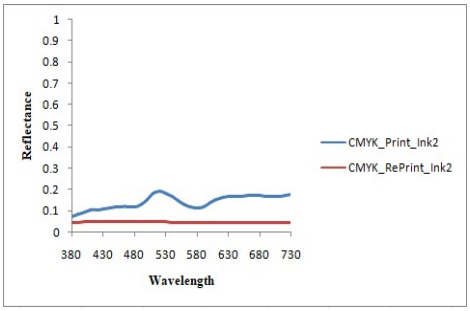

Fig 8.93: Reflectance spectrum of solid color CMYK of Ink2 for Printer3 (P3)

Figures 8.76 to 8.93 illustrate the reflectance spectrums of solid color cyan, magenta, yellow,black,blue,green,red,CMY and CMYK of two different inks used to print and reprintthe reference artwork on blister foil by same gravure printer. Same printing conditions, same output device (gravure printer), same substarte (blister foil), were used for print and reprint, but printing cylinders were different (one for print and another one for reprint process) and inks were different between first print (with Ink 1) and second print (with Ink 2).Whatever the ink, for solid colors cyan, magenta, yellow and red patches the intensity of reflectance spectrum of the print sample is higher than the scanned reprint sample. Such difference could be used to authenticate an original print sample among different reprint samples. Some differences have been observed from reflectance spectrums when using another ink (Ink2) by keeping the same output device and substrate (under same printing condition). These spectral differences has been analyzed using the Root Mean Squared Error (RMSE) values between the two inks used for gravure printing (Ink 2 vs Ink 1). The RMSE values between an original print artwork and a scanned reprinted sample are reported in Table8.13.The RMSE values are quite similar.

Table8.13: Comparisons of reflectance spectrum of solid colors Cyan, Magenta, Yellow Black between a print and a reprint artwork, printed withInk1 & Ink2, for one gravure printer (Printer 3).

Samples	P3&Ink1	P3&Ink2
Solid Cyan(C)_RMSE	0.201	0.155
Solid Magenta(M)_RMSE	0.268	0.386
Solid Yellow(Y)_RMSE	0.219	0.239
Solid Black(K)_RMSE	0.079	0.048
Solid Blue(CM)_RMSE	0.185	0.193
Solid Green(CY)_RMSE	0.187	0.155
Solid Red(MY)_RMSE	0.129	0.22
Solid CMY_RMSE	0.165	0.19
Solid CMYK_RMSE	0.098	0.101

From the comparisons done between printed samples (original) and scanned reprinted samples,it also noticed that the consistency of gravure printed samples changes when printing cylinders are changed. Few variations have also been observed when same cylinders are used with different gravure printing machines. The differences are higher when duplicate cylinders are made after capturing or scanning the printed samples.

In this study it has been demonstrated that the use of spectral signature, colorimetric values, color gamut difference, RMSE statistical analysis, ANN model and YNSN models for prediction and comparison purpose, they could provide low cost security solutions to protect medicine packaging. These methods could also be used to authenticate gravures printed samples on blister foil substrate. Since most of the medicines are packed with blister foil material(printed by gravure printers) then the proposed security solutions could be used in pharmaceutical industry to define the originality of products at manufacturing level.

CHAPTER 9

9. CONCLUSION

Pharmaceutical products are used to prevent any disease and save lives if they are authentic, good quality, safe, effective, and packed with original package. If the medicines are duplicated, then the use of counterfeited medicines could be harmful and create severe health hazard for patient. The packaging of medicines also plays an important role to the society to provide original medicines. Beside this, the original manufacturers are also worried as their profitability is affected by the counterfeiters. Moreover, the brand reputation of company is affected by the counterfeited medicine packaging. The current study has been focused on the medicine packaging and it shows that the color consistency can be used to authenticate the original print sample. Due to the inertness, temper evident features, blister foil are mostly used for medicine packaging. The image or text has been printed on the package to provide the information of product. Counterfeiters imitate the medicine packaging by different devices or technologies. For a bulk production of medicine packaging, gravure printing machines have been used in pharmaceutical packaging industry. Different camera, scanner devices are used as simple way to duplicate the medicine packages and the samples are then reprinted to produce counterfeited packages. From the current study it has been analyzed that different basic color features can be used to differentiate between original and counterfeited samples. For the unique feature of reflectance spectrum of color, the difference of nature of spectrum of cyan, magenta, yellow and black colors and their combinations have been studied to compare the print samples with the scanned reprint samples. It has been observed that if an image is printed with single color, the counterfeiters may try to match it with several color matching solution though it is not possible to match the spectrum. It would be much more difficult if it is multicolor printing. Hence, in this study, multicolor printing is proposed. To measure color consistency of multicolor printing, IT 8.7/3 color chart designed by International Color Consortium has been used which has all possible combination of single color cyan, magenta, yellow and black.A statistical analysis like Root Mean Square Error (RMSE) has been applied to compute the difference and authenticate the printed (original) output sample from three gravure printers within visible range of spectrum. It has been noticed that even if the substrate and ink same, the reflectance spectrums of print and reprint samples are different as two different print cylinders have been used

for same gravure output device. When cylinders are same but gravure printers are different, then the color difference is lesser compared to when two different cylinders (one is original and another is counterfeited) are used for same gravure machine. To establish the difference between original and counterfeited samples, the color difference is one of basic feature for authentication purpose. This property can be used to detect the original print samples.

By using the spectral curves of CMYK colors, it has been shown that the spectral curves of cyan, magenta, yellow and black inks printed and reprinted on blister foils are different for different printers. When a printed sample is scanned and reprinted by same output device, the spectral signature of the reprint differs from the original print. This property has been used to identify the original printer. In this study, the shape of spectral curves of few color inks printed and reprinted by different printers has been studied. The shape of spectral curves of few color inks printed and reprinted with same printer has been also studied. It has been observed that the shape of each spectral curve is unique for each specific ink/substrate combination. Hence if a print is scanned and reprinted, it can easily demonstrate whether it was printed by an original printer or not. It has been also shown that between print and reprinted samples, the RMSE (Root mean square error) values are different for different printers, especially in the red (380nm-490nm), green (500nm-600nm) and blue (610nm-730nm) regions of the visible domain. Hence, RMSE (Root mean square error) between print and reprinted samples can be used to authenticate the printer used among different printers. Other spectral or color difference metrics could be also used additionally to the RMSE metric used, but for this preliminary study RMSE of spectral differences was sufficient to identify the original printer.

For medicine packaging, the work has immense importance to identify counterfeited or fake medicines which has great social impact.In this study, it has been shown that the colorimetric values of the IT 8.7/3 color chart printed on blister foils are different for different printers even if the same gravure cylinder has been used. An Artificial Neural Network (ANN) model has been used to predict the L*a*b* colorimetric values of color patches for a printer. For the predicted values of a print sample (printed with printer P1 taken as reference) has compared with measured values of three printers. The

lightness difference and color differences of different printers are measured. It has shown that the color features can be seen as a very efficient tool to differentiate between print and reprint sample. It has been found that the lightness difference and color difference are much higher for scanned reprint samples with the predicted values in comparison to the original print samples. Hence the method can be used to identify whether a packaged print is printed by original manufacturers or their authorized printers or it is reprinted after scanning or taking image of the original artwork by the counterfeiters. From the study it may concluded that it is difficult for counterfeiters to counterfeit any multicolor artwork on blister foil through gravure printing process after scanning or capturing image of original (print) sample.

For an image reproduction printing workflow, color gamut volume is useful to analyze an image gamut against printer device gamut. In this study, it has showed that after scan and print process (i.e. a reprint) the volume and the size of the color gamut of a gravure printer differ from the one of an original print. In both cases print samples were printed on blister foil. Experimental results show that the volume and the size of the color gamut of a scanned reprint samples are smaller than those of the color gamut of an original print samples for three different gravure printing machines. It has been demonstrated that the color gamut of print artworks is primarily affected by the change of input gravure cylinders and also by a change of output device (gravure printing machines). The reduced color gamut is responsible of color inconsistencies observed between an original print artwork and a reprint artwork after scanned and print process. To minimize these color inconsistencies color management may be applied, but it is very challenging to compensate out-of-gamut colors resulting from the reprint process (i.e. to expand the volume of the color gamut of a reprint artwork to fit the wider gamut of an original print artwork). In the experiments, it is also investigated the effect on gamut boundaries related to a change of ink for same gravure printer and same printing conditions. It has also been analyzed that, using of two different inks, some color inconsistencies are observed between an original print artwork and a reprint artwork after scanned and print process. These inconsistencies are observed when the corresponding colors gamuts are compared as well as the shape of the spectral curves of solid colors are compared. From this study, it is found that as the shape of spectral curve of each ink is unique and may be treated as spectral signature for a specific printer. When a printed sample is scanned and reprinted by same output device (gravure

printer) than also the spectral curves of reprint samples differ significantly from the original print. It has also been observed that the differences are much higher in case of other printers. Naturally, the difference will be significant if it is printed by some other printers as it would be done in case of counterfeiting.

Hence, if a print is scanned and reprinted by counterfeiters, it could be easily found whether it was printed by an original printer or not from its color consistencies. This work has immense importance for pharmaceutical industries with a huge social impact.

FUTURE WORK

In future, similar studies may be done with paper laminations, other polymeric substrates which are widely used for food or cosmetics packaging. Experiments may be done for other printing process like flexography, offset printing. The process may be extended to more image capture devices.The extended process may be focused on the effect of different printing parameters to authenticate prints output for other printers and substrates used. The robustness of the methods will be evaluated against counterfeit packaging and provide secure product to the society. At present, color stability of digital printing of medicine packages on metal foils is not satisfactory and hence not widely used. However, in future, a color consistency of digital printing is another area which needs to be explored.

REFERENCES:

1. Roger D. Hersch, Patrick Emmel, Fabien Collaud, FrédériqueCrété, "Spectral reflection and dot surface prediction models for color halftone prints", Journal of Electronic Imaging 14(3), 033001,Jul–Sep, 2005.
2. Silvia Zuffi, Raimondo Schettini, "An innovative method for spectral-based printer characterization", Color Imaging: Device-Independent Color, 2001.
3. Roger David Hersch, Frédérique Crété, "Improving the Yule-Nielsen modified spectral Neugebauer model by dot surface coverage depending on the ink superposition conditions", IS&T/SPIE Electronic Imaging Symposium, Conf. Imaging X: Processing, Hardcopy and Applications, , SPIE Vol. 5667, 434-44, Jan. 05.
4. Roger David Hersch, Adish Kumar Singla, "An Ink Spreading Model for Dot-On-Dot Spectral Prediction", Proc. IS&T 14th Color Imaging Conference (CIC 14), Scottsdale, AZ, Vol. 14, 38-43, 2006.
5. R. D. Hersch, M. Brichon, T. Bugnon and M. Hebert, "Deducing Ink Spreading Curves from Reflection Spectra Acquired Within Printed Color Images", Journal of Imaging Science and Technology, 53(3): 030502–030502-7, 2009.
6. L Iovine, S Westland and TLV Cheung, "Application of Neugebauer-Based Models to Ceramic Printing", IS&T/SID Twelfth Color Imaging Conference,https://www.academia.edu/60131389.
7. R. D. Hersch, F. Collaud, F. Crété , P. Emmel, "Spectral prediction and dot surface estimation models for halftone prints" , IS&T/SPIE Electronic Imaging Symposium, Conf. Imaging IX: Processing, Hardcopy and Applications, SPIE Vol. 5293, 356-369, Jan. 04.
8. Robert Chung, and Fred Hsu, "Predicting Color of Overprint Solid", Proc. of the 36th IARIGAI Research Conference, Advances in Color Reproduction. 2009.
9. Hansjorg Kunzlp, Anja Noser, Marcel Loher and Safer Mourad, "Prediction of colorimetric measurements in newspaper printing using neural networks", Proc. SPIE 3648, Color Imaging: Device-Independent Color, Color Hardcopy, and Graphic Arts IV, doi: 10.1117/12.334575; (22 December 1998).
10. Kiran Deshpande and Phil Green, "A simplified method of predicting the colorimetry of spot color overprints", 18th Color Imaging Conference Final Program and Proceedings, Society for Imaging Science and Technology 2010.

11. Mark Shaw, Gaurav Sharma, Raja Bala, Edul N. Dalal, "Color Printer Characterization Adjustment for Different Substrates", Color research and application, Volume 28, Number 6, December 2003.

12. Théo Phan Van Song, Christine Andraud , Luis Ricardo Sapaico , Maria V. Ortiz Segovia, "Color prediction based on individual characterizations of ink layers and print support", Society for Imaging Science and Technology, https://doi.org/10.2352/ISSN.2470-1173.2018.8.MAAP-165,2018 .

13. Fred Hsu, "The effect of dot gain linearization as a printer calibration criteria on color matching accuracy", Printer calibration, Test target 5.0.

14. Dmitry Tarasov, Oleg Milder, Andrey Tyagunov, "Inverse Problem of Spectral Reflection Prediction by Artificial Neural Networks: Preliminary Results", Ural Symposium on Biomedical Engineering, Radioelectronics and Information Technology (USBEREIT), 978-1-5386-4946-6/18, IEEE 2018.

15. Oleg B. Milder1 and Dmitry A. Tarasov, "Spectral Reflection Prediction by Artificial Neural Network", CEUR-WS.Org/VOL-2076.

16. Francisco Imai, Mitchell Rosen, Dave Wyble, Roy Bernsa and Di-Yuan Tzeng, "Spectral reproduction from scene to hardcopy I: Input and Output", SPIE Vol. 4306 (2001).

17. Patrick Jackman, Da-Wen Sun , Gamal ElMasry, "Robust color calibration of an imaging system using a color space transform and advanced regression modelling", Elsevier Ltd. Meat Science 91 402–407,(2012).

18. Kateryna Savchenko and OlenaVelychko, "Printing Inks' Characteristics", Journal of Materials Science and Engineering B 3 (7) (2013) 464-468.

19. Abhay Sharma and Xiaoying Rong, "Establishing Standards for Color and Print Quality in Large Format Inkjet Printing", Journal of Imaging Science and Technology, 58(3): 030504-1–030504-13, 2014.

20. Haoxue Liu, Min Huang, Yu Liu, Bing Wu, and Yanfang Xu, Ningfang Liao, Guihua Cui, "Color-Difference Evaluation for Digital and Printed Images", Journal of Imaging Science and Technology, 57(5): 050502-1_050502-9, 2013.

21. Renée Charrière, Mathieu Hébert, Alain Trémeau, and Nathalie Destouches, "Color calibration of an RGB camera mounted in front of a microscope with strong color distortion", Applied Optics, Vol. 52, No. 21 , 20 July 2013.

22. Henry R. Kang, Peter G. Anderson, "Neural network applications to the color scanner and printer calibrations", Journal of Electronic Imaging 1(2), 125-135 (April 1992).

23. Rui Gong, Qing Wang, Xiaopeng Shao, Jietao Liu, "A color calibration method between different digital cameras", Optik 127 (2016) 3281–3285.

24. Zhihong Pan, Ying X. Noyes, Jon Hardeberg, Lawrence Lee and Glenn Healey, "Color Scanner Characterization with Scan Targets of Different Media Types and Printing Mechanisms", https://www.researchgate.net/publication/253778997, December 2000, DOI: 10.1117/12.410774.

25. Bangyong Sun, Han Liu, Shisheng Zhou, andWenli Li, "Evaluating the Performance of Polynomial Regression Method with Different Parameters during Color Characterization", Hindawi Publishing Corporation Mathematical Problems in Engineering Volume 2014, Article ID 418651.

26. P. Emmel, R.D. Hersch, "Colour Calibration for Colour Reproduction" ISCAS 2000 - IEEE International Symposium on Circuits and Systems, Geneva, Switzerland, May 28-31, 2000.

27. V. Ostromoukhov, R.D. Hersch, C. Pe´raire, P. Emmel, I. Amidror, "Two Approaches in Scanner-Printer Calibration: Colorimetric Space-based vs. "Closed-Loop", Proceedings Conf. Device-Independent Color Imaging, SPIE Vol. 2170, pp. 133–142.

28. Hui-Liang Shen and John H. Xin, "Colorimetric and Spectral Characterization of a Color Scanner Using Local Statistics" Journal Imaging Science and Technology 48: 342–346 (2004).

29. N. P. Garg, A. K. Singlaand R. D. Hersch, "Calibrating the Yule–Nielsen Modified Spectral Neugebauer Model with Ink Spreading Curves Derived from Digitized RGB Calibration Patch Images", Journal of Imaging Science and Technology,52(4): 040908–040908-5, 2008.

30. Tuija Jetsu, Ville Heikkinen, JussiParkkinen, Markku Hauta-Kasari, Birgitta Martinkauppi, SeongDeok Lee, Hyun Wook Ok and Chang Yeong Kim, "Color Calibration of Digital Camera Using Polynomial Transformation", Society for Imaging Science and Technology,CGIV2006.

31. Pau Soler and Jordi Arnabat, "Efficient Color Printer Characterization Based on Extended Neugebauer Spectral Models", Proc. of SPIE-IS&T Electronic Imaging, SPIE Vol. 6493, 64930S, 2007.

32. Juan Martínez-García, Mathieu Hébert, Alain Trémeau, "Color calibration of an RGB Digital Camera for the Microscopic observation of highly specular materials",Proc. of SPIE-IS&T Vol. 9398 93980I-1,2015.

33. Prarthana Shrestha, Bas Hulsken, "Color accuracy and reproducibility in whole slide imaging scanners", Journal of Medical Imaging, Vol. 1(2), Jul–Sep 2014.

34. Laurence T. Maloney and Brian A. Wandell, “Color constancy: a method for recovering surface spectral - reflectance”, Optical Society of America, Vol. 3, No. 1,January 1986.

35. Mathieu Hebert, Roger D. Hersch, “Review of Spectral Reflectance Models for Halftone Prints: Principles, Calibration, and Prediction Accuracy”, Color research and application, Volume 40, Number 4, August 2015.

36. Peter Blum, “Reflectance Spectrophotometry and Colorimetry”, PP Handbook,November, 1997.

37. George Lychock, “ Dot Area, Dot Gain, and n-Factors”, X-Rite, August 22, 1995.

38. Paul D. Fleming, James E. Cawthorne, Falguni Mehta, Saurabh Halwawala, and Margaret K. Joyce, “Interpretation of Dot Fidelity of Ink Jet Dots Based on Image Analysis”, Journal of Imaging Science and Technology, Volume 47, Number 5, September/October 2003.

39. Dean Valdec , Krunoslav Hajdek , Lucia Vragovic and Robert Gecek, “Determining the Print Quality Due to Deformation of the Halftone Dots in Flexography”, Appl. Science,2021, 11, 10601,https:// doi.org/10.3390/app112210601,2021.

40. Li Yang, “Spectral Model of Halftone on a Fluorescent Substrate”, Journal of Imaging Science and Technology, Volume 49, Number 2, March/April 2005.

41. Mathieu Hébert, “Yule-Nielsen effect in halftone prints: Graphical analysis method and improvement of the Yule-Nielsen transform”, SPIE Electronic Imaging – Color Imaging XIX: Displaying, Processing, Hardcopy, and Applications, 9015-27,2-6 February 2014.

42. https://www.xritephoto.com/

43. Francisco H. Imai, Mitchell R. Rosen and Roy S. Berns, “Comparative Study of Metrics for Spectral Match Quality”, The First European Conference on Colour Graphics, Imaging, and Vision, CGIV 2002.

44. Mark Shaw, Mark Fairchild, “Evaluating the 1931 CIE Color Matching Functions”, Color research and application, February 2002.

45. Arthur D. Broadbent, “A Critical Review of the Development of the CIE1931 RGB Color-Matching Functions”, Color research and application, Volume 29, Number 4, August 2004.

46. Mehmet Volkan Sağirlibaş, “Color Recipe Prediction with Neural Networks”, Thesis,Dokuz Eylül University Graduate School of Natural and Applied Sciences, September, 2009.

47. Andrew Stockman, Lindsay T. Sharpe, Clemens Fach, "The spectral sensitivity of the human short-wavelength sensitive cones derived from thresholds and color matches", Vision Research 39 , 2901–2927,1999.

48. Gaurav Sharma, Wencheng Wu, Edul N. Dalal, "The CIEDE2000 Color-Difference Formula: Implementation Notes, Supplementary Test Data, and Mathematical Observations", Color Research and Application,Volume 30, Number 1, February 2005.

49. Robert Chung, Edline Chun, Seunga Kang Ha, Chao-Yi Hsu, "Test Targets 3.1: A Collaborative effort exploring the use of scientific methods for color imaging and process control", RIT School of Print Media, June 2003.

50. Robert Chung and Yoshikazu Shimamura, " Quantitative Analysis of Pictorial Color Image Difference", RIT, Toppan Printing Company.

51. J A Stephen Viggiano, "Modeling the Color of Multi-Colored Halftones", RIT Research Corporation, Graphics Division.

52. Brian P. Lawler, " Color management: At last we're on the road to reliable color", v.5,7/23/2002.

53. GretagMacbeth, Spectrophotometer & XY Table, SpectrolinoSpectroScan, Serial Interface, Edition 5.

54. https://www.sony-asia.com/electronics/support/a-mount-body-dslr-a300-series/dslr-a350/specifications.

55. Kiran Deshpande, Phil Green, Michael R Pointer, "Metrics for Comparing and Analyzing Two ColourGamuts", Color research and application, volume 40, Number 5, October 2015.

56. Cheol-Hee Lee, Eung-JooLee, Suk-ChulAhn, and Yeong-Ho Ha, "Color Space Conversion via Gamut-Based Color Samples of Printer", Journal of Imaging Science and Technology, Volume 45, Number 5, September/October 2001.

57. Bangyong Sun, Han Liu, Shisheng Zhou, Junhong Xing,CongjunCaoa and Yuanlin Zheng, "A colour printer calibration method based on gamut division algorithms", Coloration Technology, Society of Dyers and Colourists,2014.

58. Yongda Chen, Roy S. Berns, Lawrence A. Taplin, "Extending Printing Color Gamut by Optimizing the Spectral Reflectance of Inks", Munsell Color Science Laboratory, Chester F. Carlson Center for Imaging Science, Rochester Institute of Technology, Rochester, New York.

59. Dogan Tutak, Huseyin N. Beytut, Arif Ozcan, "Investigation of the effects of different ink density values on color gamut in offset printing", Journal of Graphic Engineering and Design, Volume 9 (1), 2018.

60. Esther Perales, Francisco M. Martinez-Verdu,ValentinViqueira, Jesus Fernandez-Reche, Jose A. Dıaz,JoanUroz, "Comparison of Color Gamuts Among Several Types of Paper with the Same Printing Technology", Color research and Application, Volume 00, Number 0, Month 2009.

61. http://www.gamutvision.com/

62. Akshay V. Joshi & Swati Bandyopadhyay, "Effect of gravure process variables on void area in shrink film, Journal of Coatings Technology and Research",Volume11, Number5,J Coat Technol Res (2014).

63. Mahasweta Mandal, Swati Bandyopadhyay, "To Predict the Waterfastness Rate of Foil Print", International Journal of Engineering Research & Technology (IJERT), Vol. 8 Issue 06, June-2019.

64. Mahasweta Mandal, Swati Bandyopadhyay, "Study of the lightfastness properties of prints on blister foils by spectral reflectance", Color Res Appl. 2019, doi: 10.1002/col.22449.

65. Mahasweta Mandal, Swati Bandyopadhyay, "Artificial neural network approach to predict the lightfastness of gravure prints on the plastic film", Color Res Appl. 2020, doi: 10.1002/col.22504.

66. Mahasweta Mandal, Swati Bandyopadhyay, "To Predict the Waterfastness Rate of Foil Print Applying Artificial Neural Network", International Journal of Computer Applications (0975 – 8887) Volume 178 – No. 35, July 2019.

67. Mahasweta Mandal, Swati Bandyopadhyay, "To Predict the Lightfastness of Prints on Foil Applying Artificial Neural Network", Society for Imaging Science and Technology,2020.

68. Ambrish Pandey, Amit Poonia, Nishant, "Study of Print Quality on Different Substrates in Gravure Printing", International Journal of Engineering Research and Development, Volume 5, Issue 5 (December 2012), PP. 19-22.

69. Yu-Ju Wu, Paul D. Fleming III and Alexandra Pekarovicova, "Quality Analysis of Gravure Spot Color Reproduction with an Ink Jet Printer", Vol.52, No.6, Journal of Imaging Science and Technology · November 2008.

70. XinguangLv, Chang Liu, Yumei Wu, Heiner Ipsen, " Variation of Gravure Printing Characteristic Curves", Proceedings of the 17th IAPRI World Conference on Packaging, 978-1-935068-36-5, 2010.

71. Donald E. Troxel, William F. Schreiber, Samuel M. Goldwasser, Malik M. A. Khan, Len Picard, Michael A. Ide, and Carolyn J. Turcio, "Automated Engraving of Gravure Cylinders", IEEE Transactions on Systems, Man, and Cybernetics, vol. SMC- 11, no. 9, September 1981.

72. Bob Chung, Rochester Institute of Technology, "Gravure Research Agenda: The Journey of a Test Form from Engraving to Proofing", Gravure/February 2006.

73. M.F.J. Bohan, A.M. Clist, T.C. Claypole and D.T. Gethin, "Characterisation of gravure cylinders", https://www.researchgate.net/publication/265491856,January 2001.

74. Philip Pimlott, "Cylinder Smarts: A Comprehensive Guide to Essential Gravure Technology", Gravure AIMCAL Alliance (gaa.org).

75. Xiaoying Rong, Jan Pekarovic, and Alexandra Pekarovicova," Gravure Printability from Laser and Electromechanically Engraved Cylinder", January 2004.

76. Helmut Kipphan, Handbook of Print Media: Technologies and Production Methods. Publisher: Springer-Verlag, Berlin Heidelberg,2001.

77. Packaging South Asia, https://packagingsouthasia.com/packaging production/engraving-of-rotogravure-cylinders/.

78. Do-Guk Kim and Heung-Kyu Lee, "Colour laser printer identification using halftone texture fingerprint", Electronics Letters, 25th June 2015 Vol. 51 No. 13 pp. 981–983.

79. Soo-Hyeon Lee ,Hae-Yeoun Lee, "Detecting Counterfeit Bills and Their Forgery Devices using CNN-based Deep Learning", ICCGI 2018 : The Thirteenth International Multi-Conference on Computing in the Global Information Technology, ISBN: 978-1-61208-641-5,2018.

80. IuliiaTkachenko, AlainTremeauandThierryFournel, "Fighting against medicine packaging counterfeits: rotogravure press vs. cylinder signatures", Proceedings of IEEE International Workshop on Information Forensics and Security (WIFS), 11 December 2020, New York, pp. 1-6. doi :10.1109/WIFS49906.2020.9360883.

81. IuliiaTkachenko, AlainTrémeau and Thierry Fournel, "Authentication of rotogravure print-outs using a regular test pattern", Journal of Information Security and Applications,66 (2022) 103133, March 2022.

82. Das, I.; Bandyopadhyay, S.; Trémeau, A. "Characterization of Prints Based on Microscale Image Analysis of Dot Patterns", Applied Sciences 11(14):6634, 2021, DOI: 10.3390/app11146634.

83. J. Kerry, "Aluminium foil packaging", Woodhead Publishing Limited, 2012.

84. A. Kailash, Kumar,N. Vishal Gupta, P. Lalasa ,SudeepgoudSandhil, "A Review on Packaging Materials with Anti-Counterfeit, Tamper Evident Features For Pharmaceuticals", Int. J. Drug Dev. & Res ,Vol. 5 , Issue 3, July-September 2013.

85. Patel Mitali, Patel Mrunali& Patel Rashmin, "Pharmaceutical Packaging and Packaging Technology: A Brief Overview", The Pharma Review, September - October 2012.

86. S. Agatonovic-Kustrin , R. Beresford, "Basic concepts of artificial neural network (ANN) modeling and its application in pharmaceutical research", Journal of Pharmaceutical and Biomedical Analysis, 22 (2000) 717–727.

87. Pranav Y. Dave, "Short Review on Printing Ink Technology to Prevent Counterfeit of the Products", Journal of Advanced Chemical Sciences, Volume 6 Issue 4 (2020) 693–697.

88. Thomas Bugnon, Mathieu Brichon and Roger David Hersc, "Model-Based Deduction of CMYK Surface Coverage from Visible and Infrared Spectral Measurements of Halftone Prints", Proc. SPIE Vol. 6493, 649310, Color Imaging XII: Processing, Hardcopy, and Applications; Reiner Eschbach, Gabriel G. Marcu; Eds., January 2007.

89. Cheol-Hee Lee, Eui-Yoon Chung, Chae-Soo Lee, Eung-Joo Lee, and Yeong-Ho Ha,"Tone reproduction technique using neural network in inkjet printers", 1999 Third International Conference on Knowledge-Based Intelligent Information Engineering Systems, 31" Aug-1" Sept 1999, Adelaide, Australia,0-7803-5578-4/99,1999.

90. A.D.Dongare, R.R.Kharde, Amit D.Kachare, "Introduction to Artificial Neural Network", International Journal of Engineering and Innovative Technology (IJEIT) Volume 2, Issue 1, July 2012.

91. I.A. Basheer, M. Hajmeer, "Artificial neural networks: fundamentals, computing, design, and application", Journal of Microbiological Methods 43, 3–31,2000.

92. Omer Deperlioglu, Utku Kose, "An educational tool for artificial neural networks", An educational tool for artificial neural networks, 37 ,392–402,2011.

93. Ankush Roy, Biswajit Halder,UtpalGarain, "Authentication of Currency Notes through Printing Technique Verification", ICVGIP '10, December 12-15, 2010.

94. Amey Thakur, Archit Konde, "Fundamentals of Neural Networks", International Journal for Research in Applied Science & Engineering Technology (IJRASET), Volume 9 Issue VIII Aug 2021.

95. Oludare Isaac Abiodun, Aman Jantan, Abiodun Esther Omolara, Kemi Victoria Dada, NachaatAbdElatif Mohamed , Humaira Arshad, "State-of-the-art in artificial neural network applications: A survey", Heliyon 4 (2018) e00938. doi: 10.1016/j.heliyon.2018.

96. Pramod Kumar Parida, Prof. S. Chakraverty, "Artificial Neural Network Based Numerical Solution of Ordinary Differential Equations", A Thesis of Master of Science In Mathematics, Department of Mathematics National Institute of Technology, Odisha, India, May, 2012.

97. Ms. Sonali. B. Maind, Ms. Priyanka Wankar, "Research Paper on Basic of Artificial Neural Network", International Journal on Recent and Innovation Trends in Computing and Communication,Volume: 2 Issue: 1, January 2014.

98. Onur Balci, S. Noyan O ulata , Cenk ahin , and R. Turul O ulata, "An Artificial Neural Network Approach to Prediction of the Colorimetric Values of the Stripped Cotton Fabric", Fibers and Polymers, Vol.9, No.5, 604-614,2008.

99. Ron Pilchik, " Pharmaceutical Blister Packaging, Part I Rationale and Materials", Pharmaceutical Technology November 2000.

100. Joshi Akshay Vijay, "Investigation of Process Parameters on Gravure Printability for Shrink Sleeves", Thesis, Printing Engineering Department, Jadavpur University, Kolkata, India,2014.

101. Gaurav Sharma, "Digital Color Imaging", Handbook, CRC Press, Boca Raton London New York Washington, D.C.,2003.

102. Abhijit Bhattacharya, Swati Bandhyopadhyay, and Phil Green, "Characterizing coated paper surface for modeling apparent dot area of halftone prints", Optics Express, Vol. 24, No. 2, DOI:10.1364/OE.24.001708,2016.

103. Paul D Fleming and Abhay Sharma, "C3.1olor Management with ICC Profiles: Can't Live without It so Learn to Live with I".

104. A. V. Joshi, S. Bandyopadhyay "Evaluation of Voids on Shrink PVC Film", ACTA Graphica 23, 2012.

105. R. H.Leach, R.J.Pierce, "Printing Ink Mannual", Fifth Edition,Springer.

106. Jun-Dong Chang, Shyr-Shen Yu, Hong-Hao Chen, and Chwei-Shyong Tsai, "HSV-based Color Texture Image Classification using Wavelet Transform and Motif Patterns", Journal of Computers Vol. 20, No. 4, January 2010.

107. Ján Morovič, "Color gamut Mapping", ISBN no. 9780470758939, 0470758937,Wiley, 15 September 2008.

108. Abhay Sharma, "Understanding color management", 2nd Edition, Hoboken, NJ: Wiley, 2018.

109. Phill Green, "Understanding Digital Color", 2nd Edition, GATF Press, 1999.

Paulomi Kundu 21.10.22

Swati Bandyopadhyay
21.10.22
(Supervisor)

Associate Professor
Printing Engineering Department
Jadavpur University
Kolkata

Prof. Alain Trémeau

LABORATOIRE HUBERT CURIEN
UMR CNRS 5516 Université Jean Monnet
18 rue Pr. Benoît Lauras - Bât. F
F-42000 SAINT-ETIENNE
(33) 04 77 91 57 80 / Fax (33) 04 77 91 57 81